KINETICS AND MECHANISMS ASSOCIATED WITH REDOX REGULATION OF PROTEIN TYROSINE PHOSPHATASE 1B (PTP1B)

A Dissertation Presented to the Faculty of the Graduate School

University of Missouri – Columbia

In Partial Fulfillment

Of the Requirements of the Degree

Doctor of Philosophy

By

Zachary D. Parsons

Prof. Kent S. Gates, Dissertation Supervisor

July 2014

The undersigned, appointed by the Dean of The Graduate School, have examined the dissertation entitled:

KINETICS AND MECHANISMS ASSOCIATED WITH REDOX REGULATION OF PROTEIN TYROSINE PHOSPHATASE 1B (PTP1B)

Presented by Zachary Daniel Parsons

A candidate for the degree Doctor of Philosophy

And hereby certify that, in their opinion, it is worthy of acceptance.

_____

Professor Kent S. Gates

_____

Professor Carol A. Deakyne

_____

Professor Thomas J. Reilly

_____

Professor John J. Tanner

ACKNOWLEDGEMENTS

I would like to thank the following for their various contributions over the years:

Our research group provides an excellent environment in which to work. It is my opinion that, in addition to guiding the direction of a group, the "character" of an academic research group starts with the advisor. I thank Dr. Kent Gates for fostering such an environment, and for sharing experience-based insights into matters of science and life in general throughout my graduate career.

I also owe thanks to my committee members – Professors Thomas Reilly, Carol Deakyne, and Jack Tanner – for their support and insight over the years. Special thanks go to Drs. Deakyne and Reilly, who patiently and expertly instructed me in their respective crafts. I couldn't imagine having better teachers.

Having a jovial and supportive set of group members made this endeavor much more fun and "smoother a ride" than it might have otherwise been. There are too many to list, so I'll pick on just one. I thank Sarah Lewis for tolerating me early on and for stepping up on more than one occasion to support me.

Any graduate student from this Department who does not thank Jerry Brightwell and Bill Vellema for their assistance either had no "paperwork-related" or instrumentation issues, or has made an error of omission. I thank them both for their help.

Thanks go to my father, Charles Esserine. Early on, he taught me the importance of asking “Why?” and seeking an answer in earnest, both in terms of exploring the natural world and in personal development.

Finally, my thesis advisor once correctly stated: in life, there are no controls (as in, control experiments). He is correct. Nevertheless, I can only speculate as to what I might have wound up doing professionally had Michael J. Van Stipdonk not invited me to join his research group as an undergraduate. I can only imagine it wouldn’t be quite as fun. Thanks, Doc.

TABLE OF CONTENTS

LIST OF FIGURES

Chapter 1

Chapter 2

Chapter 3

Chapter 4

Chapter 5

Chapter 6

Chapter 7

Chapter 8

LIST OF SCHEMES

Chapter 1

Chapter 2

Chapter 3

Chapter 4

Chapter 6

Chapter 7

Chapter 8

LIST OF TABLES

Chapter 1: A Brief Introduction to Protein Tyrosine Phosphatases

1.1 Protein Tyrosine Phosphatase Biological Function

Protein tyrosine phosphatases (PTPs) and protein tyrosine kinases (PTKs) work in tandem to regulate the dynamic "phosphorylation status" of tyrosine residues on various target proteins.[1,2,3] PTPs catalyze the hydrolytic removal of phosphoryl groups from phosphotyrosine residues, while PTKs catalyze the attachment of phosphoryl groups to the phenolic hydroxyl of free tyrosine residues, utilizing phosphoryl donors such as ATP (Figure 1.1).

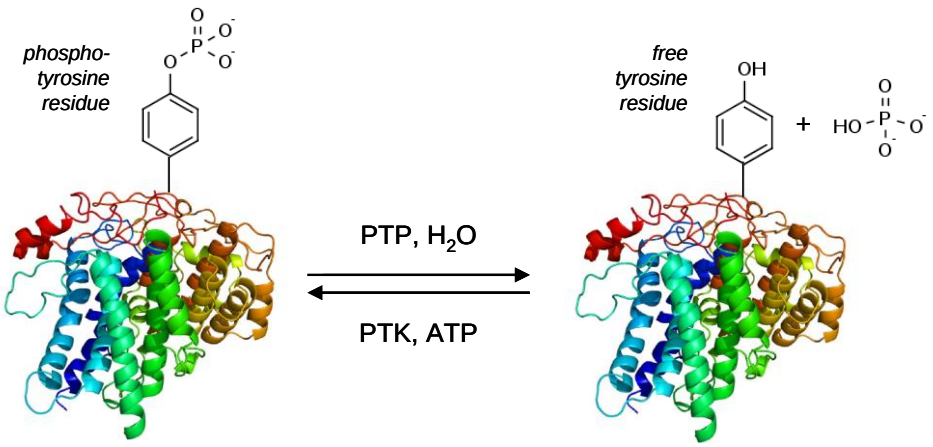

Figure 1.1 PTPs and PTKs function to control the phosphorylation status of protein tyrosine residues.

Generally speaking, phosphorylated tyrosine residues correspond to "signal on", whereas free tyrosine residues correspond to "signal off". Thus, PTKs may be crudely viewed as

cellular signaling "on-switches", and PTPs the antithetical "off-switches". Because many important cellular signaling pathways are regulated *via* modulation of tyrosine phosphorylation, it is unsurprising that aberrant PTP or PTK activity may lead to numerous disease states. Consequently, members of both the PTP and PTK families are important therapeutic targets.[2]

1.2 PTP Structure and Chemical Mechanism Employed in Catalysis

Members of the PTP family share profound structural homology. Thus, they might be expected to employ both essentially the same "catalytic machinery" in and around their active sites, and to utilize similar catalytic mechanisms.[4] For example, consider the overlain ribbon diagrams (derived from crystallographic data) of three distinct members of the PTP family: PTP1B, TCPTP, and SHP-2 (Figure 1.2).

Figure 1.2. PTPs share tremendous structural homology. Overlain are ribbon diagrams of three distinct PTPs: PTP1B (green), TCPTP (white), and SHP-2 (red; PDB codes 2CM2,

1L8K, and 3B7O, respectively). For reference, catalytic cysteine residues are shown as yellow sticks (residues 215, 216, and 459 in PTP1B, TCPTP, and SHP-2, respectively). The overlay and this image were created using PyMOL.

For this reason, much of the knowledge about structure and catalytic function gleaned from studies of the archetypical member of the PTP family, PTP1B, is extended and broadly applied to other members of the PTP family.[5,6,7]

PTPs catalyze removal of inorganic phosphate from phosphotyrosine residues by employing a crucial cysteine residue. Briefly, the anionic phosphate head group of the phosphotyrosine substrate is polarized by a series of hydrogen bonds donated by the PTP. This polarization of the substrate phospho group promotes nucleophilic attack at phosphorous by the PTP's catalytic cysteine thiolate (Cys215 in PTP1B). Nucleophilic attack displaces the tyrosine phenolic leaving group, which is protonated in flight by aspartic acid 181 (in PTP1B).[6] The nascent phospho-cysteine intermediate is then hydrolytically cleaved by an activated water molecule, affording inorganic phosphate and the PTP free cysteine thiolate (Scheme 1.1).

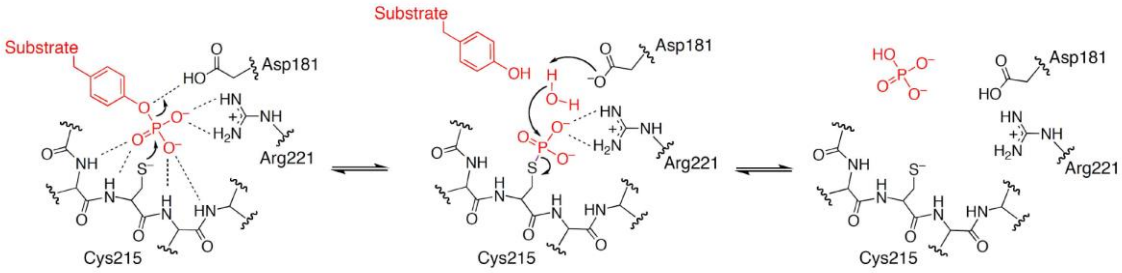

Scheme 1.1. The catalytic mechanism utilized by PTPs (numbering corresponds to residues in PTP1B).

Hydrolysis of the phospho-cysteine intermediate releases catalytically-active PTP (native PTP), which may then undergo another catalytic cycle. Importantly, any covalent modification of the catalytic cysteine sulfur results in complete loss of PTP catalytic activity.[8,9,10,11] Hence, chemically-stable modifications of the catalytic cysteine sulfur may be expected to permanently abrogate PTP activity.

1.3 Insulin Signaling, Redox Regulation of PTP1B, and Goals of this Thesis

PTP1B is a negative regulator of the insulin signaling pathway, for which it has attracted enormous attention as a potential therapeutic target for the treatment of type II diabetes *mellitus* and obesity.[12] Insulin signaling is initiated when insulin binds to the extracellular domain of the insulin receptor, triggering autophosphorylation of the insulin receptor at its intracellular (cytosolic) domain and of the insulin receptor substrate. These are the first in a series of cellular events which ultimately lead to translocation of glucose transporter Glut4 to the cell membrane, allowing the cell to draw glucose from the bloodstream for use in metabolism. The signal is terminated when active PTP1B removes these phosphoryl groups from the insulin receptor. Naturally, PTP1B catalytic activity is suppressed during active insulin signaling.

In addition to inducing autophosphorylation, insulin binding to the insulin receptor activates the NAD(P)H-dependent oxidase Nox4.[13] Nox4 catalyzes the reduction of molecular oxygen, affording hydrogen peroxide (equation 1):

$$NADPH + O_2 + H^+ \xrightarrow{Nox4} NADP^+ + H_2O_2 \qquad (1)$$

The hydrogen peroxide produced by this reaction transiently inactivates PTP1B by oxidizing the catalytic residue, Cys 215. Because the catalytic cysteine is maintained in anionic (thiolate) form, it is particularly susceptible to oxidation.[14] The reaction proceeds *via* initial nucleophilic attack of the cysteine thiolate on hydrogen peroxide, yielding a sulfenic acid intermediate (-SOH).[155] This sulfenic acid intermediate then undergoes dehydrative cyclization to afford an unusual 5-membered heterocycle, formally an isothiazolidin-3-one (more commonly referred to as a "sulfenyl amide", Scheme 1.2). Interestingly, it is the peptide backbone amide nitrogen that functions as a nucleophile in this reaction.

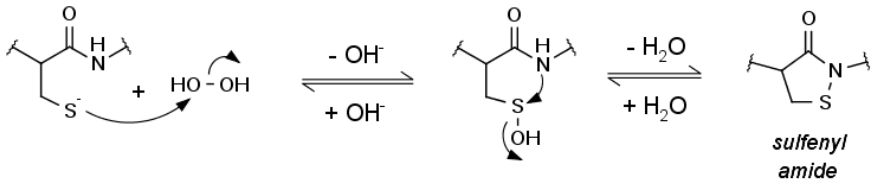

Scheme 1.2. Oxidation of PTP1B by hydrogen peroxide results in sulfenyl amide formation.

The sulfenyl amide may be reduced by biological reducing equivalents such as thiols, recovering the native PTP cysteine thiolate (Scheme 1.3).[16,17]

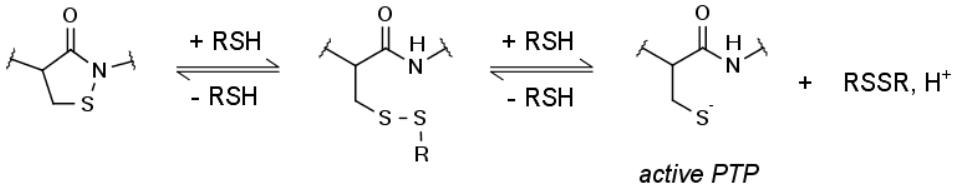

Scheme 1.3. Recovery of PTP activity *via* reduction of the sulfenyl amide by thiol agents.

This oxidative-inactivation/reductive-reactivation cycle is the basis for redox regulation of PTPs *in vivo*, and allows for control of the duration and intensity of signaling events.

Our group, in collaboration with Professor Thomas Reilly and Professor Jack Tanner's group at MU, addressed some of the kinetic, mechanistic, and structural aspects of oxidative inactivation of PTPs PTP1B and SHP2 in a 2011 publication in *JACS*.[9] Subsequently, our group undertook studies to elucidate the kinetics and mechanisms associated with recovery of PTP activity from oxidatively-inactivated PTP1B and SHP2, as described in *Biochemistry* (2013) and Chapter 2 herein.[16] In that work, we describe the rates and reactions associated with thiol-mediated recovery of the oxidatively-inactivated PTPs, and determined that oxidized PTP1B and SHP2 undergo fundamentally different processes during reductive reactivation, giving rise to two kinetically-distinct rate laws.

We also prepared a previously-reported, small molecule dipeptide model of the sulfenyl amide present in oxidized PTP1B and characterized reactions it undergoes with carbon-based nucleophiles. In Chapter 3 we report utilization of the 1,3-diketone moiety as a source of carbon nucleophiles capable of covalent capture of the sulfenyl amide. In Chapter 4, we expanded the scope of structural scaffolds capable of producing nucleophilic carbon species that react with the sulfenyl amide under mild conditions. In each case, we began developing preliminary structure-activity relationships for these carbon nucleophiles. To that effect, we measured aqueous pK_a values of the parent acids and determined both reaction order and rate constants for reactions with the model sulfenyl amide. Thereafter, we explored whether these agents might be capable of covalently trapping oxidatively-inactivated PTP1B in the context of preventing thiol-mediated recovery of the enzyme (Chapter 5). In Chapter 6 of this thesis, we explored the

possibility that PTP1B might be susceptible to so-called "over-oxidation" and subsequent hydrolytic degradation. Presumably, oxidation of the enzyme "beyond" the sulfenyl amide leads to species which might be hydrolytically-labile, though "rescuable" by thiol agents. In that work, we studied the pH-dependent rates at which "over-oxidized" PTP1B undergoes time-dependent loss of thiol-recoverable activity, and the rate at which these hydrolytically-labile species form. Interestingly, we found that the kinetics of these processes ("over-oxidation" and hydrolytic decomposition) suggest mechanisms much more complicated than that originally hypothesized. Chapters 7 of this thesis describes the development and implementation of a method by which to predict substituent electronic effects in the context of Hammett substituent constants. We used electronic structure calculations to determine optimized geometries of various aryl amines and structural analogues for prediction of nitrogen mustard reactivities. Finally, in Chapter 8 we report evidence that garlic-derived organic polysulfides are capable of alkylating biologically-relevant nucleophiles, and begin elucidating structure-activity relationships within that class of dietary electrophile.

References

(1) Hunter, T. Signaling—2000 and Beyond. *Cell* **2000**, *100*, 113–127.

(2) Tonks, N. K. Protein Tyrosine Phosphatases: From Genes, to Function, to Disease. *Nat. Rev. Mol. Cell Biol.* **2006**, *7*, 833–846.

(3) Lemmon, M. A.; Schlessinger, J. Cell Signaling by Receptor Tyrosine Kinases. *Cell* **2010**, *141*, 1117–1134.

(4) Combs, A. P. Recent Advances in the Discovery of Competitive Protein Tyrosine Phosphatase 1B Inhibitors for the Treatment of Diabetes, Obesity, and Cancer. *J. Med. Chem.* **2010**, *53*, 2333–2344.

(5) Bhattacharya, S.; LaButti, J. N.; Seiner, D. R.; Gates, K. S. Oxidative Inactivation of Protein Tyrosine Phosphatase 1B by Organic Hydroperoxides. *Bioorg. Med. Chem. Lett.* **2008**, *18*, 5856.

(6) Sarmiento, M.; Zhao, Y.; Gordon, S. J.; Zhang, Z.-Y. Molecular Basis for Substrate Specificity of Protein-Tyrosine Phosphatase 1B. *J. Biol. Chem.* **1998**, *273*, 26368–26374.

(7) Jia, Z.; Barford, D.; Flint, A. J.; Tonks, N. K. Structural Basis for Phosphotyrosine Peptide Recognition by Protein Tyrosine Phosphatase 1B. *Science* **1995**, *268*, 1754–1758.

(8) Seiner, D. R.; LaButti, J. N.; Gates, K. S. Kinetics and Mechanism of Protein Tyrosine Phosphatase 1B Inactivation by Acrolein. *Chem. Res. Toxicol.* **2007**, *20*, 1315–1320.

(9) Zhou, H.; Singh, H.; Parsons, Z. D.; Lewis, S. M.; Bhattacharya, S.; Seiner, D. R.; LaButti, J. N.; Reilly, T. J.; Tanner, J. J.; Gates, K. S. The Biological Buffer Bicarbonate/CO2 Potentiates H2O2-Mediated Inactivation of Protein Tyrosine Phosphatases. *J. Am. Chem. Soc.* **2011**, *133*, 15803–15805.

(10) Liu, S.; Zhou, B.; Yang, H.; He, Y.; Jiang, Z.-X.; Kumar, S.; Wu, L.; Zhang, Z.-Y. Aryl Vinyl Sulfonates and Sulfones as Active Site-Directed and Mechanism-Based Probes for Protein Tyrosine Phosphatases. *J. Am. Chem. Soc.* **2008**, *130*, 8251–8260.

(11) Arabaci, G.; Guo, X.-C.; Beebe, K. D.; Coggeshall, K. M.; Pei, D. A-Haloacetophenone Derivatives As Photoreversible Covalent Inhibitors of Protein Tyrosine Phosphatases. *J. Am. Chem. Soc.* **1999**, *121*, 5085–5086.

(12) Johnson, T. O.; Ermolieff, J.; Jirousek, M. R. Protein Tyrosine Phosphatase 1B Inhibitors for Diabetes. *Nat. Rev. Drug Discov.* **2002**, *1*, 696–709.

(13) Mahadev, K.; Motoshima, H.; Wu, X.; Ruddy, J. M.; Arnold, R. S.; Cheng, G.; Lambeth, J. D.; Goldstein, B. J. The NAD(P)H Oxidase Homolog Nox4 Modulates Insulin-Stimulated Generation of H2O2 and Plays an Integral Role in Insulin Signal Transduction. *Mol. Cell. Biol.* **2004**, *24*, 1844–1854.

(14) Tanner, J. J.; Parsons, Z. D.; Cummings, A. H.; Zhou, H.; Gates, K. S. Redox Regulation of Protein Tyrosine Phosphatases: Structural and Chemical Aspects. *Antioxid. Redox Signal.* **2011**, *15*, 77–97.

(15) Sivaramakrishnan, S.; Keerthi, K.; Gates, K. S. A Chemical Model for Redox Regulation of Protein Tyrosine Phosphatase 1B (PTP1B) Activity. *J. Am. Chem. Soc.* **2005**, *127*, 10830–10831.

(16) Parsons, Z. D.; Gates, K. S. Thiol-Dependent Recovery of Catalytic Activity from Oxidized Protein Tyrosine Phosphatases. *Biochemistry* **2013**, *52*, 6412–6423.

(17) Dagnell, M.; Frijhoff, J.; Pader, I.; Augsten, M.; Boivin, B.; Xu, J.; Mandal, P. K.; Tonks, N. K.; Hellberg, C.; Conrad, M.; et al. Selective Activation of Oxidized PTP1B by the Thioredoxin System Modulates PDGF-B Receptor Tyrosine Kinase Signaling. *Proc. Natl. Acad. Sci.* **2013**, *110*, 13398–13403.

Chapter 2: Thiol-Dependent Recovery of Catalytic Activity from Oxidized Protein Tyrosine Phosphatases

2.1 Introduction

Many important mammalian signaling pathways are regulated by phosphorylation of specific tyrosine residues on target proteins.[1-4] The phosphorylation status of these proteins is controlled by the coordinated action of protein tyrosine kinases that catalyze the addition of phosphoryl groups and protein tyrosine phosphatases (PTPs) that catalyze their hydrolytic removal.[2-6] The catalytic activity of selected PTPs is down-regulated as part of some signal transduction events.[3,7] This involves the activation of NADPH oxidases that generate a burst of hydrogen peroxide (H_2O_2) that oxidizes the catalytic cysteine thiolate group at the active site of selected PTPs.[8-14] The oxidatively-inactivated forms of various PTPs may exist with the catalytic cysteine residue either as a sulfenic acid, a disulfide, or a sulfenyl amide (Scheme 2.1).[15] Reaction of biological thiols with oxidized PTPs can regenerate the catalytically active enzyme, with the active site cysteine in the thiolate form (Scheme 2.2).[15]

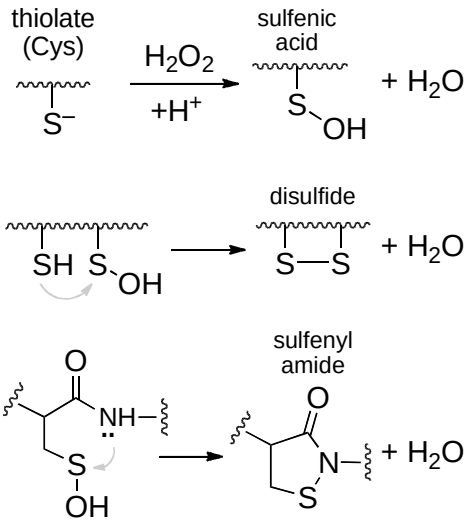

Scheme 2.1. Oxidative inactivation of protein tyrosine phosphatases.

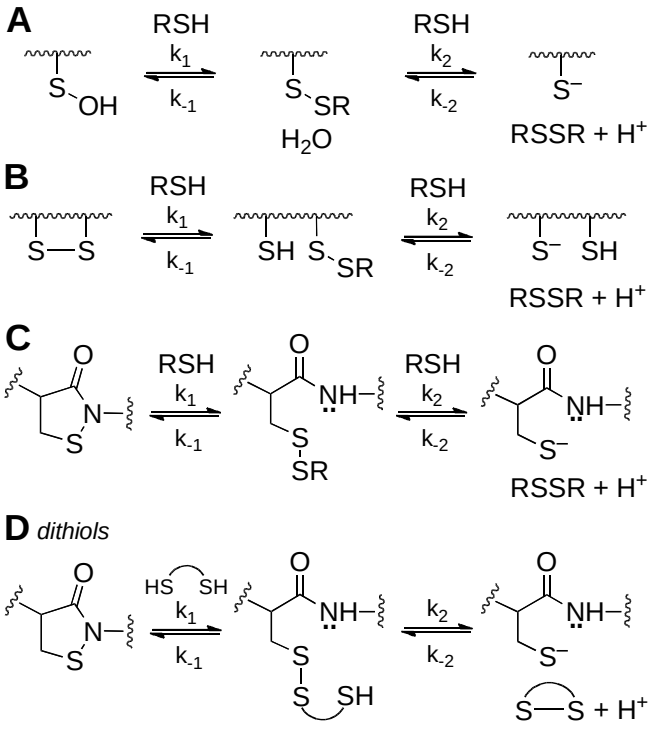

Scheme 2.2. Thiol-mediated recovery of catalytic activity from oxidized protein tyrosine phosphatases.

The oxidative inactivation and subsequent thiol-mediated reactivation of PTPs during signaling events constitutes an important biochemical "timing device" that helps control the duration and intensity of cellular responses to various stimuli.[3,7,15] A number of studies have investigated the mechanisms by which hydrogen peroxide inactivates PTPs;[9-12,16-20] however, the mechanisms by which cellular thiols regenerate the catalytic activity of these proteins has received less attention. Low molecular weight thiols, including the biological thiol glutathione (GSH), can mediate the recovery of activity from oxidized PTPs.[12,15,18,21-24] In addition, enzymes such as thioredoxin, glutaredoxin, and sulfiredoxin can repair oxidized PTPs, employing both single cysteine thiol and vicinal dithiol mechanisms in the reduction of oxidized proteins.[15,18,21,25-27] In general, the rates, mechanisms, and exact identity of the thiols that regenerate catalytic activity from oxidized PTPs remains an important, yet poorly understood, aspect of many receptor protein tyrosine kinase-mediated cell signaling pathways. In the work described here, we employed various low molecular weight thiols and the enzyme thioredoxin as probes to explore fundamental chemical and biochemical features surrounding the regeneration of catalytic activity from two structurally distinct oxidized PTPs.

Results and Discussion

2.2 Oxidative Inactivation of PTP1B.

We first examined thiol-mediated regeneration of activity from oxidized PTP1B. PTP1B is the archetypal member of the PTP superfamily and is redox regulated as part of

the insulin signaling cascade.[9,13] For these studies, we employed the catalytic domain of recombinant human PTP1B (aa 1-322). The oxidatively-inactivated enzyme was prepared by treatment of native PTP1B with H_2O_2 (1 mM) in Buffer A containing Tween-80 (0.5% v/v) for 5 min at 25 ˚C, followed by addition of catalase (100-300 units) to quench remaining H_2O_2. Enzyme prepared in this manner was completely inactive, but approximately 75% of the original activity was consistently recovered by treatment with 1,4-dithio-D-threitol (DTT, 40 mM, 20 min, 25 ˚C).

Evidence suggests that oxidative inactivation of PTP1B proceeds via conversion of the active site cysteine to the cyclic sulfenyl amide both in the crystal and in solution forms of the enzyme (Scheme 2.1).[31,32] Nonetheless, it remains possible that oxidized PTP1B exists in some other form such as the sulfenic acid (Scheme 2.1). The inability to completely recover the catalytic activity of oxidized PTP1B presumably reflects the formation of some overoxidized forms of the enzyme. These may include cyclic sulfinyl and sulfonyl amide forms of PTP1B (Structures **3** and **4**, respectively).[22,31,32] Results of previous chemical model studies indicate that the sulfinyl amide form of PTP1B may be thiol recoverable, while the sulfonyl amide likely is not.[22]

2.3 Thiol-Dependent Recovery of Activity from Oxidized PTP1B.

We treated oxidized PTP1B with a panel of structurally diverse thiol-containing compounds in the presence of the chromogenic PTP substrate *p*-nitrophenylphosphate and used a continuous spectrophotometric assay to monitor the recovery of enzyme activity engendered by each agent. All of the thiols examined caused time-dependent

recovery of activity from the oxidized enzyme (Figure 2.1). From these time courses, carried out under pseudo-first-order conditions, an apparent second-order rate constant for the recovery of enzyme activity was estimated for each thiol (Figure 2.1, legend).

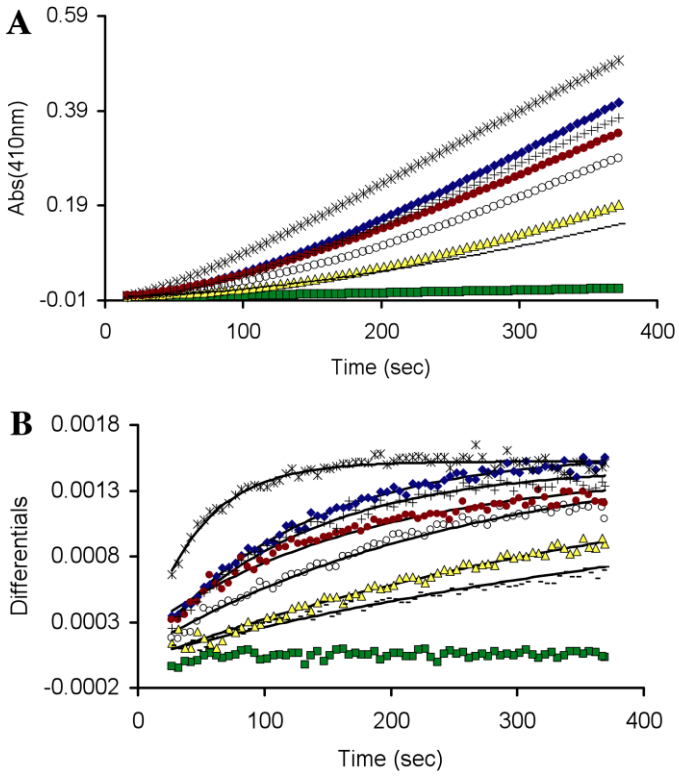

Figure 2.1. Thiol-mediated reactivation of oxidatively-inactivated PTP1B. **(A)** $PTP1B_{ox}$ (22 nM) was incubated with various thiols in Buffer A containing the chromogenic PTP substrate pNPP (20 mM), pH 7 at room temperature. The time courses monitored the increase in absorbance at 410 nm resulting from the PTP1B-catalyzed release of p-nitrophenol from the substrate. Monothiols were 50 mM and dithiols 25 mM: TGA-OMe (∗), DTT (♦), BAL (+), TGA (●), 2-ME (○), GSH (▲), NAC (-), no thiol (■). **(B)** Instantaneous rates of reactivation (slopes) versus time. Data were fit with pseudo-first order kinetic treatment to give the following estimates of the apparent bimolecular rate constants calculated in units of M^{-1} s^{-1}: TGA-OMe = 0.45, DTT = 0.33, BAL = 0.33, TGA = 0.12, 2-ME = 0.08, GSH = 0.04, NAC = 0.04.

We next undertook a more detailed kinetic examination of a subset of these thiols.

For example, treatment of oxidized PTP1B with the biological thiol GSH at concentrations ranging from 1-60 mM resulted in time- and concentration-dependent recovery of the enzyme's catalytic activity (Figure 2.2A and B). The reaction displayed second-order kinetics, with an apparent rate constant of 0.023 ± 0.004 M^{-1} s^{-1}. We examined several other structurally varied monothiols including 2-mercaptoethanol (2-ME), cysteine, and thioglycolic acid (TGA) (Table 2.1). Similar to GSH, the recovery of PTP1B activity caused by these thiols followed second-order kinetics, with the observed rate constants varying by a factor of about eight.

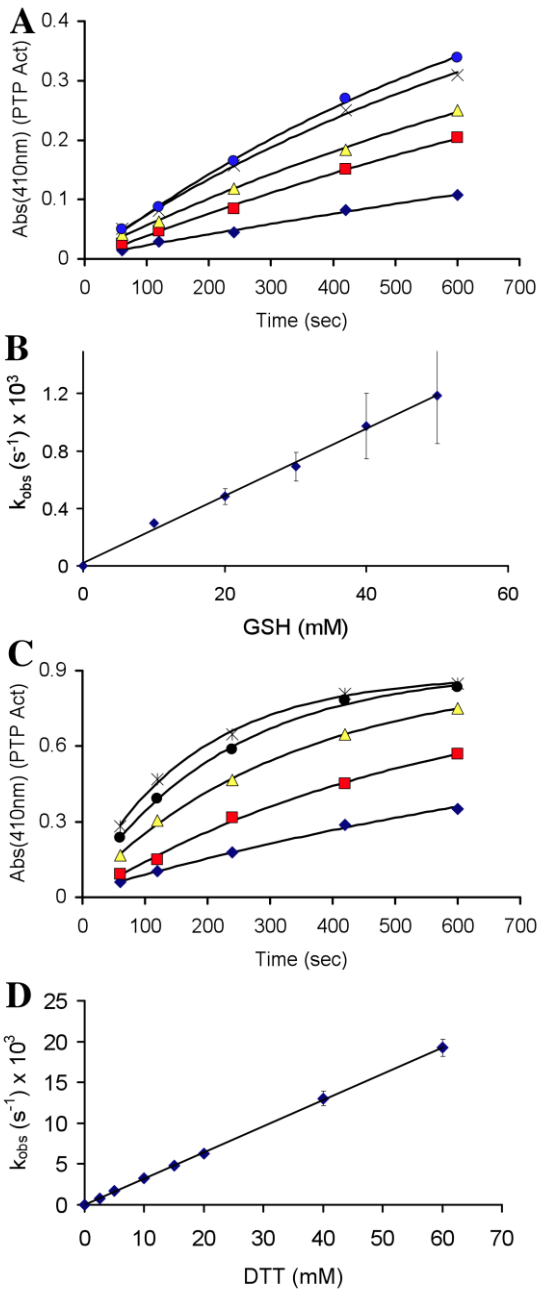

Figure 2.2. Reactivation of oxidatively-inactivated PTP1B by glutathione (GSH) and DTT. (**A**) GSH-mediated recovery of activity from oxidized PTP1B. Concentrations of GSH were 10, 20, 30, 40, and 50 mM (bottom to top). (**B**) Pseudo-first order rate constants (s^{-1} x 10^3) were plotted against corresponding concentrations of GSH (mM), affording a straight line of slope k_{obs} (M^{-1} s^{-1}) which passes through the origin. (**C**) Time-course for DTT-mediated recovery of activity from oxidized PTP1B. Concentrations of DTT were 2.5, 5, 10, 15, and 20 mM (bottom to top). (**D**) Pseudo-first order rate constants (s^{-1} x 10^3) were plotted against corresponding concentrations of DTT (mM), affording a straight line of slope k_{obs} (M^{-1} s^{-1}) which passes through the origin. A higher concentration regime of DTT (40-60 mM) was also explored in separate experiments

conducted under identical conditions. No saturation behavior was observed under any of these concentration regimes.

Thiol	Structure	k_{obs} (M^{-1} s^{-1})	pK_a
2,3-dimercaptopropanol	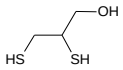	0.59 ± 0.02	8.6
Dithiothreitol	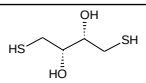	0.325 ± 0.007	9.2
Cysteamine	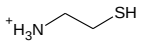	0.14 ± 0.01	8.2
Cysteine	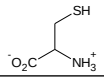	0.10 ± 0.02	8.2
Thioglycolate	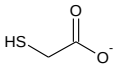	0.090 ± 0.006	10.1
2-mercaptoethane sulfonate	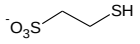	0.07 ± 0.03	9.5
2-mercaptoethanol	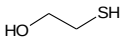	0.05 ± 0.03	9.4
Glutathione	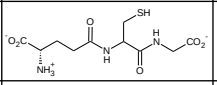	0.023 ± 0.004	9.1
3-mercaptopropionate	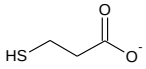	0.017 ± 0.002	10.6

Table 2.1. Structures, thiol group pK_a, and observed second-order rate constants for reactivation of oxidatively-inactivated PTP1B. Forms of thiols shown are those predominating under assay conditions (pH 7). Errors are expressed as ± 2 SE, except for cysteamine and 3-mercaptopropionate (± SD). pK_a values were taken from literature measurements.[30,35,36]

Literature precedents indicate that thiolate (RS^-) is the relevant nucleophile in the reactions of thiols with divalent sulfur electrophiles.[33,34] Consistent with these precedents, the data presented in Table 2.1 shows that, with one exception (TGA) that is discussed further below, monothiols with lower pK_a values display larger rate constants

for their reactions with oxidized PTP1B. Molecules bearing thiol groups with lower pK_a values exist with a significantly larger fraction in the reactive thiolate form near neutral pH values. The observed rate constants measured here, along with the literature pK_a values for the respective thiol groups,[30,35,36] allowed us to estimate the true rate constants for regeneration of activity from oxidized PTP1B by each thiolate (Table 2.2). This analysis accounts for differences in pK_a of the various thiol groups and highlights how structural differences influence reactivity. The results indicate that more *basic* thiolates were more reactive toward oxidized PTP1B. This is in accord with findings from the Whitesides group regarding the attack of thiolates on low molecular weight disulfides.[30,37]

Thiol	k_{RS^-} ($M^{-1} s^{-1}$)	pK_a
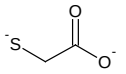	113	10.1
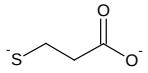	69	10.6
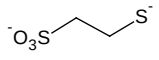	23	9.5
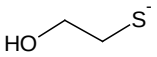	12	9.4
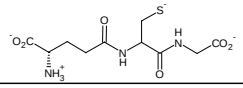	3	9.1
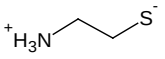	2	8.2
	2	8.2
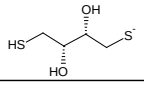	52	9.2
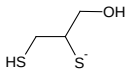	24	8.6

Table 2.2. Observed second-order rate constants, corrected for thiolate concentration under assay conditions (pH 7, 25 ˚C).

Interestingly, TGA was more reactive than pK_a considerations alone would predict. This could reflect favorable electrostatic interactions between the ionized carboxylate group of TGA with positively-charged amino acid side chains such as Arg45, Lys116, and Lys210 located near the catalytic Cys215 in the three-dimensional structure of oxidized PTP1B (see for example: pbd 3SME).[10] Alternatively, equilibrium amounts of the neutral carboxylic acid form of TGA could serve as a general acid catalyst to

increase the rate k_2 as illustrated in Scheme 2.3.

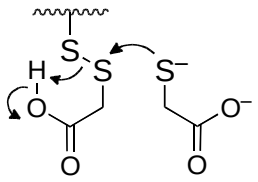

Scheme 2.3. General acid catalysis may be responsible for the unusually large rate constant (k_{RS^-}) with which thioglycolate recovers PTP activity from oxidized PTP1B.

We also examined reaction of the dithiol DTT with oxidized PTP1B. DTT has been suggested as a reasonable low molecular weight mimic of dithiol-containing enzymes involved in the repair of oxidized proteins.[15,18] Treatment of oxidized PTP1B with DTT (1-60 mM, pH 7) produced time- and concentration-dependent recovery of the enzyme's catalytic activity (Figure 2.2C and D). The data were consistent with a second-order process with a rate constant of 0.325 ± 0.007 M^{-1} s^{-1}. Importantly, the observed rate of enzyme recovery in the case of DTT was approximately 6.5-fold greater than that measured for the structurally analogous monothiol, 2-ME. Furthermore, the rate constant estimated for the regeneration of active enzyme by the thiolate form of DTT was more than double that of 2-ME thiolate (Table 2.2). Contrary to the trend identified above, in this case, the *less* basic thiolate of DTT displays a larger rate constant. The apparent discrepancy in the kinetic behavior of DTT and 2-ME likely reflects a difference in the rate-determining step for the regeneration of PTP1B activity by these two thiols. Specifically, the rate constant measured for the recovery of PTP1B activity in the case of DTT may report on the initial attack of thiolate on the oxidized enzyme (k_1 in Scheme

2.2C). This is a reasonable hypothesis given that the second step of the reaction, involving *intramolecular* attack of the pendent thiol group on the mixed disulfide intermediate, is expected to be fast (Scheme 2.2D).[30,38] In contrast, the observed rates at which monothiols reactivate oxidized PTP1B may reflect the bimolecular attack of a second equivalent of thiolate on the mixed disulfide intermediate (k_2 in Scheme 2.2C). The rate measured here for DTT (0.325 M^{-1} s^{-1}) can be compared to the value of 0.23 M^{-1} s^{-1} reported for the attack of DTT on GSH disulfide under similar conditions (pH 7, 30 °C).[30]

Unlike DTT, the dithiol 2,3-dimercapto-1-propanol (BAL) exhibited biphasic behavior in the plot of pseudo first-order rate constants versus thiol concentration (Figure 2.3).

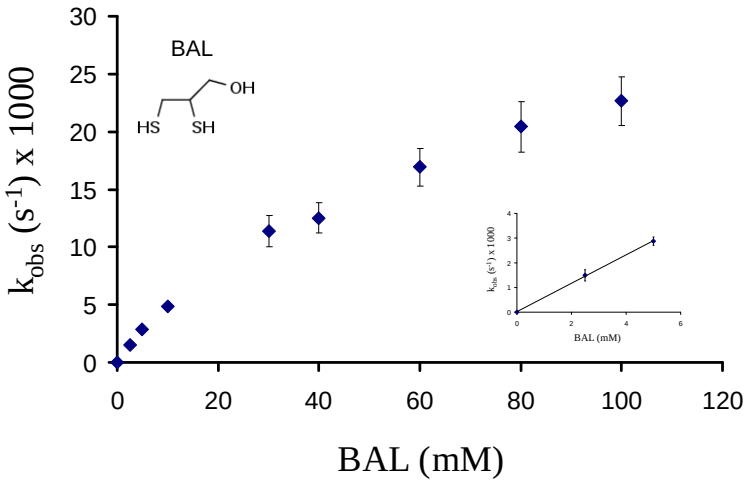

Figure 2.3. Pseudo first-order rate constants versus concentration of the dithiol BAL: biphasic kinetics in the reactivation of oxidized PTP1B. Trendline regression through data corresponding to low concentrations of BAL (0 – 5 mM) affords a straight line intercepting the origin, consistent with a simple, second-order process (inset). However, at intermediate concentrations of BAL (10 – 30 mM), curvature in the plot occurs. Rather than plateau at high concentrations of BAL (~30+ mM), a second linear region is revealed, of shallower slope than the first linear region and of non-origin intercept.

At low concentrations of BAL (up to 5 mM), a line passing through the origin with slope (second-order rate constant) equal to 0.6 M^{-1} s^{-1} was observed. At intermediate concentrations of thiol (10 – 30 mM), a "downward bend" in the plot occurs, leading to a second linear region of shallower slope, which corresponds to a *different* second-order rate constant (approximately 0.17 M^{-1} s^{-1}, with y-intercept of ~ 0.006 s^{-1}). The different kinetic behaviors of BAL and DTT may arise due to the relatively slow intramolecular ring closure in the case of the PTP-BAL mixed disulfide (k_2 in Scheme 2.2D). At low concentrations of BAL, the intramolecular ring closure of the second, pendent thiol group in the PTP-BAL mixed disulfide (k_2, Scheme 2.2D) may be faster than both the rate of initial attack of BAL on oxidized enzyme (k_1[RSH], Scheme 2.2C) *and* bimolecular attack of a second equivalent of BAL on the PTP-BAL mixed disulfide (k_2[RSH], Scheme 2.2C). Thus, in the low concentration regime, the rate-determining step for recovery of enzyme activity by BAL may be the initial attack of thiol on oxidized PTP1B, in similar fashion to that of DTT. However, at higher concentrations of BAL, the bimolecular rate associated with attack of a second equivalent of BAL on the PTP-BAL mixed disulfide (k_2[RSH], Scheme 2.2C) may surpass that of the first-order, intramolecular ring closure (k_2, Scheme 2.2D). If the two forward bimolecular rate constants in Scheme 2.2C have the relationship $k_1 > k_2$ (which is consistent with the interpretation of the data for monothiols discussed above) and the pseudo-first-order rate constant k_2[BAL] is greater than the first-order rate constant k_2 (Scheme 2.2D) then the rate-determining step for formation of the active enzyme will be the bimolecular reaction k_2 in Scheme 2C. Thus, at low concentrations BAL behaves like the dithiol DTT, while

at high concentrations BAL behaves, for all practical purposes, like a monothiol (Scheme 2.4).

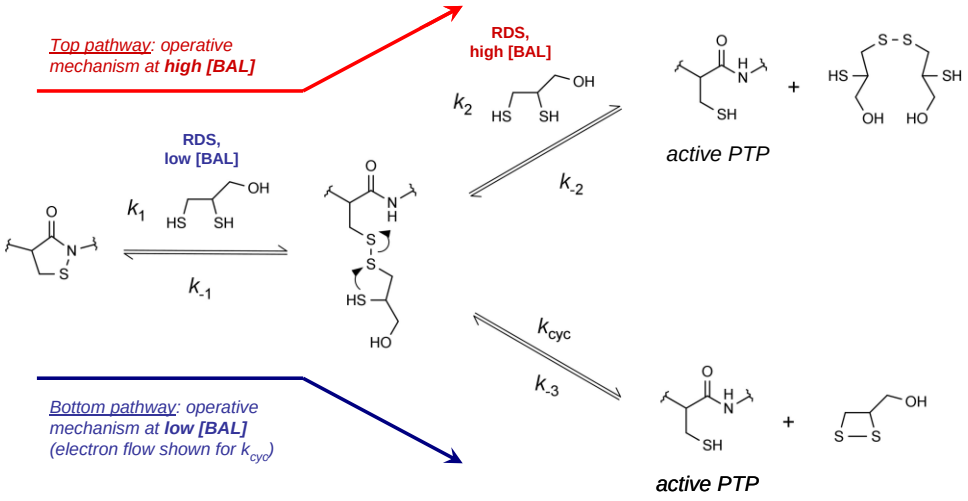

Scheme 2.4. Postulated reaction pathways at high and low concentrations of BAL during the reactivation of oxidatively-inactivated PTP1B, and associated rate-limiting steps.

Along these lines, it is worth noting that BAL typically forms cyclic dimers upon reduction of low molecular weight disulfides;[30] however, steric occlusion of the PTP-BAL mixed disulfide at the protein surface may hinder this process, rendering formation of the cyclic dimers relatively slow.

We investigated whether several known, active-site-directed reversible inhibitors of *native* PTP1B were able to inhibit thiol-mediated reactivation of the oxidized enzyme. We examined the known inhibitors phosphate (K_d = 21 mM),[39] and arsenate (K_i = 80 μM).[40] In addition, we examined the effects of two previously characterized, active-site-directed, reversible inhibitors of PTP1B, the Merck inhibitor, **1** (IC_{50} = 47 nM)[41] and 2-

(oxalylamino)benzoic acid **2** (K_i = 23 μM).[28]

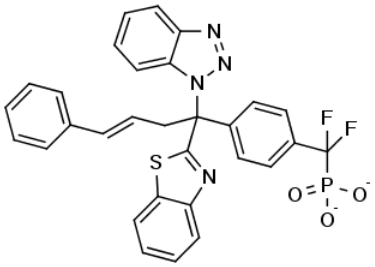

1

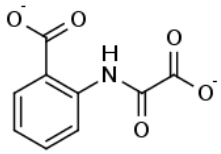

2

None of these agents inhibited the ability of thiols to restore oxidized PTP1B to its catalytically active form (data not shown). On the contrary, in the case of sodium phosphate (50 mM), a slight acceleration in the recovery of PTP1B activity by 2-ME and DTT was observed, likely because the significantly greater ionic strength of the phosphate-containing solutions depressed the pK_a of the thiol groups in these assays, leading to increased concentration of the reactive thiolate species. The failure of competitive PTP1B inhibitors to slow thiol-mediated recovery of activity from oxidized PTP1B likely reflects the simple fact that the structures of the oxidized and native enzymes are substantially different, and that traditional PTP inhibitors do not bind to the oxidized enzyme with high affinity (for example, compare pdb structures 3SME and 3HNP).[10,32]

We examined the ability of the thioredoxin/thioredoxin reductase enzyme system to regenerate catalytic activity from oxidized PTP1B. The thioredoxin/thioredoxin reductase system did regenerate active PTP1B, with an observed rate constant of 1.4 x 10^{-3} s^{-1} at a thioredoxin concentration of 2 μM (Figure 2.4).

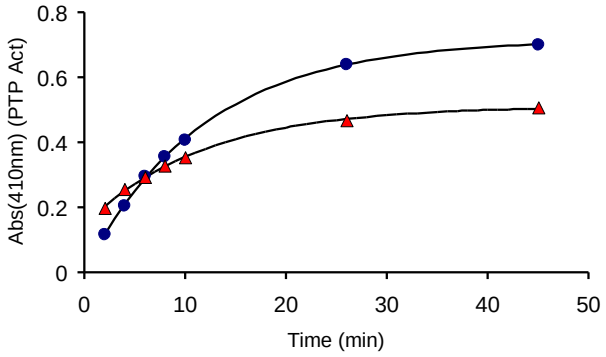

Figure 2.4. Reactivation of oxidatively-inactivated PTP1B by DTT or the thioredoxin-thioredoxin reductase system. To solutions of 2x-concentrated reducing system in Buffer R were added 1:1 (v/v) oxidatively-inactivated PTP1B to final concentrations: $PTP1B_{ox}$ (350 nM), DTT (5 mM, blue circles) or thioredoxin/thioredoxin reductase/NADPH (2 μM, 100 nM, 200 μM, respectively, red triangles). Immediately upon mixing, a timer was started, and the amount of recovered enzyme activity monitored at 2, 4, 6, 8, 10, 26, and 45 min intervals.

For comparision, a concentration of 5 mM DTT gave approximately the same pseudo-first-order rate constant as 2 μM thioredoxin (Figure 2.4). It is noteworthy that the *yield* of active PTP1B generated by the thioredoxin/thioredoxin reductase system was somewhat less than that produced by DTT (Figure 2.4). The difference in the amount of PTP1B activity regenerated by thioredoxin and the low molecular weight thiols may be explained by the presence of multiple oxoforms of PTP1B in the assay. As noted above, oxidative inactivation of PTP1B likely generates multiple oxoforms of the enzyme including the sulfenyl amide and higher oxidation states products such as the cyclic sulfinyl amide **3** and the sulfonyl amide **4**.[22,31,32] Results of previous chemical model studies suggest that low molecular weight thiols can return the sulfinyl amide **3** form of PTP1B to the active state, while the sulfonyl amide likely cannot be recovered.[22] As

described in this work, it is possible that thioredoxin may selectively process the sulfenyl amide shown in Scheme 2.1, but not the sulfinyl amide **3**. In contrast, the chemical studies reported previously indicated that DTT and other low molecular weight thiols appear indiscriminant with regard to their reactions with small molecules that model these oxoforms of PTP1B.[22] While these results suggests the possibility that a mixture of PTP1B oxoforms may be generated during the oxidation of PTP1B with H_2O_2, the simple bimolecular kinetics observed for the thiol-dependent recovery of activity from oxidized PTP1B further suggest that the oxoforms are converted to active enzyme at similar rates. If multiple processes with significantly different rate constants were operative, biphasic kinetics would be observed.

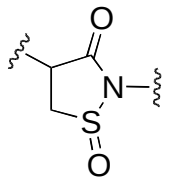

3

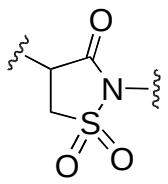

4

2.4 Disulfide Byproducts Generated in the Reaction of Thiols with Oxidized PTP1B Do Not Inactivate the Catalytically-Active Form of the Enzyme.

Thiol-mediated reactivation of PTP1B generates a disulfide byproduct (Scheme 2.2). Previous reports indicate that disulfides such as GSH disulfide, Ellman's reagent, and the natural product gymnorrhizol can inactivate PTP1B.[27,42,43] Therefore, we

investigated whether 2-ME disulfide, GSH disulfide, and oxidized DTT might inactivate PTP1B under our assay conditions. We found that none of these disulfides inactivated the native enzyme at concentrations of 1-20 mM in Buffer A containing Tween-80 (0.5% v/v) at 25 ˚C. The results suggest that the process defined by k_{-2}[RSSR] in Scheme 2.2 was not significant under the conditions of our experiments.

2.5 Trialkylphosphine-Mediated Reactivation of Oxidatively-Inactivated PTP1B.

Because trialkylphosphine-based reagents are commonly utilized for reduction of protein disulfides to free thiols,[44-46] we were curious how the efficiency of the prototypical reagent in this class, tris(2-carboxyethyl)phosphine (TCEP),[44] compares to thiols in its ability to regenerate catalytic activity from oxidized PTP1B. As shown in Figure S5, time- and concentration-dependent recovery of PTP activity was observed upon treatment of oxidized PTP1B with TCEP under assay conditions identical to those employed in our thiol experiments. The amount of recovered PTP activity was comparable to that recovered by DTT. A replot of the pseudo first-order rate constants versus concentration of TCEP afforded a straight line passing through the origin, suggesting a rate-determining step first-order in TCEP. Reduction of disulfides to two equivalents of thiol by trialkylphosphine reagents involves initial attack of the neutral phosphorus atom on the disulfide, liberating the first equivalent of thiol (Scheme 2.5).[44-46] Subsequent hydrolysis of the thio-phosphonium intermediate liberates the second equivalent of thiol, affording the corresponding trialkylphosphine oxide.

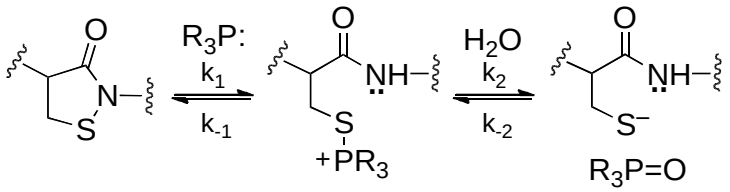

Scheme 2.5. Reactivation of oxidatively-inactivated PTP1B by phosphine-based reagents. Nucleophilic attack of the phosphine phosphorous on the sulfenyl amide sulfur and subsequent hydrolysis of the thiophosphonium intermediate affords reduced PTP and the corresponding phosphine oxide.

The simple second-order kinetics observed here suggest that the initial attack of phosphorus on the oxidized PTP1B sulfenyl sulfur is rate-limiting, and that the hydrolysis step leading to active enzyme is relatively fast (Scheme 2.5). Additionally, the phosphorus-oxygen bond is sufficiently strong to render k_{-2} in Scheme 4 negligible, and the reaction irreversible.[44-46] Under the conditions employed here (pH 7, 25 ˚C), the rate constant for reactivation of oxidized PTP1B by TCEP was 1.5 ± 0.5 M^{-1} s^{-1}. This value is appreciably larger than the rate constants observed for the thiol-containing agents examined here likely due, in large part, to the fact that a substantial fraction of TCEP exists in the unprotonated, reactive form at neutral pH. The pK_a of phosphorus-protonated TCEP (R_3PH^+) has been estimated at 7.66,[44] whereas the most acidic thiol examined in our study has a pK_a of 8.2 (cysteamine). Adjusting the observed rate constant for concentration of active nucleophile, in analogous fashion to that described above for the thiol/thiolate couples, we calculated a rate constant of 8.0 M^{-1} s^{-1} for attack of the TCEP neutral phosphorus nucleophile on oxidized PTP1B. It has been noted previously that, while TCEP reduces low molecular weight disulfides more rapidly than does DTT, the opposite is true in the case of some protein disulfides.[45] Here, this not the case. In fact, if initial attack of the phosphorus reagent on oxidized PTP1B is rate-

limiting, and the observed rate constant reports on k_1 in similar fashion to the dithiol agents, the "pK_a-corrected" rate constant is perhaps higher than one might expect for a thiol of $pK_a = 7.66$.

2.6 Thiol-Dependent Recovery of Activity from Oxidized SHP-2.

Finally, we examined thiol-dependent recovery of activity from oxidatively-inactivated SHP-2, a different member of the human PTP family. The cellular activity of SHP-2 is redox regulated in response to platelet-derived growth factor, endothelin-1, and T-cell receptor stimulation.[3,47] Our experiments employed the catalytic domain (aa 246-527) of the recombinant human enzyme and the oxidized enzyme was generated in a manner similar to that described above for PTP1B. Treatment of the oxidized enzyme with DTT (40 mM, 20 min, 25 ˚C) consistently returned approximately 95% of the original catalytic activity of the enzyme. The amount of activity recovered from oxidatively-inactivated SHP-2 is greater than that observed for PTP1B. This suggests that SHP-2 resists the generation of "overoxidized" oxoforms that cannot be returned to active enzyme upon treatment with low molecular weight thiols.

As expected, treatment of oxidized SHP-2 with a panel of thiol-containing molecules gave time-dependent recovery of the enzyme's catalytic activity and, as described above in the context of PTP1B, apparent second-order rate constants for the recovery were estimated from the continuous assay data (Figure 2.5).

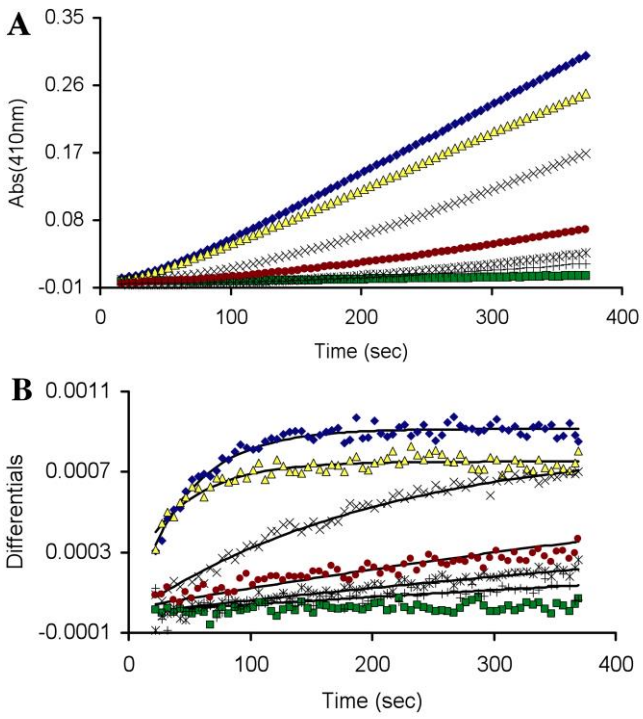

Figure 2.5. Thiol-mediated reactivation of oxidatively-inactivated SHP-2. **(A)** Oxidized SHP-2 (11 nM) was incubated with various thiols in Buffer A containing the chromogenic PTP substrate pNPP (20 mM) pNPP, pH 7 at room temperature. The time courses monitored the increase in absorbance at 410 nm resulting from the SHP-2-catalyzed release of p-nitrophenol from the substrate. Monothiols were 50 mM and dithiols 25 mM: DTT (♦), TGA-OMe (▲), TGA (X), 2-ME (●), GSH (*), NAC (+), no thiol (■). **(B)** Instantaneous rates of reactivation (slopes) versus time. Data were fit with pseudo-first order kinetic treatment to give the following estimates of the apparent bimolecular rate constants calculated in units of M^{-1} s^{-1}: DTT = 0.89, TGA-OMe = 0.44, TGA = 0.10, 2-ME = 0.02, GSH = 0.02, NAC = 0.01.

We then undertook a more detailed kinetic analysis that showed treatment of oxidized SHP-2 with DTT gave time- and concentration-dependent recovery of PTP activity consistent with a simple, second-order process with rate constant 0.8 ± 0.1 M^{-1} s^{-1} (Figure 2.6A and 5B). This value matches that measured previously for a slightly different construct (aa 268-525) of the enzyme's catalytic subunit.[21]

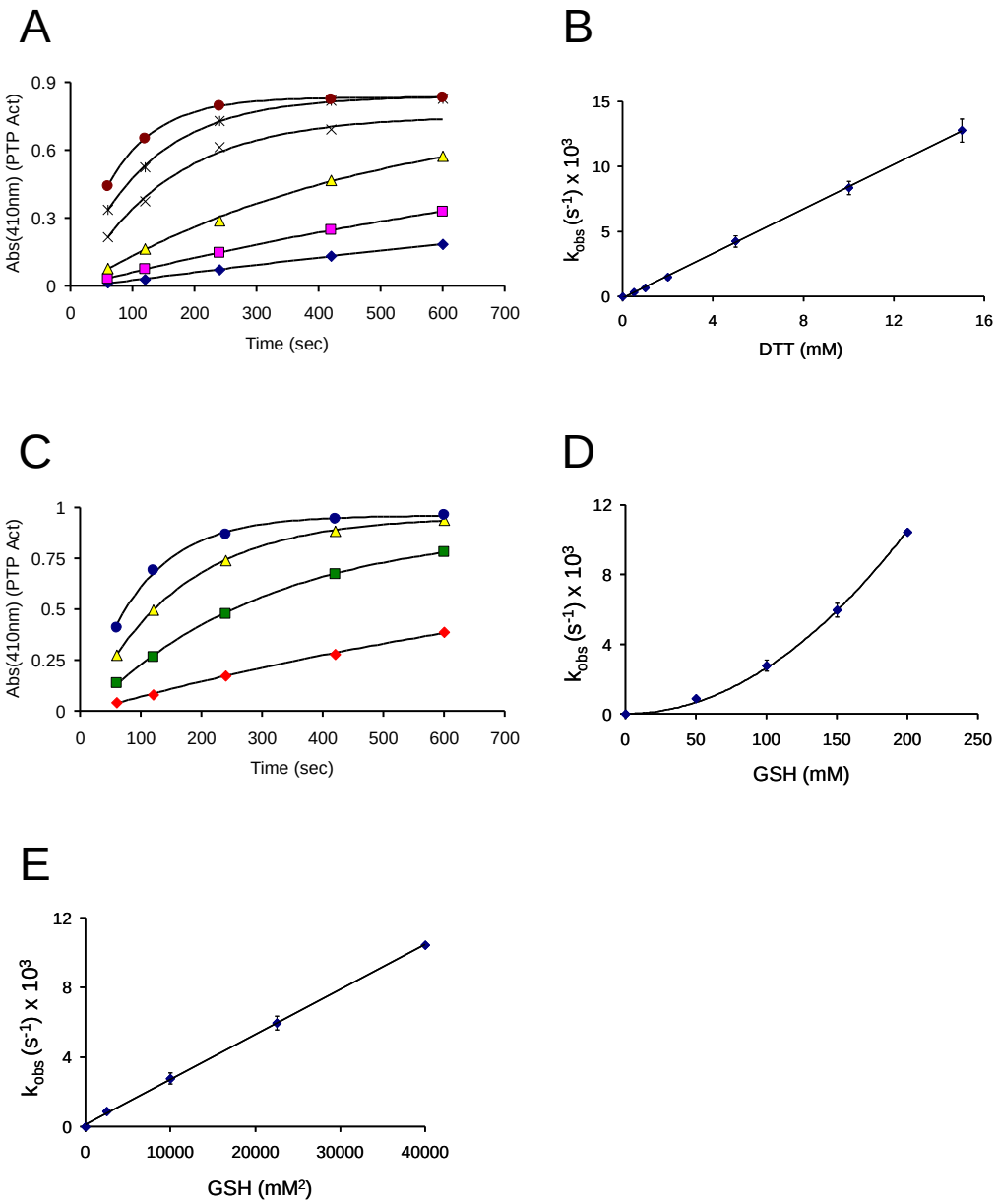

Figure 2.6. Reactivation of oxidatively-inactivated SHP-2 by DTT and GSH. Assays were conducted as described in the Experimental Section. **A**. DTT-mediated recovery of activity from oxidized PTP1B. **B**. Pseudo-first order rate constants (s^{-1} x 10^3) were plotted against DTT concentration (mM), affording a straight line of slope k_{obs} (M^{-1} s^{-1}) which passes through the origin. This data is consistent with a bimolecular process in the rate-determining step. **C**. GSH-mediated recovery of activity from oxidized SHP-2. **D**. Plotting the observed pseudo first-order rate constants versus concentration of GSH affords a curvilinear (parabolic) graphical form, indicating a non-second order kinetic process. **E**. Plotting of the observed pseudo first-order rate constants versus the square of the GSH concentration affords a linear form, which passes through the origin. This suggests a process second-order in thiol concentration in the rate-determining step, with the relevant rate constant being equal to 0.29 ± 0.02 M^{-2} s^{-1}.

The rate at which DTT regenerates SHP-2 activity, a value expected to reflect the initial attack of DTT thiolate on the oxidized enzyme (k_1 in Scheme 2.2) as discussed above, is approximately 2.5-fold faster than the analogous reaction on PTP1B. This result is particularly interesting in light of previous work suggesting that oxidation of the active site cysteine residue in SHP-2 initiates a disulfide relay that transmits the initial oxidation of the active site cysteine to a distal pair of cysteine residues (Scheme 2.6).[21]

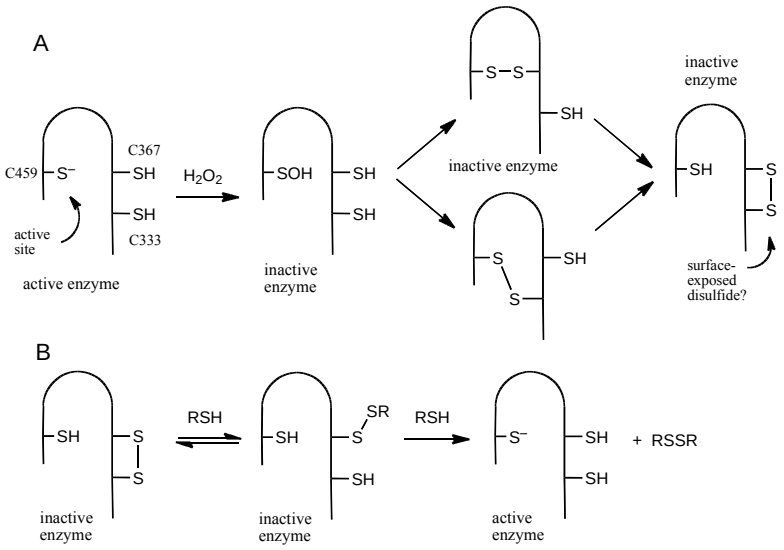

Scheme 2.6. Proposed disulfide relay initiated by oxidative inactivation of SHP-2 (Panel A) and proposed mechanism for thiol-dependent recovery of activity from oxidized SHP-2 (Panel B).

While no structural information is available regarding oxidized SHP-2, our result suggests that the proposed disulfide relay in SHP-2 generates a surface-exposed disulfide that is readily accessible to low molecular weight thiols. In contrast, oxidized PTP1B is thought to exist with the catalytic cysteine residue in the cyclic sulfenyl amide

form.[10,23,32]

Interestingly, from our survey of thiols using the continuous assay, it was clear that monothiols such as the biological thiol GSH were rather inept at regeneration of activity from oxidized SHP-2, when compared to their action on oxidized PTP1B (Figures 2.1 and 2.5). Intrigued, we examined the ability of various concentrations of GSH to regenerate SHP-2 activity. A plot of the resulting observed rate constants versus GSH concentration gave a rising curve that was *not* consistent with simple second-order kinetics. Indeed, a plot of the observed rate constants obtained under pseudo-first-order conditions versus the *square* of GSH concentration gave a straight line consistent with the rate law $k[RSH]^2$ and corresponding rate constant of $0.29 \pm 0.02\ M^{-2}\ s^{-1}$. Such a rate law could reasonably result from a mechanism involving reversible attack of thiol on a protein disulfide followed by irreversible, rate limiting generation of the active enzyme via attack of a second equivalent of thiol (Scheme 2.6B). We assume that the thiolated protein intermediate generated by the intial attack of thiol on the oxidized enzyme is catalytically inactive (Scheme 2.6B), although this assumption need not be true if the species exists at a low steady state concentration. This notion is broadly consistent with the original proposal suggesting that oxidized SHP-2 is inactive despite possessing a native (unoxidized) cysteine thiol group at its active site (Scheme 2.6A).[15,21] This scheme is kinetically analogous to the reduction of flavin by monothiols and dithiols reported previously.[38,48-50] Notably, the rate at which physiologically-relevant concentrations of GSH regenerate of active enzyme from oxidized SHP-2 was negligible compared to the analogous reaction with oxidized PTP1B. This behavior is not limited to GSH, as the monothiol 2-ME also displayed kinetics second-order in thiol, with the

overall third-order rate constant of 0.25 ± 0.05 M^{-2} s^{-1}.

2.7 Conclusions

All of the thiol-containing molecules examined in this study were able to regenerate active enzyme from oxidized PTP1B. Agents that contain lower pK_a thiol groups are superior in their ability to regenerate active enzyme, likely because these compounds present larger amounts of thiolate (RS^-) for reaction with the oxidized PTP. Along these lines, our studies suggest that the relatively low pK_a of cysteamine (8.3) renders this an effective monothiol reagent for maintaining PTP1B in the active form during biochemical assays. In fact, for this particular application, cysteamine may be superior to DTT from an economical perspective. Approximately two-fold higher concentrations of cysteamine are required to match the rate of DTT under our conditions, but cysteamine is less than one-eighth the cost of DTT on a mole-for-mole basis. Methylthioglycolate (TGA-OMe) also could be effective and economical for such applications but is practically undesirable due to its foul odor.

We found that that the biological thiol GSH regenerates catalytic activity from oxidized PTP1B with an apparent second-order rate constant of 0.023 ± 0.004 M^{-1} s^{-1}. To provide a general reference point for comparison, this value is approximately 20-times less than the rate at which GSH attacks oxidized GSSG (GSH/GSSG disulfide exchange, 0.41 M^{-1} s^{-1}, 25 ˚C, pH 7).[51] Based on the rate constant reported here, we can estimate that a physiologically-relevant concentration GSH (5 mM) will convert oxidized PTP1B to the active form with a half-life of 1.7 h ($t_{1/2}$ = ln 2/(0.023 M^{-1} s^{-1} x 0.005 M).

Furthermore, the results suggested that, in the case of monothiols, the initial attack on oxidized PTP1B (k_1[RSH]) was faster than the second step leading to recovery of the native enzyme (k_2[RSH]). This kinetic scenario allows for accumulation of the intermediate enzyme-thiol mixed disulfide (PTP1B-SSR) and may explain why the glutathionylated form of PTP1B has been detected in cell lysates following stimulation of alveolar macrophage respiratory burst.[24] Accordingly, enzymes such as the glutaredoxins or sulfiredoxin that repair glutathionylated proteins may be involved in the intracellular conversion of glutathionylated PTP1B to its catalytically active form.[25-27] The thioredoxin enzyme system repairs oxidized PTP1B more effectively than the low molecular weight thiols, with comparable rates for the reactivation of oxidized PTP1B obtained at 2 μM Trx, 4 mM DTT and 60 mM GSH. We observed a greater yield of recovered enzyme activity when oxidized PTP1B was treated with low molecular weight thiols than when treated with thioredoxin. This suggests that enzymatic reduction of oxidized PTP1B may occur in an oxoform-selective manner. For example, thioredoxin may rapidly regenerate PTP1B catalytic activity from the sulfenyl amide oxoform, while the higher oxidation states of PTP1B such as the sulfinyl and sulfonyl amide oxoforms are not processed by the enzyme. The rate of reactivation of PTP1B by Trx reported here is substantially faster than the published rate of Trx-dependent reactivation rate measured for a different PTP family member, SHP-2, under somewhat different conditions.[21] The observed pseudo-first-order rate constant measured here for the reactivation of oxidized PTP1B by 2 uM Trx, allows us to estimate an apparent second-order rate constant of 700 M^{-1} s^{-1} for this process.[14] This suggests that the thioredoxin-mediated recovery of oxidized PTP1B proceeds roughly 20-fold faster than the recovery of SHP-2.[21]

We observed profound kinetic differences between the thiol-dependent regeneration of activity from oxidized PTP1B and SHP-2. This may reflect structural differences between the oxidized enzymes. Along these lines, oxidation of the active site cysteine residue in SHP-2 was proposed to initiate a disulfide relay that transmits the initial oxidation of the active site cysteine to a distal pair of cysteine residues (Scheme 2.6),[21] while oxidized PTP1B is thought to exist with the catalytic cysteine residue in the cyclic sulfenyl amide form.[10,23,32] Regeneration of activity from oxidized SHP-2 by monothiols appears to be second-order in thiol concentration and, at physiological concentrations of GSH, recovery of SHP-2 is expected to be quite slow, relative to oxidized PTP1B. An earlier study that examined the regeneration of oxidized SHP-2 by excess glutathione did not note a non-linear dependence on glutathione concentration, although the data was not shown.[21] Using the rate constant measured in this work we estimate that, at a steady-state GSH concentration of 5 mM, the half-life for recovery of oxidized SHP-2 would be approximately 27 h (compared to 1.7 h for oxidized PTP1B). The observed kinetics lead us to speculate that the recovery of SHP-2 activity by GSH proceeds via an unfavorable equilibrium addition of the thiol to an enzyme disulfide, followed by irreversible, rate-limiting generation of the active enzyme via attack of a second equivalent of thiol. This kinetic scenario suggests that glutathionylated SHP-2 will not accumulate in cells. Consistent with this analysis, glutathionylated SHP-2 *was not* observed in cell lysates under conditions where glutathionylated PTP1B *was* detected.[24] From a practical point of view, our results suggest that monothiols will be remarkably poor reagents for protecting SHP-2 against oxidative inactivation, when compared with their activity in the context of PTP1B. On the other hand, the ability of

DTT to maintain SHP-2 in its catalytically active form is superior to its activity against oxidized PTP1B. The results presented here, alongside previous work,[21] indicate that for both PTP1B and SHP-2, the rates at which the oxidized enzyme is recovered follows the trend Trx > DTT > GSH.

There is increasing recognition that cellular activity of various PTP enzymes is redox regulated as part of both normal and pathogenic processes.[3,7,52] The catalytic subunits of the classical PTPs are highly homologous, yet subtle differences among the various family members lead to significant differences in the structures of the oxidized enzymes, with the catalytic cysteine residue existing as either a sulfenic acid, a disulfide, or a sulfenyl amide (Scheme 2.1).[15] Using low molecular weight thiols as probes, we observed here very different kinetic behavior in the regeneration of catalytic activity of two different oxidized PTPs. This highlights the potential for structural differences in oxidized PTPs to play a significant role the rates at which low molecular weight thiols and enzymes such as thioredoxin and glutaredoxin return catalytic activity to these enzymes during cell signaling events.

2.8 Methods and Materials

Materials. All thiols used in this study were from Sigma-Aldrich, and were of no less than *purum* reagent grade. Buffer components Tris, Bis-Tris, sodium acetate, and diethylenetriaminepentaacetic acid (DTPA) were also from Sigma. Sodium chloride was from Fisher Scientific, and the non-ionic detergent Surfact-Amps® 80 (Tween 80) was from Thermo Scientific. Catalase from *Corynebacterium glutamicum* (844,000 U/mL)

and 30% (wt/wt) aqueous hydrogen peroxide were from Sigma. The chromogenic substrate 4-nitrophenyl phosphate disodium salt hexahydrate (pNPP), and sodium hydroxide were also from Sigma. Recombinant thioredoxin from *E. coli* (product T0910), thioredoxin reductase (product T7915), and NADPH-tetra(cyclohexylammonium) salt (product N5130) were from Sigma-Aldrich and were used as received. Absorption spectra were recorded on an Agilent 8453 Hewlett-Packard G1103A spectrophotometer. Zeba mini buffer exchange/desalting columns used in the preparation of thiol-free PTP1B or SHP-2 were from Pierce (catalog no. 89882), and were used according to the manufacturer's protocol. The catalytic domains of PTP1B and SHP-2 were expressed and purified as previously described.[10] The previously characterized active site-directed PTP1B inhibitor **1** was a gift from Dr. Ernest Asante-Appiah (Merck). The previously characterized active-site directed PTP1B inhibitor **2** was prepared as described previously.[28]

Oxidative Inactivation of Native PTP1B and SHP-2. Prior to use in kinetics assays, both PTPs were removed from stock storage solutions and exchanged into Buffer A (Tris (50 mM), Bis-Tris (50 mM), DTPA (10 mM), and sodium acetate (100 mM), pH 7.0) containing 0.5% (v/v) Tween 80. Subsequently, the PTPs were diluted in the same buffer and completely inactivated by treatment with hydrogen peroxide (1 mM) for 5 min at 25 ˚C. Following the inactivation incubation period, catalase (100-300 units, final) was added to quench excess H_2O_2. The reaction tube was then allowed to stand open to air for 2 min to ensure complete evolution of O_2 gas, and the oxidized PTPs stored on ice until used. Generally 0.7 μM oxidized PTP1B and 0.35 μM oxidized SHP-2 were the final concentrations for discontinuous assays. The aqueous solubility of PTP1B is greatly

decreased upon oxidation, and protein precipitation was observed at concentrations of oxidized PTP1B as low as 4 μM.

Determination of Approximate Rate Constants Via Continuous Spectrophotometric assay. Stock solutions of 25.5 mM pNPP, 250 mM monothiol, and 125 mM dithiol were prepared in Buffer A. For thiols bearing acidic functionalities (thioglycolic acid (TGA), GSH, and *N*-acetyl-L-cysteine (NAC)), one mole equivalent of acid was neutralized via addition of the appropriate amount of 10 M NaOH in ddH_2O to prevent acidification of the assay buffer, and the pH checked against buffer alone using a four-color pH test strip. In a manner similar to that described above, oxidized PTP1B (1.5 μM) and oxidized SHP-2 (0.75 μM) were prepared. To a 1 mL quartz cuvette were added 628 μL of 25.5 mM pNPP and 160 μL of 250 mM monothiol, or 125 mM dithiol. Following zeroing of the spectrophotometer against this solution, 12 μL of oxidized PTP1B or SHP-2 were added, the mixture immediately mixed by gentle vortexing, and the release of 4-nitrophenol followed at 410 nm (5 sec cycle times). Because the concentration of substrate in the assay (20 mM) was saturating (as determined in a separate experiment) and effectively constant, we may express the approximation:

$$[E_{act}] = [E \bullet S],$$

where $[E_{act}]$ is the concentration of native (active) PTP, and [E•S] is the concentration of the PTP-substrate complex. Under conditions of saturating substrate, we may write:

$$[P]_t = (k_{cat}\,[E \bullet S]) * (t),$$

where [P] is the concentration of product 4-nitrophenol and k_{cat} has its usual meaning in the context of Michaelis-Menten kinetics. Thus, if k_{cat} and $[E_{act}]$ are constant during the experiment, [E•S] would also be constant, and the term *dP/dt* would be constant and

described by a line with the slope, k_{cat}[E•S] (this being the basis for determination of "traditional" kinetic constants K_m and V_{max}). Here, however, since the concentration of active PTP changed (increased) with time during thiol-mediated reactivation, rising curves are observed in the plot of [P] versus time. Under the pseudo first-order conditions employed, and for a given k_{cat}, these rising curves can be described by the expression:

$$\frac{dP}{dt} = \frac{d[E \bullet S]}{dt} = \frac{d[E_{act}]}{dt} = \frac{D_t - D_\infty}{D_o - D_\infty} = e^{-k_\psi * t},$$

where k_ψ is the pseudo first-order rate constant of reactivation in the presence of excess thiol, and D_o, D_t, and D_∞ are the instantaneous rates of change in [P] versus time initially, at time t during the reactivation process, and at the completion of the reaction. Thus, computing instantaneous rates of change in Abs_{410} (differentials, D) at time t and replotting D_t versus the median of the time interval considered affords kinetic data that describes the thiol-mediated recovery of PTP activity versus time under pseudo-first-order conditions. It is worth noting that this method for extracting kinetic data from a continuous spectrophotometric assay is reminiscent of that described by Hart and O'Brien for inactivation of acetylcholinesterase by paraoxon in the presence of 4-nitrophenyl acetate.[29]

Determination of Rate Constants of Reactivation of Oxidatively-Inactivated PTPs Via Discontinuous Assay Methods. Stocks of oxidatively-inactivated PTPs were prepared as described (0.7 μM PTP1B and 0.35 μM SHP-2, *vide supra).* In the same buffer were prepared 2x-concentrated stocks of thiol. Prior to initiation of the reactivation reaction, the stocks were incubated separately at 25 ˚C for 5 min to allow thermal equilibration. Immediately upon 1:1 (v/v) mixture of the two stocks, a timer was

started, and at 1, 2, 4, 7, and 10 min intervals, 10 μL aliquots were removed from the reaction mixture and placed in 2 mL microcentrifuge tubes containing 490 μL of 20 mM pNPP in activity assay buffer (50 mM Bis-Tris, 10 mM DTPA, 150 mM NaCl, pH 6, 30 ˚C). The activity assays were allowed to proceed for 10 min at 30 ˚C prior to quenching with 500 μL of 2 M NaOH.[14] The absorbance at 410 nm was recorded and the data analyzed as described below.

To account for any potential residual activity in the oxidized PTP stocks, the appropriate concentration of oxidized PTP was added to the blank series, subjected to identical conditions in the activity assay, and the instrument zeroed against this sample. For thiols of limited solubility and/or sluggish reaction times, DTT or 2-mercaptoethanol (2-ME) were used to determine the endpoint of the reaction. In a separate experiment, it was found that these thiol agents all recovered similar amounts of enzyme activity for PTP1B.

Data from these assays were analyzed in Microsoft Excel by fitting to the general form for a first-order reaction:

$$\frac{[A]_t - [A]_\infty}{[A]_o - [A]_\infty} = e^{-k_\psi * t},$$

where k_ψ is the pseudo-first-order rate constant and $[A]_o$, $[A]_t$, and $[A]_\infty$ are the absorbances at 410 nm initially, at time *t*, and at the end of the reactivation process, respectively. From this data, apparent bimolecular rate constants and rate constants for thiolate attack on oxidized PTP1B were calculated according to the method of Szajewski and Whitesides.[30]

Similar methodologies to those described above were utilized in determination of the rate of recovery of catalytic activity of oxidized PTP1B by the trialkylphosphine

reagent TCEP. Because the material was received as the hydrochloride salt and additionally bears three acidic carboxylic acid groups, 3.5 equiv of base were added to the stock solution via addition of the appropriate volume of NaOH (10 M) to prevent acidification of the assay buffer. The resulting mixture was confirmed to have the same pH as buffer alone by four-color pH strip. The amount of total recoverable activity by treatment of oxidized PTP1B with TCEP (20 mM) or DTT (40 mM) for 30 min (pH 7, 25 ˚C) was found to be effectively the same (within ~7% of one another).

Reactivation of oxidatively-inactivated PTP1B by the thioredoxin-thioredoxin reductase system. A concentrated (40 μM) stock solution of thioredoxin (a lyophilized powder) was prepared via dissolution in Buffer A lacking Tween, and was stored at -20^{0}C until used. Solutions of thioredoxin reductase (a 16 μM suspension in ammonium sulfate) were prepared fresh via dilution from the stock into Buffer A. Solutions of NADPH in Buffer A were prepared fresh and stored on ice until used. Solutions of the reducing system (thioredoxin/thioredoxin reductase/NADPH) were prepared fresh from stock solutions and used immediately. In general, the ratio of thioredoxin:thioredoxin reductase was held at 20:1, and it was found that these conditions were more than adequate to ensure that reduction of thioredoxin by thioredoxin reductase in the presence of excess NADPH (100 – 200 μM) was not rate-limiting. For kinetics runs with oxidized PTP1B, the thioredoxin system was prepared (thioredoxin/thioredoxin reductase/NADPH : 4 μM/200 nM/200 μM) and allowed to equilibrate at 25 ˚C several minutes prior to the start of the assay. Recovery of PTP1B activity was measured as described above.

References

(1) Hunter, T. and Sefton, B. M. (1980) Transforming gene product of Rous sarcoma virus phosphorylates tyrosine. *Proc. Nat. Acad. Sci. USA 77*, 1311-1315.

(2) Hunter, T. (2000) Signaling - 2000 and beyond. *Cell 100*, 113-127.

(3) Tonks, N. K. (2006) Protein tyrosine phosphatases: from genes, to function, to disease. *Nature Rev. Cell. Biol. 7*, 833-846.

(4) Lemmon, M. A. and Schlessinger, J. (2010) Cell signaling by receptor tyrosine kinases. *Cell 141*, 1117-1134.

(5) Tonks, N. K., Diltz, C. D. and Fischer, E. H. (1988) Purification of the major protein-tyrosine phosphatases of human placenta. *J. Biol. Chem. 263*, 6722-6730.

(6) Tarrant, M. K. and Cole, P. A. (2009) The chemical biology of protein phosphorylation. *Ann. Rev. Biochem. 78*, 797-825.

(7) Östman, A., Frijhoff, J., Sandin, A. and Böhmer, F.-D. (2011) Regulation of protein tyrosine phosphatases by reversible oxidation. *Biochem. J. 150*, 345-356.

(8) Jiang, F., Zhang, Y. and Dusting, G. J. (2011) NADPH Oxidase-Mediated Redox Signaling: Roles in Cellular Stress Response, Stress Tolerance, and Tissue Repair. *Pharmacol. Rev. 63*, 218-242.

(9) Mahedev, K., Motoshima, H., Wu, X., Ruddy, J. M., Arnold, R. S., Cheng, G., Lambeth, J. D. and Goldstein, B. J. (2004) The NAD(P)H oxidase homolog Nox4 modulates insulin-stimulated generation of H_2O_2 and plays an integral role in insulin signal transduction. *Mol. Cell Biol. 24*, 1844-1854.

(10) Zhou, H., Singh, H., Parsons, Z. D., Lewis, S. M., Bhattacharya, S., Seiner, D. R., LaButti, J. N., Reilly, T. J., Tanner, J. J. and Gates, K. S. (2011) The biological buffer, bicarbonate/CO2, potentiates H2O2-mediated inactivation of protein tyrosine phosphatases. *J. Am. Chem. Soc. 132*, 15803–15805.

(11) LaButti, J. N., Chowdhury, G., Reilly, T. J. and Gates, K. S. (2007) Redox regulation of protein tyrosine phosphatase 1B by peroxymonophosphate. *J. Am. Chem. Soc. 129*, 5320-5321.

(12) Denu, J. M. and Tanner, K. G. (1998) Specific and reversible inactivation of protein tyrosine phosphatases by hydrogen peroxide: evidence for a sulfenic acid intermediate and implications for redox regulation. *Biochemistry 37*, 5633-5642.

(13) Meng, T.-C., Buckley, D. A., Galic, S., Tiganis, T. and Tonks, N. K. (2004) Regulation of insulin signaling through reversible oxidation of the protein tyrosine phosphatases TC45 and PTP1B. *J. Biol. Chem. 279*, 37716-37725.

(14) Parsons, Z. D. and Gates, K. S. (2013) Redox Regulation of Protein Tyrosine Phosphatases: Methods for Kinetic Analysis of Covalent Enzyme Inactivation. *Methods Enzymol. 528(C)*, 129-154.

(15) Tanner, J. J., Parsons, Z. D., Cummings, A. H., Zhou, H. and Gates, K. S. (2011) Redox Regulation of Protein Tyrosine Phosphatases: Structural and Chemical Aspects. *Antioxid. Redox Signal. 15*, 77-97.

(16) LaButti, J. N. and Gates, K. S. (2009) Biologically relevant properties of peroxymonophosphate (=O3POOH). *Bioorg. Med. Chem. Lett. 19*, 218-221.

(17) Hecht, D. and Zick, Y. (1992) Selective inhibition of protein tyrosine phosphatase activities by H2O2 and vanadate in vitro. *Biochem. Biophys. Res. Commun. 188*, 773-779.

(18) Lee, S. R., Kwon, K. S., Kim, S. R. and Rhee, S. G. (1998) Reversible inactivation of protein-tyrosine phosphatase 1B in A431 cells stimulated with epidermal growth factor. *J. Biol. Chem. 273*, 15366-15372.

(19) Weibrecht, I., Boehmer, S.-A., Dagnell, M., Kappert, K., Oestman, A. and Boehmer, F.-D. (2007) Oxidatiion sensitivity of the catalytic cysteine of the protein tyrosine phosphatases SHP-1 and SHP-2. *Free Rad. Biol. Med. 43*, 100-110.

(20) Woo, H. A., Yim, S. H., Shin, D. H., Kang, D., Yu, D.-Y. and Rhee, S. G. (2010) Inactivation of peroxiredoxin I by phosphorylation allows localized hydrogen peroxide accumulation for cell signaling *Cell 140*, 517-528.

(21) Chen, C.-Y., Willard, D. and Rudolph, J. (2009) Redox regulation of SH2-domain-containing protein tyrosine phosphatases by two backdoor cysteines. *Biochemistry 48*, 1399-1409.

(22) Sivaramakrishnan, S., Cummings, A. H. and Gates, K. S. (2010) Protection of a single-cysteine redox switch from oxidative destruction: on the functional role of sulfenyl amide formation in the redox-regulated enzyme PTP1B. *Bioorg. Med. Chem. Lett. 20*, 444-447.

(23) Sivaramakrishnan, S., Keerthi, K. and Gates, K. S. (2005) A chemical model for the redox regulation of protein tyrosine phosphatase 1B (PTP1B). *J. Am. Chem. Soc. 127*, 10830-10831.

(24) Rinna, A., Torres, M. and Forman, H. J. (2006) Stimulation of the alveolar macrophage respiratory burst by ADP causes selective glutathionylation of protein tyrosine phosphatase 1B *Free Rad. Biol. Med. 41*, 86-91.

(25) Vlamis-Gardikas, A. and Holmgren, A. (2002) Thioredoxin and glutaredoxin isoforms. *Methods Enzymol. 347*, 286-296.

(26) Findlay, V. J., Townsend, D. M., Morris, T. E., Fraser, J. P., He, L. and Tew, K. D. (2006) A novel role for human sulfiredoxin in the reversal of glutathionylation. *Cancer Res. 66*, 6800-6806.

(27) Barrett, W. C., DeGnore, J. P., König, S., Fales, H. M., Keng, Y.-F., Zhang, Z.-Y., Yim, M. B. and Chock, P. B. (1999) Regulation of PTP1B via glutathionylation of the active site cysteine 215. *Biochemistry 38*, 6699-6705.

(28) Andersen, H. S., Olsen, O. H., Iversen, L. F., Sørensen, A. L. P., Mortensen, S. B., Christensen, M. S., Branner, S., Hansen, T. K., Lau, J. F., Jeppesen, L., Moran, E. J., Su, J., Bakir, F., Judge, L., Shahbaz, M., Collins, T., Vo, T., Newman, M. J., Ripka, W. C. and Møller, N. P. H. (2002) Discovery and SAR of a novel selective and orally bioavailable nonpeptide classical competitive inhibitor class of protein tyrosine phosphatase 1B. *J. Med. Chem. 45*, 4443-4459.

(29) Hart, G. J. and O'Brien, R. D. (1973) Recording spectrophotometric method for determination of dissociation and phosphorylation constants for the inhibition of acetylcholinesterase by organophosphates in the presence of substrate. *Biochemistry 12*, 2940-2945.

(30) Szajewski, R. P. and Whitesides, G. M. (1980) Rate constants and equilibrium constants for thiol-disulfide interchange reactions involving oxidized glutathione. *J. Am. Chem. Soc. 102*, 2011-2026.

(31) van Montfort, R. L. M., Congreeve, M., Tisi, D., Carr, R. and Jhoti, H. (2003) Oxidation state of the active-site cysteine in protein tyrosine phosphatase 1B. *Nature 423*, 773-777.

(32) Salmeen, A., Anderson, J. N., Myers, M. P., Meng, T.-C., Hinks, J. A., Tonks, N. K. and Barford, D. (2003) Redox regulation of protein tyrosine phosphatase 1B involves a sulphenyl-amide intermediate. *Nature 423*, 769-773.

(33) Fava, A., Iliceto, A. and Camera, E. (1957) Kinetics of the Thiol-Disulfide Exchange. *J. Am. Chem. Soc. 79*, 833-838.

(34) Senatore, L., Ciuffari, E., Fava, A. and Levita, G. (1973) Nucleophilic substitution at sulfur. Effect of nucleophile and leaving group basicity as probe of bond formation and breaking. *J. Am. Chem. Soc. 95*, 2918-2922.

(35) Bracher, P. J., Snyder, P. W., Bohall, B. R. and Whitesides, G. M. (2011) The relative rates of thiol-thioester exchange and hydrolysis for alkyl and aryl thioalkanoates in water. *Orig. Life Evol. Biosph. 41*, 399-412.

(36) Harris, D. C. (2010) *Quantitative Chemical Analysis*, 8th ed., W. H. Freeman and Co., New York.

(37) Whitesides, G. M., Lilburn, J. E. and Szajewski, R. P. (1977) Rates of thiol-disulfide interchange reactions between mono- and dithiols and Ellman's reagent. *J. Org. Chem. 42*, 332-338.

(38) Loechler, E. L. and Hollocher, T. C. (1980) Reduction of flavins by thiols. 3. The case for concerted N,S-acetal formation in attack and an early transition state in breakdown. *J. Am. Chem. Soc. 102*, 7328-7334.

(39) Zhang, Y.-Z. and Zhang, Z.-Y. (1998) Low-affinity binding determined by titration calorimetry using a high-affinity coupling ligand: a thermodynamic study of ligand binding to protein tyrosine phosphatase 1B. *Anal. Biochem. 261*, 139-148.

(40) Sarmiento, M., Zhao, Y., Gordon, S. J. and Zhang, Z.-Y. (1998) Molecular basis for substrate specificity of protein-tyrosine phosphatase 1B. *J. Biol. Chem. 273*, 26368-26374.

(41) Montalibet, J., Skorey, K., McKay, D., Scapin, G., Asante-Appiah, E. and Kennedy, B. P. (2006) Residues Distant from the Active Site Influence Protein-tyrosine Phosphatase 1B Inhibitor Binding. *J. Biol. Chem. 281*.

(42) Pregel, M. J. and Storer, A. C. (1997) Active site titration of tyrosine phosphatases SHP-1 and PTP1B using aromatic disulfides. *J. Biol. Chem. 272*, 23552-23558.

(43) Gong, J.-X., Shen, X., Yao, L.-G., Jiang, H., Krohn, K. and Guo, Y.-W. (2007) Total synthesis of gymnorrhizol, an unprecedented 15-membered macrocyclic polydisulfide from the Chinese Mangrove Bruguiera gymnorrhiza. *Org. Lett. 9*, 1715-1716.

(44) Burns, J. A., Butler, J. C., Moran, J. and Whitesides, G. M. (1991) Selective reduction of disulfides by tris(2-carboxyethyl)phosphine. *J. Org. Chem. 56*, 2648-2650.

(45) Cline, D. J., Redding, S. E., Brohawn, S. G., Psathas, J. N., Schneider, J. P. and Thorpe, C. (2004) New water-soluble phosphines as reductants of peptide and protein disulfide bonds: reactivity and membrane permeability. *Biochemistry 43*, 15195-15203.

(46) Getz, E. B., Xiao, M., Chakrabarty, T., Cooke, R. and Selvin, P. R. (1999) A comparison between the sulfhydryl reductants tris(2-carboxyethyl)phosphine and dithiothreitol for use in protein biochemistry. *Anal. Biochem. 273*, 73-80.

(47) Michalek, R. D., Nelson, K. J., Holbrook, B. C., Yi, J. S., Stridiron, D., Daniel, L. W., Fetrow, J. S., King, S. B., Poole, L. B. and Grayson, J. M. (2007) The requirement of reversible cysteine sulfenic acid formation for T-cell activation and function. *J. Immunol. 179*, 6456 -6467

(48) Loechler, E. L. and Hollocher, T. C. (1980) Reduction of flavins by thiols. 1. Reaction mechanism from the kinetics of the attack and breakdown steps. *J. Am. Chem. Soc. 102*, 7312-7321.

(49) Yokoe, I. and Bruice, T. A. (1975) Oxidation of thiophenol and nitroalkanes by an electron deficient isoalloxazine. *J. Am. Chem. Soc. 97*, 450-451.

(50) Holden, J. W. and Main, L. (1977) The kinetics and mechanism of the oxidation of mercaptoethanol by riboflavin. *J. Aust. Chem. 30*, 1387-1391.

(51) Rabenstein, D. L. and Weaver, K. H. (1996) Kinetics and equilibria of the thiol/disulfide exchange reactions of somatostatin with glutathione. *J. Org. Chem. 61*, 7391-7397.

(52) Samet, J. M. and Tal, T. L. (2010) Toxicological disruption of signaling homeostasis: tyrosine phosphatases as targets. *Annu. Rev. Pharmacol. Toxicol. 50*, 215-235.

Chapter 3: Covalent Capture of a Dipeptide Model Isothiazolidin-3-one (Sulfenyl Amide) by 1,3-diketo-based Carbon Nucleophiles

3.1 Introduction

Protein tyrosine phosphatases (PTPs) and protein tyrosine kinases (PTKs) function in tandem to regulate signal transduction pathways within the cell.[1234] PTPs catalyze the hydrolytic removal of phosphoryl groups from phosphotyrosine residues on target proteins, while PTKs catalyze the transfer of a phosphoryl group from ATP to tyrosine residues.[5] The human genome encodes approximately 90 distinct PTKs and 107 PTPs.[4] Aberrant PTK or PTP activity can lead to a large number of unique disease states, and members of both enzyme families are important therapeutic targets.[67]

PTP1B is a negative regulator of the insulin signaling cascade, a role which has drawn tremendous attention to this enzyme as a potential therapeutic target for the treatment of type II diabetes.[8] When active, PTP1B terminates insulin signaling by catalyzing dephosphorylation of the intracellular domain of the insulin receptor and insulin receptor substrates.[9] A crucial cysteine thiolate nucleophile (Cys215) is required for catalysis,[10] and oxidation of this cysteine thiolate by biological or exogenous oxidants converts the enzyme to a catalytically-inactive form ($PTP1B_{ox}$).[111213141516] For example, during normal insulin signaling processes, PTP1B is transiently inactivated by a burst of hydrogen peroxide (H_2O_2) produced by the NAD(P)H-dependent oxidase Nox4 – itself activated during the insulin signaling process.[17] Oxidation of the catalytic cysteine in

PTP1B by H_2O_2 or the H_2O_2-bicarbonate system *in vitro* converts the active site cysteine residue to an unusual 5-membered sulfenyl amide moiety (formally known as a 1,2-thiazolidin-3-one, or isothiazolidin-3-one).[181911] The reaction proceeds by initial oxidation of the active site cysteine thiolate to the corresponding sulfenic acid, followed by a dehydrative cyclization involving the adjacent amide nitrogen (Scheme 3.1, top pathway).[20]

Reactions of biological thiols with $PTP1B_{ox}$ can restore catalytic activity of the enzyme.[21221223] Both low molecular weight thiols such as glutathione[24] (GSH) and enzyme systems such as thioredoxin can regenerate catalytic activity from $PTP1B_{ox}$.[2123] This reduction proceeds in stepwise fashion, wherein attack by the first equivalent of thiol on the electrophilic sulfur atom of the sulfenyl amide generates a ring-opened, protein-thiol mixed disulfide. The mixed disulfide is then readily cleaved by attack of a second equivalent of thiol, affording fully reduced, catalytically-active PTP1B and glutathione disulfide (GSSG).[21] Redox regulation of PTP1B may help control the duration and intensity of the cellular responses to insulin.

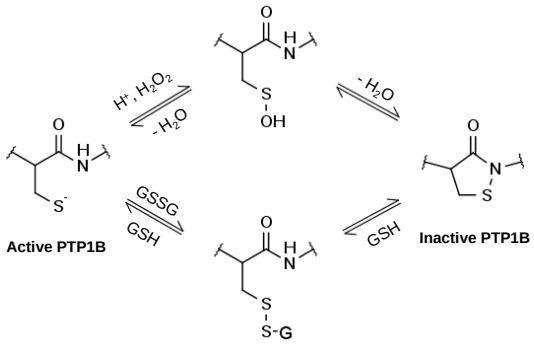

Scheme 3.1. Redox regulation of PTP1B: oxidative inactivation by hydrogen peroxide (H_2O_2) is reversible by thiol agents such as glutathione (GSH).

$PTP1B_{ox}$ may represent a therapeutic target that is structurally distinct from the catalytically-active form of the enzyme.[18] This is a significant observation because native PTP1B has proven refractory to intense drug development efforts, leaving some to categorize this enzyme as an "undruggable target".[25] Broadly speaking, most of the traditional small molecule inhibitors developed against PTP1B have either lacked selectivity for the target enzyme over other structurally homologous PTP family members or are large, polar molecules with poor bioavailability.[8] However, capture of $PTP1B_{ox}$ may have the same effect as inhibition of native PTP1B. Indeed, Tonks and coworkers recently showed that an intracellular antibody that binds to $PTP1B_{ox}$ and blocks thiol-mediated recovery of its catalytic activity resulted in enhanced phosphorylation of the insulin receptor following insulin stimulation.[26] Agents that target $PTP1B_{ox}$ may enjoy built-in selectivity, arising from the fact that only a small subset of cellular PTPs are oxidized in response to insulin stimulation.[27] Further selectivity may result from structural differences between various oxidized PTPs.[28]

We anticipated that the $PTP1B_{ox}$ sulfenyl amide might be a chemically-unique electrophilic sulfur target that can be covalently captured by reaction with small molecule nucleophiles (Scheme 3.2). More specifically, we sought nucleophiles that would react with the sulfenyl amide sulfur, but would *not* react with the electrophilic sulfurs present in various cellular disulfides. Additionally, the bond formed by reaction of the nucleophile with the sulfenyl amide sulfur in $PTP1B_{ox}$ must be stable in the presence of thiol in order to "survive" in a cell. This presents a particular challenge because the S-nucleophile bond generated by reaction of common nitrogen, sulfur, oxygen, or

phosphorus nucleophiles with the sulfenyl amide typically are thiol-labile (or hydrolytically-labile, in the case of P).[29303132]

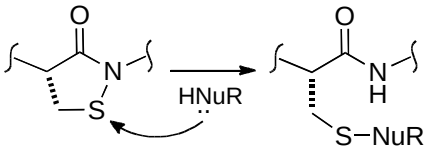

Scheme 3.2. Nucleophilic attack on a sulfenyl amide.

These issues led us to consider carbon-based nucleophiles derived from 1,3-diketones. In general, carbon-sulfur bonds are expected to be stable under physiological conditions. It was reported decades ago that the 1,3-diketone dimedone (5,5-dimethyl-1,3-cyclohexanedione) reacts with the electrophilic sulfur atom in protein sulfenic acid residues.[3334] More recently, dimedone-based probes have been developed for the detection of oxidized cysteine residues in various proteins, including PTP1B.[35] One example of an acyclic 1,3-diketone probe for protein sulfenic acids has been reported.[333635] To our knowledge, there is no evidence that dimedone or other 1,3-diketones react with dialkyl disulfide groups under physiologically-relevant conditions. Thus, we set out to explore the ability of 1,3-diketones to react with the sulfenyl amide residue in $PTP1B_{ox}$. In these initial studies, we wished to examine fundamental reaction processes under well-defined conditions. Accordingly, we employed a dipeptide model **2** containing a sulfenyl amide moiety that was first prepared by Morin and coworkers.[37] We characterized the products resulting from reactions between the dipeptide sulfenyl amide and a group of structurally-diverse 1,3-diketones. Reaction products appear to form via

nucleophilic attack of carbon on the electrophilic sulfenyl sulfur atom. We observed three different types of products, depending upon the structure of the 1,3-diketone reactant. We then provided evidence that the three product types are stable in the presence of thiol. Additionally, kinetic measurements for a subset of the 1,3-diketones allowed us to define structure-activity relationships controlling the reactivity of carbon acids toward the sulfenyl amide residue.

Results

3.2 Synthesis and Characterization of the Dipeptide Sulfenyl Amide (3).

We prepared the dipeptide sulfenyl amide **3** by the general route of Morin and coworkers involving coupling of *N*-Boc-protected cystine **1** with valine methyl ester, followed by treatment of the disulfide-bridged dipeptide **2** with Br_2 in dichloromethane containing pyridine (Scheme 3.3). The sulfenyl amide (72%) was separated from other oxidation products including the sulfinyl and sulfonyl amides **4** and **5** (17% and 6% yields, respectively) by column chromatography and was characterized by ^{1}H-NMR, ^{13}C-NMR, high resolution mass spectrometry, and single-crystal X-ray crystallography.

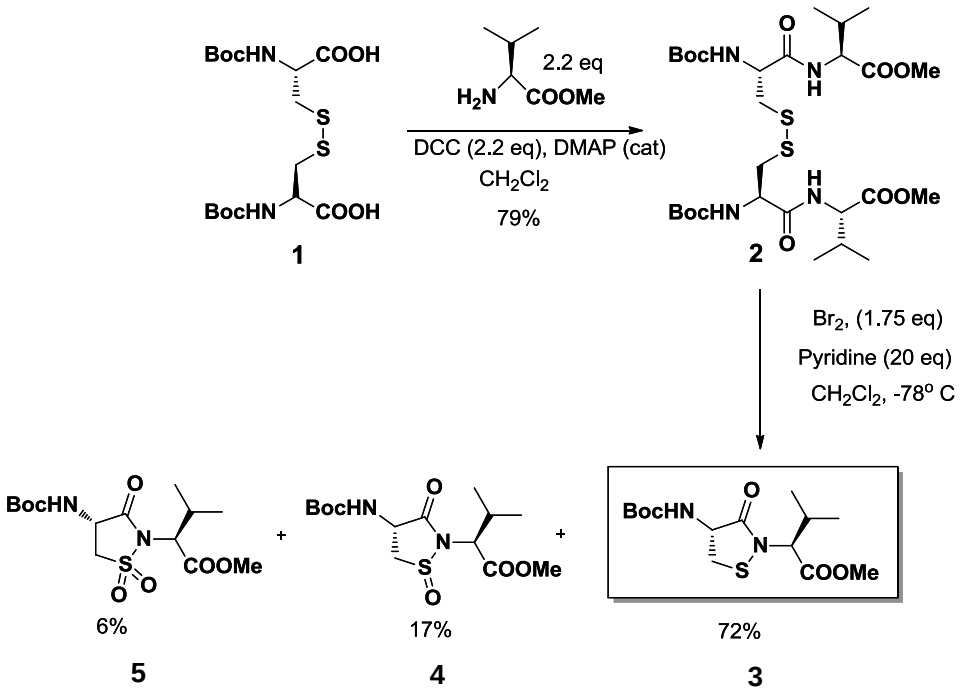

Scheme 3.3. Synthesis of the model dipeptide sulfenyl amide

3.3 Excess thiol regenerates the native cysteine residue.

To confirm that the model compound **3** recapitulates important redox transformations of $PTP1B_{ox}$ under our reaction conditions, we treated the dipeptide sulfenyl amide with excess (5 equiv.) of *D,L*-cysteine in a solvent system composed of a 2:1 mixture of methanol and HEPES buffer (50 mM, pH 7), NaCl (100 mM), and EDTA (1 mM). Importantly, work conducted previously by our group showed that cysteine is an effective reagent for reduction of the $PTP1B_{ox}$ sulfenyl amide to native PTP1B cysteine thiol.[21] Here, we found that reaction of the dipeptide model sulfenyl amide with 5 equiv

of cysteine rapidly (within ~1 min) afforded free dipeptide thiol residue, isolated in 85 % yield (Scheme 3.4).

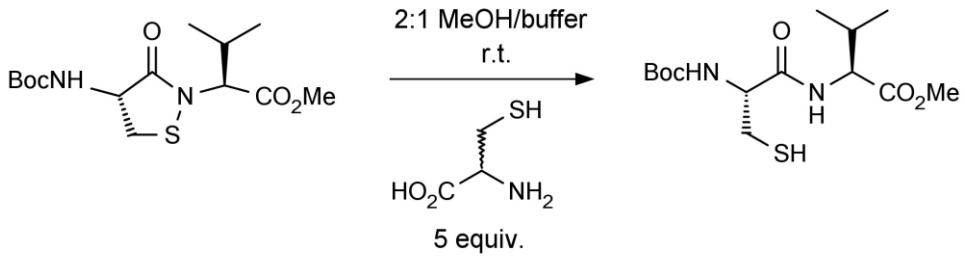

Scheme 3.4. Excess thiol reduces **3** to the corresponding free thiol.

3.4 Reactions of Aliphatic 1,3-Diketones With 3.

Treatment of **3** with a panel of structurally-diverse cyclic and acyclic 1,3-diketo carbon acids in the 2:1 methanol/buffer mixture described above afforded the adducts expected from the attack of the carbon nucleophile on the electrophilic sulfenyl amide sulfur (59% – 87% isolated yields, Table 3.1, Scheme 3.5). Presumably the reaction proceeds *via* initial ionization of the carbon acid to form the corresponding enolate, which attacks the sulfenyl sulfur of the isothiazolidin-3-one; concomitant ring opening and proton transfer affords the thioether adduct. Reaction of the model sulfenyl amide with the β-diketone acetylacetone (**A**), the β-keto ester methyl acetoacetate (**B**), and the β-diester dimethyl malonate (**C**) gave the expected adducts **3a-3c** in comparable yields (70% - 78%). The NMR spectral signatures of isolated **3a** and **3b** suggest these products

exist exclusively as the enol tautomers. For example, in the ^{1}H NMR spectrum of **3a**, the relative integral of the enolic –OH proton appearing at ~17 ppm is 1H, while no resonance corresponding to the C-H_α proton of the keto tautomer is observed.[38] Although β-keto esters typically tend to prefer the keto form in organic solvent,[39] evidently the presence of the α-thio group in **3b** promotes enolization. Conversely, the ^{1}H NMR spectrum of **3c** suggests the product exists exclusively in keto form, as no signals downfield from that of $CHCl_3$ (from NMR solvent $CDCl_3$) were observed, but an additional overlapping resonance at ~4.4 ppm was, consistent with the presence of an α-proton. Peak splitting due to the presence of two diastereomers of **3c** was observed, but signals were too poorly resolved to be integrated separately. Finally, identifying the dimedone adduct **3d** as the α-thio enol tautomer was expected, as (a) dimedone is known to exist preferentially as the enol in solution,[40] and (b) previous work by Shiau and coworkers showed that the product isolated from reaction of 1,3-cyclopentanedione and the same dipeptide sulfenyl amide was an α-thio enol.[41]

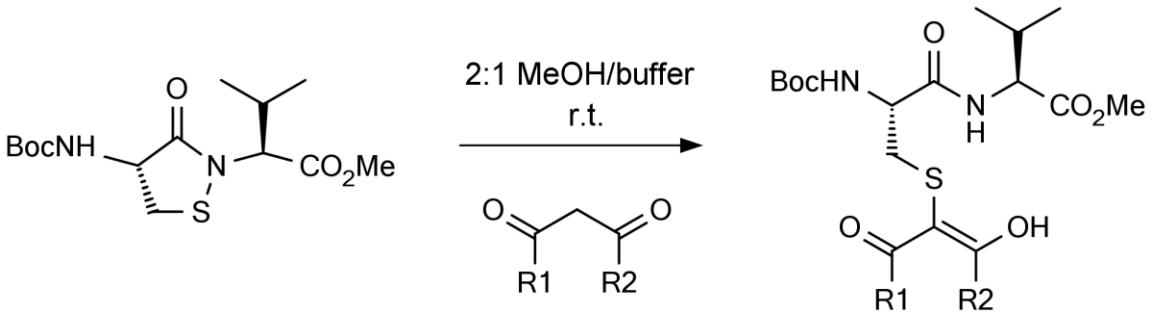

3a; R1 = CH_3, R2 = CH_3
b; R1 = OCH_3, R2 = CH_3
d; R1,R2 = $CH_2C(CH_3)_2CH_2$

Scheme 3.5. Reaction of **3** with 1,3-diketones acetyl acetone (**A**), methyl acetoacetate (**B**), and dimedone (**D**) afford enolic products.

1,3-diketone	Structure	Adduct	(%) Yield
A		3a	77
B	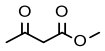	3b	78
C	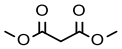	3c	70
D	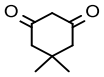	3d	70
E	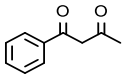	3e	87
F	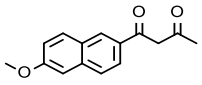	3f	81
G	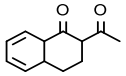	3g	77
H	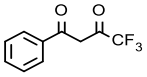	3h	72
I	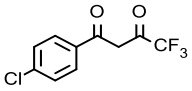	3i	68
J	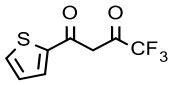	3j	65
K	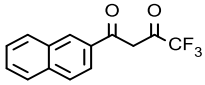	3k	59
L	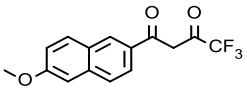	3l	69
M	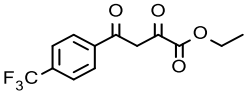	3m	83

Table 3.1. Diketone structures and yields of thioether products. 1,3-diketo carbon nucleophiles (1.1 equiv) were allowed to react with the model sulfenyl amide (1.0 equiv) in 2:1 MeOH : Buffer A at r.t. Yields are isolated following column chromatography.

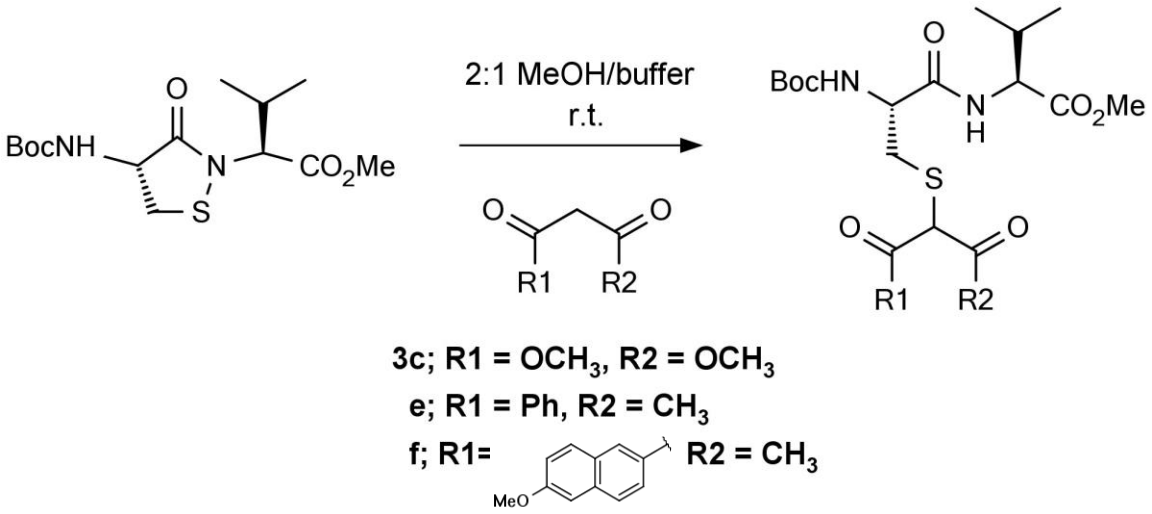

Scheme 3.6. Capture of the model sulfenyl amide by diketo compounds **C**, **E**, and **F** afford α-sulfenyl keto products.

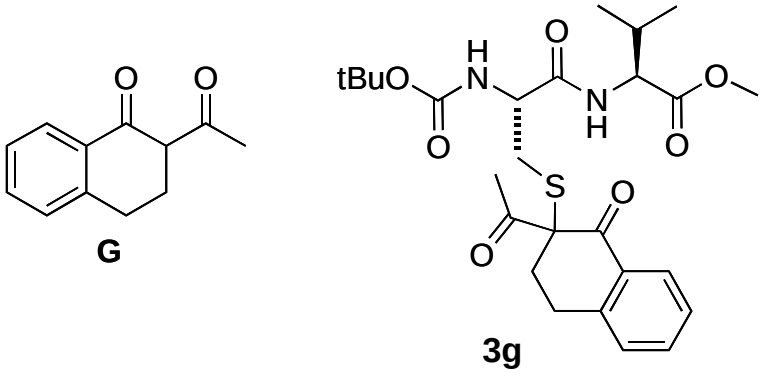

3.5 Reactions of aromatic 1,3-diketones with the sulfenyl amide.

To our knowledge, no aryl-based 1,3-diketo carbon acids have yet been reported to trap biologically-relevant sulfenylating agents (i.e. sulfenic acids and sulfenyl amides).

Thus, we examined reactions between a series of structurally-diverse aryl 1,3-diketones and the sulfenyl amide. Indeed, treatment of the model sulfenyl amide with aryl 1,3-diketones **E**, **F**, and **G** afforded the expected adducts **3e**-**3g** in very good yields (77% - 87%, Table 1, Scheme 3.6). Products **3e** and **3f** exhibited complex ^{1}H NMR spectra, presumably due to the presence of both keto and enol product forms. In both cases, extensive overlapping of signals in the ^{1}H NMR spectra precluded positive peak assignments to either isomer. However, because product **3g** lacks a second acidic proton, we were able to infer that **3g** forms a mixture of diastereomeric keto products, as evinced by the presence of two peaks each at 2.3 ppm and 3.7 ppm, corresponding to keto and ester methyl groups in the two isomers, respectively. These peaks were too poorly resolved to be reliably integrated separately, but the fact that the two pairs of singlets are of comparable *height* leads us to believe that diastereomers of **3g** formed in roughly a 1:1 ratio.

3.6 Reactions of the model sulfenyl amide with 1,3-diketones bearing α-electron withdrawing-groups.

We envisioned that stronger carbon acids would afford greater fractions of reactive enolate at neutral pH, and might thus afford greater reactivity with the sulfenyl amide under physiologically-relevant conditions. Therefore, we examined reactions of the sulfenyl amide with a series of aryl 1,3-diketones bearing electron-withdrawing α-trifluoromethyl or oxalyl substituents. In general, 1,3-diketones bearing either a $–CF_3$ or oxalyl group were found to have aqueous pK_a values between 5 and 6 (compare to pK_a

values 8-9 for acyclic 1,3-diketones). Indeed, compounds **H**-**M** reacted with the model sulfenyl amide, forging the expected carbon-sulfur bond (Scheme 3.7). However, these compounds were not isolated as sulfenylated adducts of the starting 1,3-diketone, but rather as α-sulfenylated *monoketone* products, presumably due to hydrolysis of the α-thio 1,3-diketone intermediate (Scheme 3.8). For example, in the product ^{13}C NMR spectra of **3h**-**3l**, the characteristic splitting pattern associated with the $–CF_3$ group was absent, corresponding to loss of the terminal trifluoromethyl ketone fragment. These losses were then confirmed by mass spectrometry. Corroborating the presence of an intermediate in these decomposition reactions, we noted that the reaction mixture quickly became yellow-green upon addition of 1,3-diketone to sulfenyl amide, and that this coloration slowly faded back to clear over the period of ~ 25 min. Presumably, the coloration was due to formation of α-sulfenyl trifluoromethyl or oxalyl 1,3-diketone adducts, and decoloration due to decomposition of these intermediates. Importantly, neither starting diketones **H**-**M** nor the sulfenyl amide alone produced coloration of solution. These observations suggest rapid diketone ionization and fast reaction with the sulfenyl amide, followed by relatively slow decomposition of the initially-formed α-sulfenylated 1,3-diketone. Decomposition of α-sulfenyl 1,3-diketone adducts may be driven by the presence of an α-electron withdrawing group ($-CF_3$ or oxallyl), as electron-withdrawing groups are known to increase both the rate and extent of carbonyl hydration.[424344] Interestingly, despite large differences in acidity between diketones bearing or lacking α-electron withdrawing groups, we did not observe a marked difference in product yields between the two classes (59% - 83% for those with α-EWGs, 77% - 87% for those without).

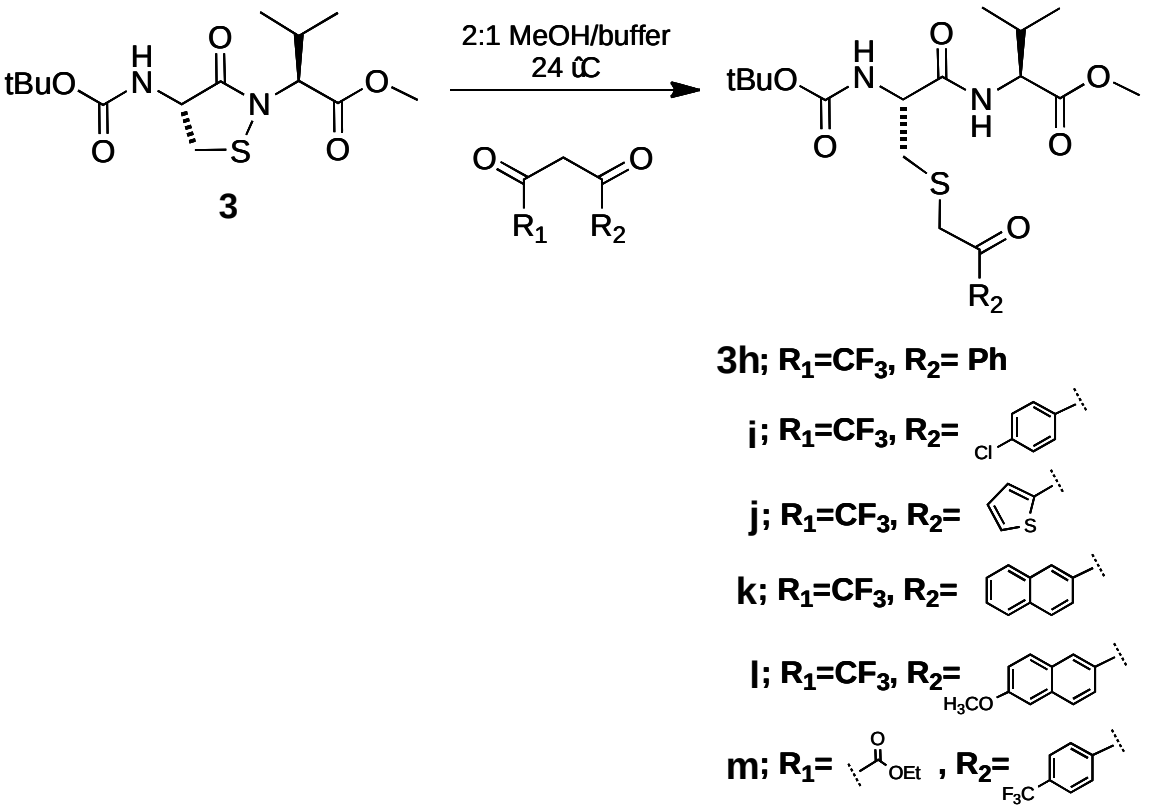

Scheme 3.7. Capture of the model sulfenyl amide by 1,3-diketones bearing α-electron-withdrawing groups and associated α-sulfenyl monoketone product structures.

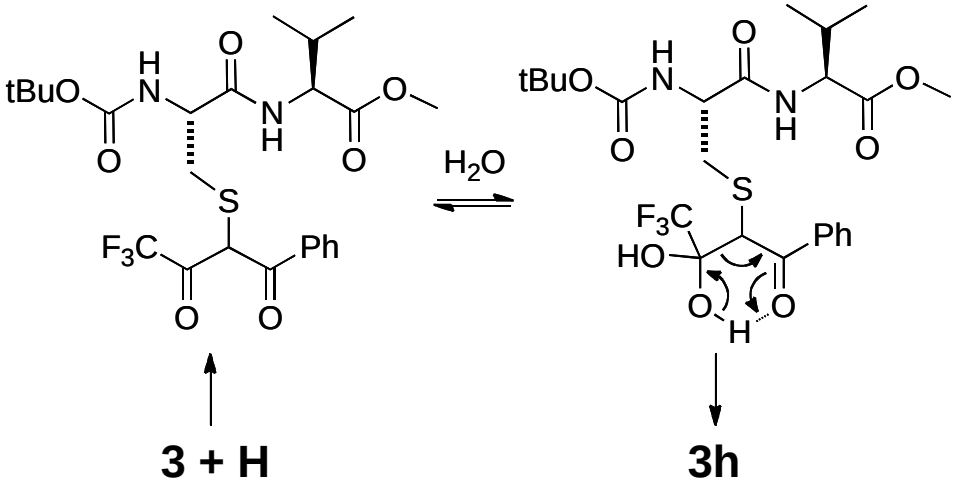

Scheme 3.8. Proposed mechanism for hydrolytic decomposition leading to formation of **3h** and associated products.

3.7 The products of covalent capture of the sulfenyl amide by 1,3-diketones are resistant to thiol attack.

Because the cellular milieu contains millimolar concentrations of the thiol glutathione,[24] any molecular probe or therapeutic agent designed to covalently capture an electrophilic sulfur *in vivo* must forge a bond to sulfur that is resistant to thiol-mediated cleavage. Thus, we assayed representative members of each product class for stability against thiol agent. Products **3a**, **3e**, **3g**, and **3k** were incubated with 50 mM dithiothreitol (DTT) at 50°C for 6 hours; no reaction was observed as judged by thin layer chromatography (TLC). These results suggest that adducts formed by attack of 1,3-diketo carbon nucleophiles on a sulfenyl amide are stable in the presence of thiol agents.

3.8 Determination of reaction kinetics for trapping of the model sulfenyl amide.

We next set out to determine rate constants associated with covalent capture of the dipeptide sulfenyl amide with 1,3-diketones. Along these lines, we designed an assay to monitor sulfenyl amide concentration spectrophotometrically, using the colorimetric aryl thiol 2-nitro-5-sulfanylbenzoic acid (TNB – the reduced form of Ellman's reagent).[45] In this assay, diketone nucleophile and sulfenyl amide were allowed to react under conditions similar to those employed in the syntheses of the thioether adducts (1:1 MeOH : Buffer B – 50 mM Tris, 50 mM Bis-Tris, 100 mM NaOAc, 10 mM DTPA, pH 7.0, 23 ± 2°C). At various times, aliquots were removed from the reaction mixture and diluted into

an assay buffer (pH 5.0) containing TNB. Reaction of TNB with remaining **3** afforded a decrease in the absorbance at 410 nm. As the "trapping" reaction proceeded over time, the concentration of free sulfenyl amide *decreased*, thus affording *increasing* absorbances at 410 nm.

Both **H** and **E** captured the sulfenyl amide in a time- and concentration-dependent manner (Figure 3.1A and 3.1C). The observed pseudo first-order rate constants (k_ψ, s^{-1}) depended linearly on diketone concentration in each case (Figure 3.1B and 3.1D), and both reactions were found to be first-order in nucleophile, consistent with an overall second-order process, for which the relevant rate law is:

$$Rate = k_{trap}[SA][Nu]$$

where k_{trap} is the apparent second-order rate constant, [SA] is the concentration of sulfenyl amide, and [Nu] is the concentration of carbon nucleophile. The rate constants measured for these processes were 9.2 ± 0.6 M^{-1} s^{-1} for **E** and 1.24 ± 0.07 M^{-1} s^{-1} for **H**. Approximate second-order rate constants were also determined for **A** (12 M^{-1} s^{-1}), **D** (6 M^{-1} s^{-1}), **K** (2 M^{-1} s^{-1}), and two additional diketones, **N** (13 M^{-1} s^{-1}) and **O** (3 M^{-1} s^{-1}). In these runs, pseudo first-order rate constants were determined at a single concentration of diketone and divided by that molar concentration of diketone to afford the apparent second-order rate constant in units of M^{-1} s^{-1}.

Finally, in order to develop a quantitative relationship between structure and reactivity, we measured the aqueous acidity constants for these diketones (Table 3.2). We found that the aqueous acidities of the 1,3-diketones examined spanned a range of roughly four orders of magnitude (pK_a 4.8 – 9.0).

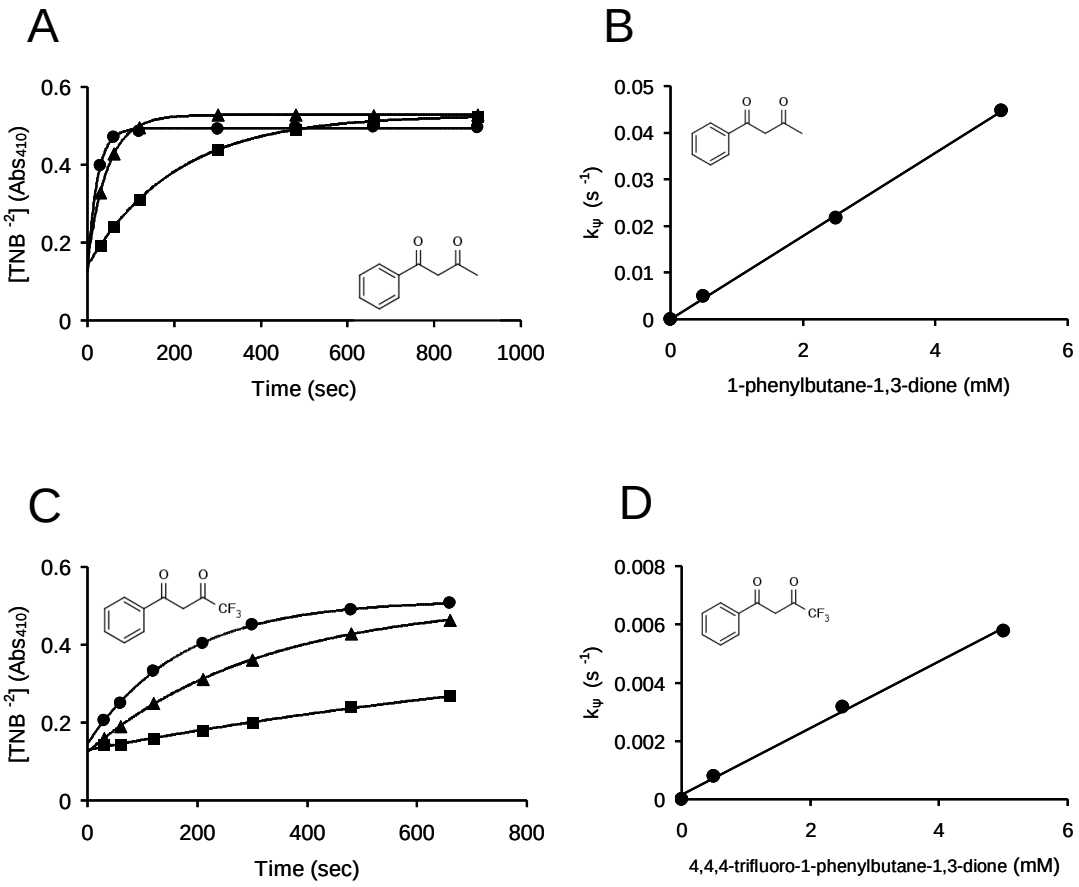

Figure 3.1. Reaction kinetics for trapping the model sulfenyl amide by compounds **E** and **H**. Kinetics runs were conducted at 23 ± 2 °C in 1:1 MeOH : Buffer B (50 mM Tris, 50 mM Bis-Tris, 10 mM DTPA, 100 mM NaOAc, pH 7.0) under pseudo first-order conditions (excess diketone). (**A**,**C**) 50 μM sulfenyl amide was allowed to react with either **E** or **H**. At various time points, aliquots were removed from the reaction mixture and assayed for remaining, unreacted sulfenyl amide *via* dilution into assay buffer containing TNB. Time-dependent consumption of sulfenyl amide was observed at varying rates as a function of diketone concentration (0.5, 2.5, and 5 mM diketone, squares, triangles, and circles, respectively). (**B**,**D**) Pseudo first-order rate constants depend linearly on diketone concentration, consistent with a second-order process. Bimolecular rate constants were calculated by division of the corresponding pseudo first-order rate constants (s^{-1}) by the molar concentration of nucleophile in excess (affording apparent second-order rate constants in units M^{-1} s^{-1}). The apparent second-order rate constants calculated at each concentration of diketone were then averaged and the standard deviations computed: k_{trap} for **E** 9.2 ± 0.6 M^{-1} s^{-1} and **H** 1.24 ± 0.07 M^{-1} s^{-1}.

1,3-diketone	Structure	pK_a
O		4.8
D		4.9
N	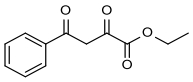	5.6
K	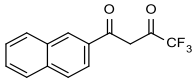	6.0
H	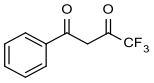	6.0
E	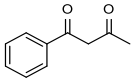	8.3
A		9.0

Table 3.2. Aqueous pK_a values for diketones examined in kinetics studies. Aqueous pK_a values were determined spectrophotometrically, as described in Methods and Materials.

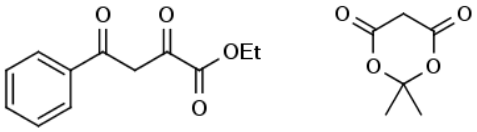

N **O**

3.9 Discussion

We first verified that the dipeptide model isothiazolidin-3-one underwent redox transformations analogous to those of the $PTP1B_{ox}$ sulfenyl amide. Namely, treatment of the model sulfenyl amide with excess thiol (5 equiv *D,L*-cysteine) afforded fully-reduced

dipeptide cysteine thiol. Work conducted previously by our group[21] showed that cysteine effectively reduced the $PTP1B_{ox}$ sulfenyl amide, affording native PTP cysteine thiol(ate). Additionally, work conducted by Shiau *et. al.* showed that treatment of the dipeptide sulfenyl amide with 1 equiv of 4-mercaptobenzoic acid under the same reaction conditions afforded exclusively the mixed disulfide product. These results suggest that the initial attack of thiolate on the sulfenyl amide is faster than subsequent attack of thiolate on the mixed disulfide. This scenario is in agreement with the kinetics observed during reactivation of $PTP1B_{ox}$ by monothiols.[21] Taken together, these results suggest that the dipeptide sulfenyl amide may serve as a reasonable chemical model for the $PTP1B_{ox}$ sulfenyl amide.

We found that structurally-diverse 1,3-diketones captured the model sulfenyl amide in 59 – 87 % isolated yields. Interestingly, we observed no apparent trend between product yield and diketone structure or pK_a. Products isolated as α-sulfenylated unsymmetrical 1,3-diketones formed mixtures of diastereomers, due to the generation of a new stereocenter in the reaction. It is not yet clear whether the isomeric distribution is due to the initial attack of either the *re* or *si* face of the enolate on the sulfenyl amide (kinetic product distribution), or from post-reaction isomerization *via* proton exchange at the central α-carbon (thermodynamic product distribution). Product **3g** deserves special mention, as – to our knowledge – this is the first reported reaction wherein an α-substituted acyclic 1,3-diketone has been successfully α-functionalized with a biologically-relevant sulfenylating agent. This suggests that molecular probes or therapeutic agents may be α-functionalized without hindering reaction with biological sulfur electrophiles. It is worth noting that, in an effort to synthesize oudenone, Bates and

Farina previously showed that sulfenylation of an α-functionalized *cyclic* diketone (1,3-cyclopentanedione) by N-(phenylthio)succinimide proceeds smoothly in dry dichloromethane with TEA as base.[46] However, the fact that product **3g** readily forms remains an important discovery, as the chemical differences between cyclic and acyclic 1,3-dicarbonyl compounds are well-documented (for example, the acidity of the acyclic β-diester dimethyl malonate is enhanced roughly *one billion-fold* upon cyclization to Meldrum's acid).[40]

We then examined the stabilities of structurally-distinct adducts **3a**, **3e**, **3g**, and **3k** against the thiol dithiothreitol (DTT). We found that when these adducts were treated with 50 mM DTT in 2:1 MeOH/HEPES buffer at 50°C for 6 hrs, no reaction occurred as judged by thin layer chromatography (TLC). These results suggest that the adducts formed by covalent capture of a sulfenyl amide by 1,3-diketones are highly resistant to thiol-mediated cleavage. It is worth noting that these stability tests were performed at elevated temperature, relative to physiological temperature (37°C), and at roughly 10-fold higher thiol concentration.[24]

Finally, we measured representative reaction rates and determined reaction order for these sulfenyl amide "trapping" processes. We found that diketones **E** and **H** captured the sulfenyl amide in time- and concentration-dependent manners. Pseudo first-order rate constants for these processes depended linearly on diketone concentration, consistent with an overall second-order process. The kinetic data may be explained by a mechanism involving rapid ionization of the diketone, followed by rate-limiting attack of enolate on sulfenyl amide (Scheme 3.9). Diketone **E** captured the model sulfenyl amide with rate constant $9.2 \pm 0.6\ M^{-1}\ s^{-1}$, compared to $1.24 \pm 0.07\ M^{-1}\ s^{-1}$ for trifluoromethyl diketone **H**.

These results were surprising, as diketone **H** is roughly 200x more acidic than **E**. Thus, it may be expected that **H** would form larger fractions of enolate than **E** under the conditions employed, affording a correspondingly larger apparent rate constant, k_{trap} (Scheme 3.9). However, **H** captured the sulfenyl amide roughly 10-fold more slowly than **E**. To further explore the relationship between diketone pK_a and rate constant k_{trap}, we measured aqueous pK_a values and determined approximate rate constants for sulfenyl amide capture by five additional 1,3-diketones: **A**, **D**, **K**, **N**, and **O**. We found that, though the acidities of these diketones varied by up to ~16,000-fold (pK_a 4.8 – 9.0), rate constants varied by only a single order of magnitude (1.3 – 13 $M^{-1} s^{-1}$). Indeed, plotting log k_{trap} versus diketone pK_a afforded no apparent correlation between the two (Figure 3.2).

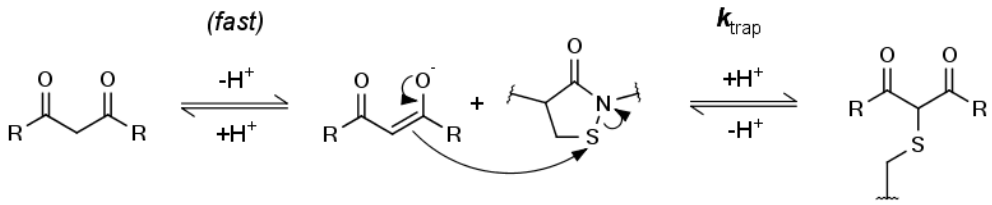

Scheme 3.9. Postulated reaction mechanism for trapping of the sulfenyl amide by 1,3-diketo nucleophiles.

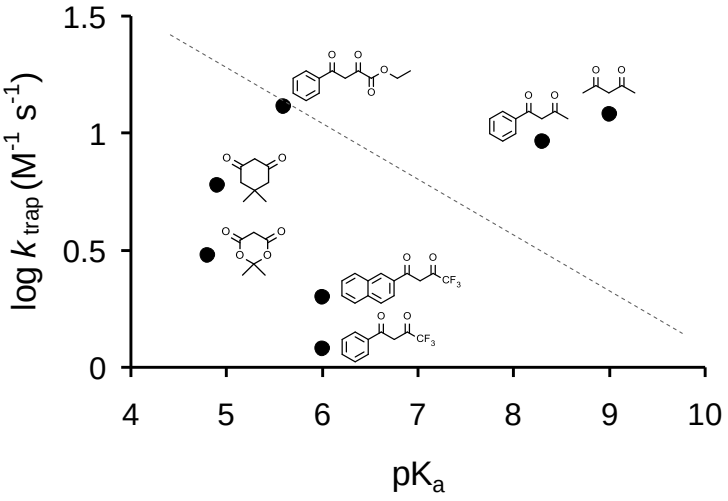

Figure 3.2. Plotting log k_{trap} versus diketone pK$_a$ affords no apparent correlation between the two (inset line represents direction of *expected* correlation).

We postulate that the observed kinetics were a result of competing factors, such as the intrinsic nucleophilicity of various enolates towards the sulfenyl amide, extent of diketone ionization, and the extent to which parent keto compounds were hydrated. Regarding the latter, hydration of a carbonyl *via* 1,2-addition of water results in formation of the corresponding *gem*-diol. This process diminishes the acidity of α-protons and renders the molecule unable to enolize at that position. Thus, the ability of a carbonyl compound to function as a carbon nucleophile is abrogated upon hydration. Although methyl ketones are poorly hydrated in solution (K_{eq}, defined as [*gem*-diol]/[>C=O], is 10^{-3} and $10^{-5.2}$ for acetone and acetophenone, respectively), α,α,α-trifluoromethyl ketones are extensively hydrated (K_{eq} for trifluoroacetone and trifluoroacetophenone are 32 and 80, respectively).[424743] This observation may explain why trifluoromethyl diketones **H** and **K** were found to capture the model sulfenyl amide

more slowly than methyl ketones **A** or **E**, though both **H** and **K** were much more acidic. Also, isolation of adducts **3h** and **3k** as monoketone fragments may corroborate this hypothesis.

3.10 Conclusion

We have demonstrated that covalent capture of a dipeptide sulfenyl amide by 1,3-diketones exhibits broad structural tolerance in diketone structure and pK_a. Furthermore, the adducts formed by these reactions as resistant to thiol-mediated cleavage. Importantly, we verified that the model sulfenyl amide recapitulated important redox transformations of oxidatively-inactivated PTP1B ($PTP1B_{ox}$), suggesting that the dipeptide sulfenyl amide is a reasonable chemical model for that existing in $PTP1B_{ox}$. We measured reaction rates and determined representative rate constants for covalent capture of the model sulfenyl amide by various 1,3-diketones, finding that although the acidities of these compounds varied greatly (by up to ~16,000-fold), rate constants for trapping the model sulfenyl amide fell within roughly one order of magnitude (1.3 – 13 $M^{-1} s^{-1}$). The kinetics of these processes were found to be first-order in diketone, suggesting an overall second-order process. The kinetic data were consistent with a mechanism wherein the diketone ionizes rapidly in solution, and then engages in rate-limiting attack on the sulfenyl amide electrophile.

Covalent capture of the sulfenyl amide in $PTP1B_{ox}$ represents a novel strategy for suppressing the enzyme's activity for therapeutic gain. This approach may permit "side-stepping" of traditional pitfalls associated with PTP inhibitor development. Additionally,

because this approach calls for nucleophilic agents to capture the sulfenyl amide electrophile, it benefits from inherent selectivity arising from bioorthogonal reaction pairing.

3.11 Methods and Materials

Spectrophotometric Determination of Carbon Acid Ionization Constants. A buffer containing glycine, sodium acetate, and sodium phosphate (all 50 mM, final concentrations) was prepared in ddH_2O. Portions of the buffer were prepared at pH 3 and pH 13, and at half pH unit intervals between. All measurements were made at room temperature (23 ± 2°C) on an Agilent 8453 Hewlett-Packard G1103A spectrophotometer. The approximate ionic strength of the buffer was 0.2 M (that due to buffer component contributions). Concentrated stock solutions of the carbon acids were prepared in DMSO (typically 1-10 mM) and stored at -20°C until used. Because molar absorptivity may vary greatly as a function of molecular structure, concentrations of carbon acids suitable for use in the spectrophotometer were determined separately for each molecule, but typically ranged from 50 – 250 μM.

In order to determine which carbon acid UV-Vis absorption maxima might be suitable for use in pK_a determination, we first examined the absorption spectra of a fixed concentration of carbon acid at the pH extremes (3 and 13), and looked for spectral changes as a function of pH. Generally, spectral peaks were blue-shifted and/or attenuated upon acidification (at pH 3), relative to those appearing at pH 13, consistent with anions being the relevant absorbing species at high pH (Figure 3.3A). Having thus

determined suitable concentrations of carbon acids and the associated wavelength(s) to monitor during titration experiments, fixed concentrations of each carbon acid were introduced to each buffer (pH 3 to 13), briefly allowed to equilibrate, and the pH–dependent spectral peak intensities recorded. Consistently, the final composition of the mixture assayed in the cuvette was 4 % DMSO in buffer (v/v; 40 μL carbon acid in DMSO, 960 μL buffer). Finally, absorption at λ_{max} for the wavelengths monitored was plotted as a function of pH, and the pK_a determined by fitting to the equation:

$$A_{pH} = A_{\min} + \frac{(A_{\max} - A_{\min})}{1+10^{pK_a - pH}}$$

where A_{min}, A_{max}, and A_{pH} are the absorbances at minimum pH (pH 3), maximum pH (pH 13), and intermediate pH values, respectively, at the wavelength being monitored for a given carbon acid (Figure 3.3B). To validate both the solvent system employed (aqueous buffer components + 4 % DMSO, μ = 0.2 M) and the method used in data analysis, a set of benchmark carbon acids and heteroatom-based acids of known aqueous pK_a were examined, and the ionization constants determined in our hands matched excellently those reported in the literature, determined by various means.

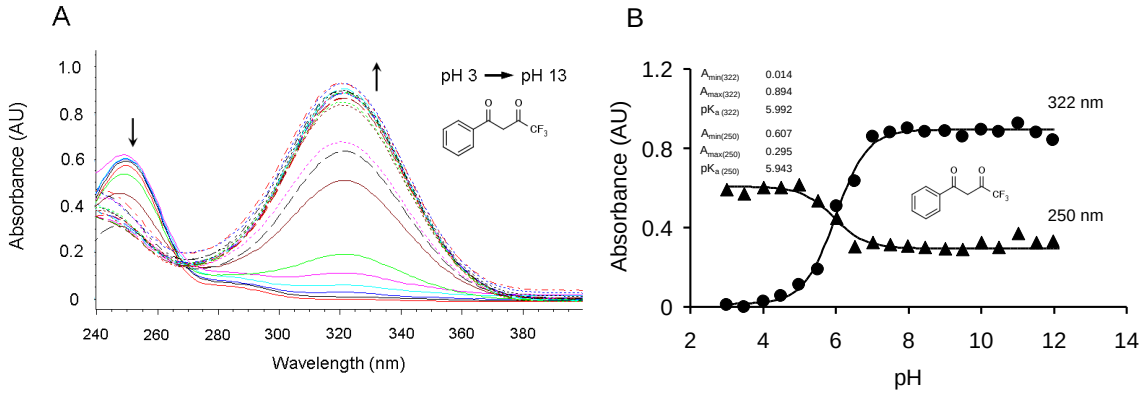

Figure 3.3. Spectrophotometric determination of carbon acid ionization constants. **A.** To 960 µL samples of "universal buffer" pH 3 – 13 (see text) were added 40 µL of 1.25 mM compound **H** in dmso to final concentration 50 µM. The solution was briefly allowed to equilibrate and the absorption spectrum versus buffer blank recorded. **B.** The absorbances of spectral peaks that varied as a function of pH were plotted versus the corresponding pH and the data fitted to afford the apparent pK_a.

Development of Assay Methodology for the Selective Detection of Sulfenyl Amide via Spectrophotometry. In order to follow the reaction of interest spectrophotometrically, we first prepared the colorimetric reagent 2-nitro-5-sulfanylbenzoic acid (TNB, Abs_{410nm} in aqueous media). Synthesis of TNB was accomplished by reduction of Ellman's reagent (5,5′-Dithiobis(2-nitrobenzoic acid)) with 8 equivalents of cysteamine hydrochloride in water brought to pH 8 with $NaHCO_3$. The reaction was stirred at room temperature for 2 hours, acidified to pH 1 with 12 M HCl, and then extracted with EtOAc. Drying of the organic layer with Na_2SO_4 and rotary evaporation afforded pure TNB as an orange solid. NMR spectral data matched that previously reported in the literature.[48]

We determined that TNB reacts selectively and stoichiometrically (1:1) with the model sulfenyl amide; that is, loss of absorbance at 410 nm from a solution of TNB was observed upon addition of sulfenyl amide to solution, but not when disulfides such as 2-mercaptoethanol disulfide or thioethers such as product **3a** were added. Stoichiometric (1:1) reaction of TNB with sulfenyl amide suggests the process proceeds to the mixed disulfide, but further reduction of the mixed disulfide to the free peptide thiol, accompanied by formation of DTNB, does not occur. Failure of TNB to fully reduce the model sulfenyl amide to the corresponding thiol is in agreement with precedented thiol-disulfide reaction equilibria involving low-pK_a aryl thiols, wherein equilibrium heavily favors the free aryl thiol.[49] Thus, we established that (a) the assay reading (Abs_{410}) changes solely as a function of concentration of sulfenyl amide in solution, in 1:1 fashion, and (b) that instrument response is linearly dependent on analyte (sulfenyl amide) concentration within the concentration regime considered. Accordingly, the assay employed a slight molar excess (1.25 equiv) of TNB over sulfenyl amide.

A concentrated (50 mM) stock of TNB in ethanol was prepared and stored at -20^{o}C until use. During use, the solution was stored on ice. When handled this way, the stock thiol was found to be stable for weeks (no appreciable loss of Abs_{410} at fixed concentration of TNB). *Note: dmso was found to be unsuitable for storage of TNB, as the solution rapidly decolored, presumably due to dmso-mediated oxidation of TNB to colorless DTNB.*[50] Stock solutions of all carbon nucleophiles and of the sulfenyl amide were prepared in dmso and stored at -20^{o}C before use.

Determination of Rate Constants for Reaction of 1,3-Diketo Nucleophiles with the Model Sulfenyl Amide. Approximately 10 minutes prior to the start of the assay, an

aliquot (1 – 120 μL) of concentrated stock (250 – 500 mM) of carbon nucleophile in dmso was added to the reaction buffer (1:1 MeOH : Buffer B – 50 mM Tris, 50 mM Bis-Tris, 10 mM DTPA, 100 mM NaOAc, pH 7.0, 11.88 mL total volume). To this solution was added additional dmso, as needed, to bring the final volume of the reaction buffer to 12.0 mL total (1 % dmso v/v, final). This afforded final diketone nucleophile concentrations of 500 μM – 5 mM. The 10 min pre-incubation period was intended to allow for ionization of the carbon acid to proceed roughly to equilibrium.[51] Following the pre-incubation period, 2 mL of the mixture (now containing diketone), were removed and set aside for determination of initial (A_o) and endpoint (A_∞) measurements for the reaction.

Assay buffer solutions were prepared via addition of 10 μL of 50 mM TNB in EtOH to 1990 μL of Buffer C (500 mM NaOAc, 100 mM Bis-Tris, 75 mM DTPA, pH 5.0), affording 2 mL final volume and 250 μM TNB final concentration. The 2 mL of assay buffer solution were subsequently divided into nine 200 μL aliquots and stored on ice until used; 7 aliquots were dedicated to reaction kinetics time point measurements, and the last 2 to endpoint determinations (A_o and A_∞, *vide supra*).

To the remaining 10 mL of reaction buffer were added 10 μL of the model sulfenyl amide (50 mM in dmso), to final concentration 50 μM. Immediately upon introduction of the sulfenyl amide to the reaction mixture, a timer was started and aliquots (800 μL) were periodically removed from the reaction mixture and assayed for remaining (unreacted) sulfenyl amide by dilution into ready-made 200 μL aliquots of assay buffer containing TNB (*vide supra*). Reaction progress was typically assayed at 0.5, 1, 2, 3.5, 5, 8, and 11 minute time points. The assay mixture, strongly buffered at pH

5, permitted simultaneous quenching of the enolate/sulfenyl amide reaction and quantitation of unreacted sulfenyl amide.[52] The quenched time point mixtures (1 mL total; 800 μL reaction mixture, 200 μL assay buffer + TNB) afforded 50 μM TNB and 40 μM sulfenyl amide formal concentrations (final). Prior to measuring Abs_{410} of these samples, they were allowed to thermally equilibrate by standing at room temperature for 5-10 min. The Abs_{410} at time zero (A_o) and infinite time (A_∞) were determined separately by preparation of two independent endpoint samples; 800 μL of the set-aside 2 mL of reaction mixture were added to 200 μL assay buffer (done for two samples). Then, to the initial reading sample (A_o), 0.8 μL of dmso were added, and to the endpoint sample (A_∞) 0.8 μL of sulfenyl amide (50 mM) in dmso were added. Use of these samples for determination of A_o and A_∞ account for any contribution the diketone/enolate might have to Abs_{410}.

Plots of Abs_{410} with respect to reaction time afforded monophasic rising curves, consistent with consumption of sulfenyl amide by carbon nucleophile (Figure 4A). Because the concentration of carbon nucleophile in the kinetics experiment was at least 10-fold higher than that of the sulfenyl amide, the data were analyzed using pseudo first-order kinetics by fitting to the equation:

$$A_t = [(A_o - A_\infty) \times e^{-k_\psi \times t}] + A_\infty$$

where A_o, A_∞, and A_t are the Abs_{410} initially, finally, and intermediately during the reaction, and k_ψ is the pseudo first-order rate constant for reaction at a given concentration of carbon nucleophile. Note that the expression above is merely a rearranged form of the equation that describes any (pseudo) first-order process:

$$\frac{A_t - A_\infty}{A_o - A_\infty} = e^{-k*t}$$

Indeed, first-order kinetic models fit excellently to the data, and plotting the observed pseudo first-order rate constants versus concentration of the carbon nucleophile in excess afforded a straight line passing through the origin (Figure 3.2). This kinetic "profile" is consistent with a simple bimolecular process being involved in the rate-determining step, described by rate law:

$$Rate = -\frac{d[SA]}{dt} = +\frac{d[P]}{dt} = k_{obs}[SA][Nu]$$

where k_{obs} is the second-order rate constant (also referred to as k_{trap} herein), and [SA], [P], and [Nu] are the concentrations of the sulfenyl amide, product thioether, and enolate nucleophile, respectively.

References

(1) Hunter, T. Signaling—2000 and Beyond. *Cell* **2000**, *100*, 113–127.

(2) Hunter, T. Protein Kinases and Phosphatases: The Yin and Yang of Protein Phosphorylation and Signaling. *Cell* **1995**, *80*, 225–236.

(3) Pawson, T.; Scott, J. D. Protein Phosphorylation in Signaling – 50 Years and Counting. *Trends Biochem. Sci.* **2005**, *30*, 286–290.

(4) Alonso, A.; Sasin, J.; Bottini, N.; Friedberg, I.; Friedberg, I.; Osterman, A.; Godzik, A.; Hunter, T.; Dixon, J.; Mustelin, T. Protein Tyrosine Phosphatases in the Human Genome. *Cell* **2004**, *117*, 699–711.

(5) Ward, W. H. J.; Cook, P. N.; Slater, A. M.; Davies, D. H.; Holdgate, G. A.; Green, L. R. Epidermal Growth Factor Receptor Tyrosine Kinase: Investigation of Catalytic Mechanism, Structure-Based Searching and Discovery of a Potent Inhibitor. *Biochem. Pharmacol.* **1994**, *48*, 659–666.

(6) Tonks, N. K. Protein Tyrosine Phosphatases: From Genes, to Function, to Disease. *Nat. Rev. Mol. Cell Biol.* **2006**, *7*, 833–846.

(7) Manning, G.; Whyte, D. B.; Martinez, R.; Hunter, T.; Sudarsanam, S. The Protein Kinase Complement of the Human Genome. *Science* **2002**, *298*, 1912–1934.

(8) Combs, A. P. Recent Advances in the Discovery of Competitive Protein Tyrosine Phosphatase 1B Inhibitors for the Treatment of Diabetes, Obesity, and Cancer. *J. Med. Chem.* **2010**, *53*, 2333–2344.

(9) Johnson, T. O.; Ermolieff, J.; Jirousek, M. R. Protein Tyrosine Phosphatase 1B Inhibitors for Diabetes. *Nat. Rev. Drug Discov.* **2002**, *1*, 696–709.

(10) Scapin, G.; Patel, S.; Patel, V.; Kennedy, B.; Asante-Appiah, E. The Structure of Apo Protein-Tyrosine Phosphatase 1B C215S Mutant: More than Just an S → O Change. *Protein Sci.* **2001**, *10*, 1596–1605.

(11) Zhou, H.; Singh, H.; Parsons, Z. D.; Lewis, S. M.; Bhattacharya, S.; Seiner, D. R.; LaButti, J. N.; Reilly, T. J.; Tanner, J. J.; Gates, K. S. The Biological Buffer, Bicarbonate/CO2, Potentiates H2O2-Mediated Inactivation of Protein Tyrosine Phosphatases. *J. Am. Chem. Soc.* **2011**, *133*, 15803–15805.

(12) Denu, J. M.; Tanner, K. G. Specific and Reversible Inactivation of Protein Tyrosine Phosphatases by Hydrogen Peroxide: Evidence for a Sulfenic Acid Intermediate and Implications for Redox Regulation†. *Biochemistry (Mosc.)* **1998**, *37*, 5633–5642.

(13) LaButti, J. N.; Chowdhury, G.; Reilly, T. J.; Gates, K. S. Redox Regulation of Protein Tyrosine Phosphatase 1B by Peroxymonophosphate (O3POOH). *J. Am. Chem. Soc.* **2007**, *129*, 5320–5321.

(14) Bhattacharya, S.; LaButti, J. N.; Seiner, D. R.; Gates, K. S. Oxidative Inactivation of Protein Tyrosine Phosphatase 1B by Organic Hydroperoxides. *Bioorg. Med. Chem. Lett.* **2008**, *18*, 5856.

(15) Meng, F.-G.; Zhang, Z.-Y. Redox Regulation of Protein Tyrosine Phosphatase Activity by Hydroxyl Radical. *Biochim. Biophys. Acta* **2013**, *1834*, 464–469.

(16) Rhee, S. G. H2O2, a Necessary Evil for Cell Signaling. *Science* **2006**, *312*, 1882–1883.

(17) Mahadev, K.; Motoshima, H.; Wu, X.; Ruddy, J. M.; Arnold, R. S.; Cheng, G.; Lambeth, J. D.; Goldstein, B. J. The NAD(P)H Oxidase Homolog Nox4 Modulates Insulin-Stimulated Generation of H2O2 and Plays an Integral Role in Insulin Signal Transduction. *Mol. Cell. Biol.* **2004**, *24*, 1844–1854.

(18) Salmeen, A.; Andersen, J. N.; Myers, M. P.; Meng, T.-C.; Hinks, J. A.; Tonks, N. K.; Barford, D. Redox Regulation of Protein Tyrosine Phosphatase 1B Involves a Sulphenyl-Amide Intermediate. *Nature* **2003**, *423*, 769–773.

(19) Van Montfort, R. L. M.; Congreve, M.; Tisi, D.; Carr, R.; Jhoti, H. Oxidation State of the Active-Site Cysteine in Protein Tyrosine Phosphatase 1B. *Nature* **2003**, *423*, 773–777.

(20) Sivaramakrishnan, S.; Keerthi, K.; Gates, K. S. A Chemical Model for Redox Regulation of Protein Tyrosine Phosphatase 1B (PTP1B) Activity. *J. Am. Chem. Soc.* **2005**, *127*, 10830–10831.

(21) Parsons, Z. D.; Gates, K. S. Thiol-Dependent Recovery of Catalytic Activity from Oxidized Protein Tyrosine Phosphatases. *Biochemistry (Mosc.)* **2013**, *52*, 6412–6423.

(22) Chen, C.-Y.; Willard, D.; Rudolph, J. Redox Regulation of SH2-Domain-Containing Protein Tyrosine Phosphatases by Two Backdoor Cysteines. *Biochemistry (Mosc.)* **2009**, *48*, 1399–1409.

(23) Dagnell, M.; Frijhoff, J.; Pader, I.; Augsten, M.; Boivin, B.; Xu, J.; Mandal, P. K.; Tonks, N. K.; Hellberg, C.; Conrad, M.; et al. Selective Activation of Oxidized PTP1B by the Thioredoxin System Modulates PDGF-B Receptor Tyrosine Kinase Signaling. *Proc. Natl. Acad. Sci.* **2013**, *110*, 13398–13403.

(24) Lushchak, V. I. Glutathione Homeostasis and Functions: Potential Targets for Medical Interventions. *J. Amino Acids* **2012**, *2012*, e736837.

(25) Cheng, A. C.; Coleman, R. G.; Smyth, K. T.; Cao, Q.; Soulard, P.; Caffrey, D. R.; Salzberg, A. C.; Huang, E. S. Structure-Based Maximal Affinity Model Predicts Small-Molecule Druggability. *Nat. Biotechnol.* **2007**, *25*, 71–75.

(26) Haque, A.; Andersen, J. N.; Salmeen, A.; Barford, D.; Tonks, N. K. Conformation-Sensing Antibodies Stabilize the Oxidized Form of PTP1B and Inhibit Its Phosphatase Activity. *Cell* **2011**, *147*, 185–198.

(27) Meng, T.-C.; Buckley, D. A.; Galic, S.; Tiganis, T.; Tonks, N. K. Regulation of Insulin Signaling through Reversible Oxidation of the Protein-Tyrosine Phosphatases TC45 and PTP1B. *J. Biol. Chem.* **2004**, *279*, 37716–37725.

(28) Tanner, J. J.; Parsons, Z. D.; Cummings, A. H.; Zhou, H.; Gates, K. S. Redox Regulation of Protein Tyrosine Phosphatases: Structural and Chemical Aspects. *Antioxid. Redox Signal.* **2011**, *15*, 77–97.

(29) Craine, L.; Raban, M. The Chemistry of Sulfenamides. *Chem. Rev.* **1989**, *89*, 689–712.

(30) Irwin, R. S.; Kharasch, N. Derivatives of Sulfenic Acids. XXXVII. Studies of Sulfenyl Esters (Thioperoxides). Part 5. Thermal Decompositions1. *J. Am. Chem. Soc.* **1960**, *82*, 2502–2505.

(31) Kice, J. L.; Cleveland, J. P. Nucleophilic Substitution Reactions Involving Sulfenic Acids and Sulfenyl Derivatives. Nucleophile- and Acid-Catalyzed Oxygen-18 Exchange of Phenyl Benzenethiolsulfinate. *J. Am. Chem. Soc.* **1973**, *95*, 104–109.

(32) Burns, J. A.; Butler, J. C.; Moran, J.; Whitesides, G. M. Selective Reduction of Disulfides by tris(2-Carboxyethyl)phosphine. *J. Org. Chem.* **1991**, *56*, 2648–2650.

(33) Allison, W. S. Formation and Reactions of Sulfenic Acids in Proteins. *Acc. Chem. Res.* **1976**, *9*, 293–299.

(34) Seo, Y. H.; Carroll, K. S. Quantification of Protein Sulfenic Acid Modifications Using Isotope-Coded Dimedone and Iododimedone. *Angew. Chem. Int. Ed.* **2011**, *50*, 1342–1345.

(35) Pan, J.; Carroll, K. S. Chemical Biology Approaches to Study Protein Cysteine Sulfenylation. *Biopolymers* **2013**.

(36) Qian, J.; Wani, R.; Klomsiri, C.; Poole, L. B.; Tsang, A. W.; Furdui, C. M. A Simple and Effective Strategy for Labeling Cysteine Sulfenic Acid in Proteins by

Utilization of B-Ketoesters as Cleavable Probes. *Chem. Commun.* **2012**, *48*, 4091–4093.

(37) Morin, R. B.; Gordon, E. M.; Lake, J. R. Chemistry of Dehydropeptides. Formation of Isothiazolones and Isothiazolidones from Cysteinyl Peptides. *Tetrahedron Lett.* **1973**, *14*, 5213–5216.

(38) Pretsch, E.; Bühlmann, P.; Badertscher, M. *Structure Determination of Organic Compounds: Tables of Spectral Data*; 4th ed. 2009 edition.; Springer: Berlin, 2009.

(39) Rogers, M. T.; Burdett, J. L. KETO–ENOL TAUTOMERISM IN B-DICARBONYLS STUDIED BY NUCLEAR MAGNETIC RESONANCE SPECTROSCOPY: II. SOLVENT EFFECTS ON PROTON CHEMICAL SHIFTS AND ON EQUILIBRIUM CONSTANTS. *Can. J. Chem.* **1965**, *43*, 1516–1526.

(40) Arnett, E. M.; Harrelson, J. A. Ion Pairing and Reactivity of Enolate Anions. 7. A Spectacular Example of the Importance of Rotational Barriers: The Ionization of Meldrum's Acid. *J. Am. Chem. Soc.* **1987**, *109*, 809–812.

(41) Shiau, T. P.; Erlanson, D. A.; Gordon, E. M. Selective Reduction of Peptide Isothiazolidin-3-Ones. *Org. Lett.* **2006**, *8*, 5697–5699.

(42) Guthrie, J. P. Carbonyl Addition Reactions: Factors Affecting the Hydrate–Hemiacetal and Hemiacetal–Acetal Equilibrium Constants. *Can. J. Chem.* **1975**, *53*, 898–906.

(43) Hilal, S. H.; Bornander, L. L.; Carreira, L. A. Hydration Equilibrium Constants of Aldehydes, Ketones and Quinazolines. *QSAR Comb. Sci.* **2005**, *24*, 631–638.

(44) Rendina, A. R.; Hermes, J. D.; Cleland, W. W. A Novel Method for Determining Rate Constants for Dehydration of Aldehyde Hydrates. *Biochemistry (Mosc.)* **1984**, *23*, 5148–5156.

(45) Whitesides, G. M.; Lilburn, J. E.; Szajewski, R. P. Rates of Thiol-Disulfide Interchange Reactions between Mono- and Dithiols and Ellman's Reagent. *J. Org. Chem.* **1977**, *42*, 332–338.

(46) Bates, H. A.; Farina, J. Oxonium Ion Electrophiles: Synthesis of the Hypotensive Oudenone. *J. Org. Chem.* **1985**, *50*, 3843–3845.

(47) Guthrie, J. P. Equilibrium Constants for a Series of Simple Aldol Condensations, and Linear Free Energy Relations with Other Carbonyl Addition Reactions. *Can. J. Chem.* **1978**, *56*, 962–973.

(48) Van Berkel, S. S.; Brem, J.; Rydzik, A. M.; Salimraj, R.; Cain, R.; Verma, A.; Owens, R. J.; Fishwick, C. W. G.; Spencer, J.; Schofield, C. J. Assay Platform for Clinically Relevant Metallo-B-Lactamases. *J. Med. Chem.* **2013**, *56*, 6945–6953.

(49) Hupe, D. j.; Pohl, E. R. A Demonstration of the Reactivity—Selectivity Principle for the Thiol—Disulfide Interchange Reaction. *Isr. J. Chem.* **1985**, *26*, 395–399.

(50) Yiannios, C. N.; Karabinos, J. V. Oxidation of Thiols by Dimethyl Sulfoxide. *J. Org. Chem.* **1963**, *28*, 3246–3248.

(51) Pearson, R. G.; Dillon, R. L. Rates of Ionization of Pseudo Acids.1 IV. Relation between Rates and Equilibria. *J. Am. Chem. Soc.* **1953**, *75*, 2439–2443.

(52) Parsons, Z. D.; Gates, K. S. Redox Regulation of Protein Tyrosine Phosphatases: Methods for Kinetic Analysis of Covalent Enzyme Inactivation. *Methods Enzymol.* **2013**, *528*, 129–154.

Chapter 4: Covalent capture of a dipeptide model isothiazolidin-3-one (sulfenyl amide) by novel sulfone-based carbon nucleophiles

4.1. Introduction

Protein tyrosine phosphatases (PTPs) are important cell signaling enzymes that catalyze the hydrolytic removal of phosphoryl groups from phosphotyrosine residues on target proteins.[12] PTPs bear a cysteine thiolate nucleophile at their active site, and covalent modification of this crucial catalytic residue leads to inactivation of the enzyme.[34567] Because PTP catalytic cysteine residues are maintained in thiolate form at physiological pH (pK_a catalytic –SH ~ 5.0),[2] the sulfur atom is highly susceptible to oxidation. Along those lines, oxidative modification of the catalytic cysteine serves as part of the cellular control mechanism for regulation of some PTPs *in vivo*.[89] Indeed, during some cell signaling events, NAD(P)H-dependent oxidases produce a burst of hydrogen peroxide (H_2O_2) which may inactivate select PTPs.[9] Subsequently, biological reducing agents such as the thiol glutathione can regenerate PTP catalytic activity by reducing the oxidized PTP, restoring the catalytic cysteine thiolate (Scheme 1).[10116] This oxidative-inactivation/reductive-reactivation couple serves as a regulatory mechanism for control of the duration and intensity of some PTP-mediated signaling pathways *in vivo*.

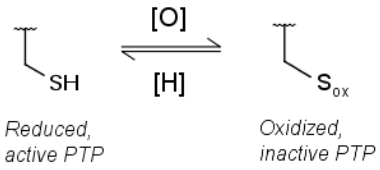

Scheme 4.1. General schematic for redox regulation of PTPs

A member of the PTP family, PTP1B, has attracted considerable attention as a potential therapeutic target for the treatment of type II diabetes and obesity.[12131415] Through its ability to dephosphorylate the insulin receptor and insulin receptor substrate, PTP1B serves as a negative regulator of insulin signaling.[16] Inhibition of native PTP1B by small molecules has been found to prolong the duration for which the insulin receptor remains phosphorylated, and thus the duration of insulin signaling.[17] This observation has driven intense efforts by academic and pharmaceutical laboratories to develop selective, orally-bioavailable inhibitors of PTP1B for the treatment of type II diabetes *mellitus*. However, despite more than 10 years of combined efforts, there are no currently no inhibitors of PTP1B in use or in clinical trials. This failure is generally attributed to the structure of native PTP1B, and to that of PTPs in general.[12] Namely, PTPs bear active sites of high positive polarity to recognize their anionic phosphotyrosine substrates. Inhibitors that are phosphotyrosine isosteres tend to be of high negative polarity/charge, resulting in poor cell permeability/bioavailability. Furthermore, PTP active site architecture is highly conserved, lending to difficulty in developing selective PTP inhibitors. For these reasons, clinically-useful inhibition of PTP1B by targeting the active site with competitive inhibitors has been deemed an "intractable" approach.[18]

Consequently, pursuing alternative approaches to inhibiting PTP1B activity *in vivo* is an important task.

During normal insulin signaling processes, NAD(P)H-dependent oxidase Nox4 produces a burst of hydrogen peroxide which oxidatively inactivates PTP1B.[9] Oxidation of PTP1B leads to an unusual 5-membered heterocycle involving the catalytic cysteine residue (Cys215) and neighboring residue serine 216 (Scheme 4.2).[19203] The 5-membered heterocycle is formally an isothiazolidin-3-one, but is more commonly called a sulfenyl amide.

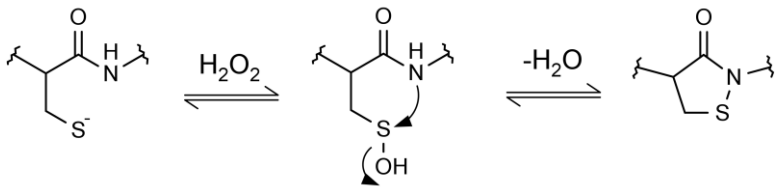

Scheme 4.2. Oxidation of PTP1B affords a 5-membered sulfenyl amide.

Recently, Tonks' group showed that an antibody specific for *oxidatively-inactivated* PTP1B ($PTP1B_{ox}$) effectively "traps" the oxidized enzyme in cells, resulting in enhanced phosphorylation of the insulin receptor.[21] Also in that work, the antibody was shown to inhibit phosphine-mediated reduction of $PTP1B_{ox}$ *in vitro*, thereby preventing recovery of phosphatase activity from $PTP1B_{ox}$. Work conducted by our group has shown that phosphine agents are comparable to thiol agents in their ability to recover PTP activity from $PTP1B_{ox}$.[10] Taken together, these results suggested that the mechanism of action by which the antibody potentiated insulin signaling was *prevention*

of recovery of PTP activity from $PTP1B_{ox}$ in the cell. Thus, this may suggest that blocking thiol-mediated recovery of $PTP1B_{ox}$ *in vivo* may be a viable approach for suppressing its phosphatase activity for therapeutic purposes. Furthermore, because $PTP1B_{ox}$ structure differs appreciably from that of native PTP1B,[2] this approach may potentially avoid the "traditional pitfalls" associated with inhibiting native PTP1B (*vide supra*). Hence, we set out to identify small molecules capable of irreversibly capturing oxidatively-inactivated PTP1B.

The sulfenyl amide sulfur is known to be electrophilic, as evinced by its propensity to undergo reaction with nucleophilic agents such as thiols and phosphines. Thus, we envisioned that small molecule nucleophiles might be capable of irreversibly "capturing" the sulfenyl amide (Scheme 4.3). Here, we sought to identify such a set of small molecule nucleophiles. Because the cellular milieu contains millimolar concentrations of the thiol glutathione (GSH),[22] we were interested in identifying nucleophilic agents which might form bonds to sulfur resistant to cleavage by thiols. As sulfur-heteroatom bonds are known to generally be thiol- or hydrolytically-labile,[1023] we narrowed our consideration of candidate molecules to those which might be nucleophilic at carbon under physiological conditions. This requirement effectively demands identification of carbon acids sufficiently strong to ionize (to some extent) under physiological conditions (pH 7.4).

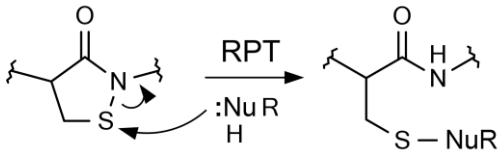

Scheme 4.3. Covalent capture of a sulfenyl amide by a nucleophilic agent.

Compounds containing methylene groups bearing α,α-electron-withdrawing substituents may exhibit unusually low pK_a values for the methylene C-H bonds.[2425] Thus, we considered a variety of molecules containing such functionalities (EWG-CH_2-EWG). In a separate work, we report the results of covalent capture of a model sulfenyl amide by 1,3-diketones (Chapter 3 herein). It is worth noting that 1,3-diketones have been successfully used in capturing protein sulfenic acids (-SOH) formed in cells.[2627] Here, we sought to expand the library of scaffolds which afford carbon nucleophiles capable of trapping biological sulfur electrophiles under mild conditions. We anticipated that select sulfone-containing compounds might afford carbon acids of sufficient strength to ionize under mild conditions.[24] Additionally, we envisioned that the sulfone functionality might afford tremendous structural diversity. Sulfones are synthetically accessible by oxidation of sulfides,[282930] and sulfides are readily accessible *via* nucleophilic substitution reactions with thiols. In some cases, deprotonation of a methyl sulfone with strong base (*n*-BuLi, MeONa, or NaH) followed by nucleophilic substitution may afford target molecules (Scheme 4.4).[3132]

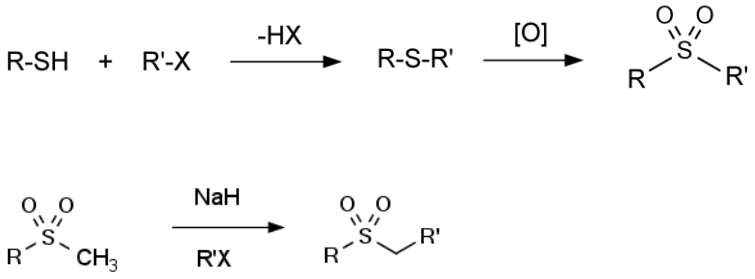

Scheme 4.4. General synthetic routes for preparation of sulfones.

To explore whether various sulfone-based carbon acids might be capable of trapping a sulfenyl amide electrophile, we first prepared a model dipeptide isothiazolidin-3-one (**1**) according to the method of Morin and coworkers.[33] We found that several sulfones bearing β-electron-withdrawing groups were commercially available. Of these, we selected representative members from three "classes" for screening against reaction with the model sulfenyl amide. We treated the model sulfenyl amide with a slight excess (1.1 equiv) of either β-keto sulfone (**A**), β-disulfone (**B**), or β-cyano sulfone (**C**) under mild conditions (2:1 MeOH/pH 7 buffer, r.t.). Indeed, all three classes of sulfone-based carbon nucleophile were found to form thioether (C-S-C) linkages upon reaction with the sulfenyl amide, consistent with nucleophilic attack of the acidic methylene unit on the sulfenyl amide sulfur (Scheme 4.5). Interestingly, products isolated from these reactions suggested capture of either one or two equivalents of the sulfenyl amide (so-called "monoadducts" **1a – 1c** or "diadducts" **2a – 2c**, respectively). Monoadduct formation presumably resulted from ionization of the parent sulfone carbon acid and subsequent attack on the sulfenyl amide. Diadducts presumably formed *via* ionization of the remaining acidic proton present in monoadducts, followed by nucleophilic attack on a second equivalent of sulfenyl amide. Total yields of these reactions (sum of monoadducts and diadducts) ranged from 12 – 62%. In an effort to identify structure-activity relationships, we then turned our attention to measuring the kinetics of these trapping reactions. We first determined the aqueous pK_a values of several sulfone-based carbon acids. We then conducted kinetics experiments to determine the rates of these trapping processes under conditions similar to those employed in the synthetic efforts (1:1 MeOH/pH 7 buffer). We found that all three classes of carbon acid trapped the model

sulfenyl amide in time- and concentration-dependent fashions, and that these processes were first-order with respect to nucleophile. This data was consistent with overall second-order reaction kinetics. Apparent second-order rate constants spanned a range of roughly 5-fold across all types of carbon nucleophile (12 – 61 M^{-1} s^{-1}) though aqueous acidity constants varied up to roughly 60-fold (pK_a 9.2 – 11.0). We found that neither reaction yields nor reaction rates seemed to depend to any great extent on pK_a of carbon acid. These results have important ramifications on design considerations for molecules intended to trap biological sulfur electrophiles under physiologically-relevant conditions.

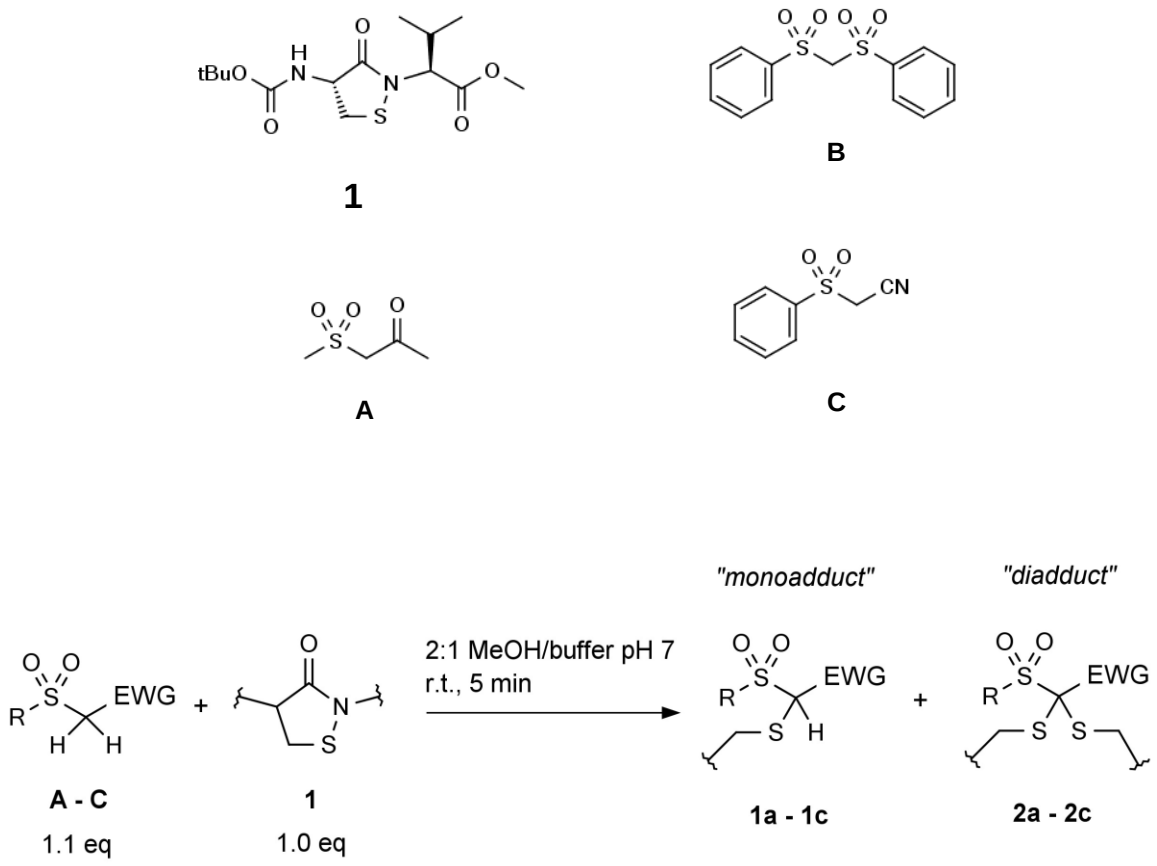

Scheme 4.5. Reaction of model sulfenyl amide **1** with various sulfone-based carbon nucleophiles affords a mixture of monoadducts and diadducts.

Results

4.2 Sulfone-based carbon nucleophiles react with the model sulfenyl amide to afford thioether-linked products.

We first prepared a small chemical model of the $PTP1B_{ox}$ sulfenyl amide (**1**) by the method of Morin and coworkers.[33] In work reported elsewhere, we verified that this dipeptide model isothiazolidin-3-one recapitulated important redox transformations that $PTP1B_{ox}$ is known to undergo, thus validating the dipeptide as a reasonable chemical model for the oxidized enzyme (Chapter 3 herein). We then screened representative β-keto sulfone (**A**), β-disulfone (**B**), and β-cyano sulfone (**C**) molecules for reaction with the isothiazolidin-3-one (Scheme 4.5). All three "classes" of carbon nucleophile afforded the anticipated carbon-sulfur linkages, consistent with nucleophilic attack of the sulfone α-carbon on the sulfenyl amide sulfur.

Interestingly, we found that the products isolated from the reaction mixtures following column chromatography fell into two general categories: "monoadducts" **1a – 1c**, and "diadducts" **2a – 2c**. Presumably, diadducts **2a – 2c** arise from loss of the remaining ionizable proton from monoadducts **1a – 1c**, followed by nucleophilic attack on a second equivalent of sulfenyl amide. Isolated total yields from these reactions (sum of monoadducts and diadducts) ranged from 12 – 62% (Table 4.1).

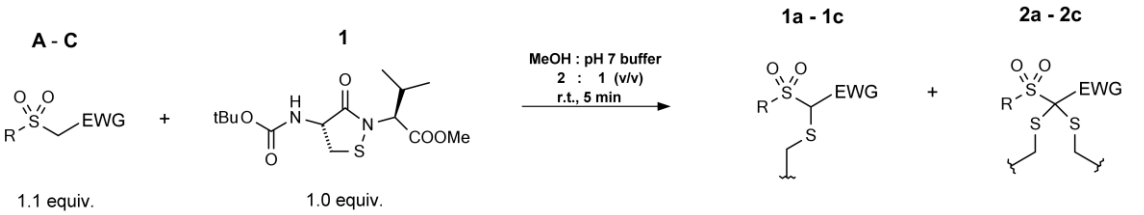

Cmpd	Structure	adduct	(%) yield	adduct	(%) yield	total (%) yield	pK_a [a]
A	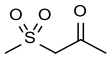	**1a**	12	**2a**	n/a	12	10.0
B	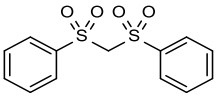	**1b**	16	**2b**	46	62	10.9
C	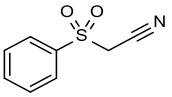	**1c**	n/a	**2c**	40	40	11.0

Table 4.1. Isolated yields of various adducts from reaction of the model sulfenyl amide with carbon nucleophiles. To a stirred solution of carbon acid (1.1 equiv) in 2:1 MeOH : Buffer A was added sulfenyl amide (1.0 equiv), and the mixture allowed to stir at r.t. for approx. 5 min. After this time, the methanol was evaporated under reduced pressure and the remaining aqueous layer was extracted with DCM (2 x 1 mL). The mixture was then purified over silica gel with ethyl acetate:hexane eluent, and the pooled fractions evaporated under reduced pressure. Finally, residual solid was reconstituted in acetonitrile, washed with hexane (2 x 1 mL), and evaporated to dryness under vacuum to afford pure product. [a]Aqueous pK_a values for parent carbon acids **A**, **B**, and **C** (determined as described below).

4.3 Covalent capture of the model sulfenyl amide by β-keto sulfone (A).

Reaction of the sulfenyl amide with methanesulfonylacetone (**A**) afforded exclusively monoadduct **1a** in 12% yield (Table 4.1). Diadduct **1b** was neither isolated nor observed by thin layer chromatography (TLC). Product **1a** was isolated as a mixture of diastereomers, which relative ^{1}H NMR integrals suggest exist in roughly a 2:1 ratio

(Figure 4.1). Extensive signal overlap in the ^{1}H NMR spectrum of **1a** precluded integration of peaks separately in many cases, such as for the *i*-Pr group at 1.0 ppm and the *t*-Bu group at 1.5 ppm. However, well-resolved singlets at circa 5.0 ppm and 5.3 ppm, which we attribute to the central α-protons of the two isomers (proton ***k*** in Figure 4.1),[34] exhibit an integral ratio of 1:2.2. It is not yet clear whether the isomeric distribution observed is a kinetic or thermodynamic product distribution. Namely, the isomeric distribution afforded by the initial attack on the sulfenyl amide by either the *re* or *si* face of the enolate of **A** would afford a kinetic product distribution, whereas post-reaction isomerization *via* exchange of proton ***k*** would afford a thermodynamic product distribution.

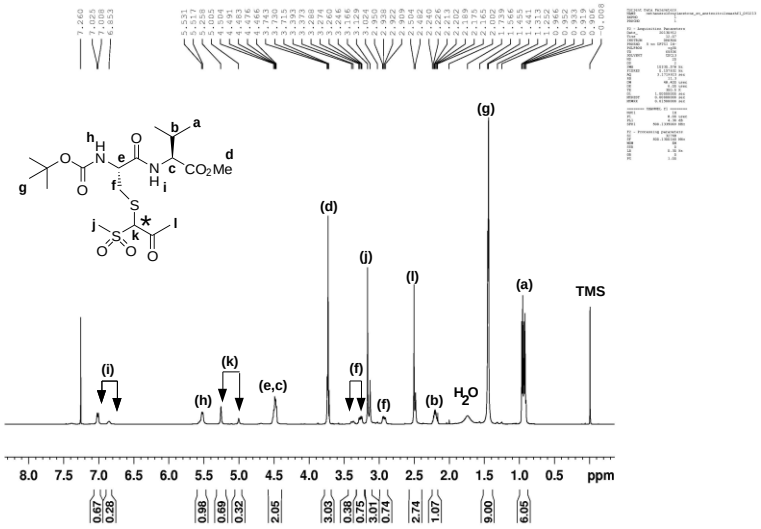

Figure 4.1. ^{1}H NMR spectrum of product **1a** revealing a roughly 2:1 distribution of diastereomers.

4.4 Covalent capture of the sulfenyl amide by β-sulfonyl sulfone B.

Reaction of β-disulfone **B** with the sulfenyl amide afforded both monoadduct **1b** and diadduct **2b** in 16% and 46% yields, respectively (62 % overall yield, Table 4.1). These adducts were readily differentiable by ^{1}H NMR spectroscopy: in the ^{1}H NMR spectrum of monoadduct **1b**, the disulfone α-proton ***k*** appeared as a singlet at 6.2 ppm and the ratio of total aryl protons to those in the Boc *t*-butyl group was 10:9. Conversely, the ^{1}H NMR of diadduct **2b** lacked the peak corresponding to α-proton ***k***, and doubling of the *t*-butyl integral relative to those of aryl protons was observed (18:10). Mass spectrometry confirmed these assignments. Because ionization of disulfone **B** affords a symmetrical carbanion, reaction with the sulfenyl amide yielded a single diastereomer in **1b**.

4.5 Covalent capture of the model sulfenyl amide by β-cyano sulfone C.

Reaction of β-cyano sulfone **C** with the sulfenyl amide afforded exclusively diadduct **2c** in 40 % yield. Interestingly, the intermediate monoadduct **1c** was not isolated or observed by TLC. Product **2c** was readily identifiable as a "diadduct" by ^{1}H NMR spectroscopy, as the NMR spectrum lacked the singlet between ~ 5 – 6 ppm characteristic of the sulfone α-proton present in monoadducts, and doubling of the Boc *t*-butyl integral relative to those of aryl protons was observed.

4.6 Determination of aqueous acid dissociation constants for various sulfone-based carbon acids.

Aqueous pK_a values were determined spectrophotometrically at 23 ± 2°C in a "universal" buffer containing 50 mM each of glycine, sodium acetate, and sodium phosphate prepared in ddH_2O (μ = 0.2 M, due to buffer components). Spectral peaks sensitive to buffer pH were monitored at pH 3 – 13 at fixed carbon acid concentration. Peak intensities were plotted as a function of buffer pH and the apparent pK_a determined by least-squares fitting of equation 1 to the data, with pK_a, A_{min}, and A_{max} as adjustable parameters.

$$A_{pH} = A_{\min} + \frac{(A_{\max} - A_{\min})}{1+10^{pK_a - pH}} \quad (1)$$

The terms A_{min}, A_{max}, and A_{pH} are the absorbances at minimum pH (pH ≤ 3), maximum pH (pH ≥ 13), and intermediate pH values, respectively (Figure 4.2). Aqueous pK_a values under these conditions were found to fall between 9.2 – 11.0 (Table 4.2).

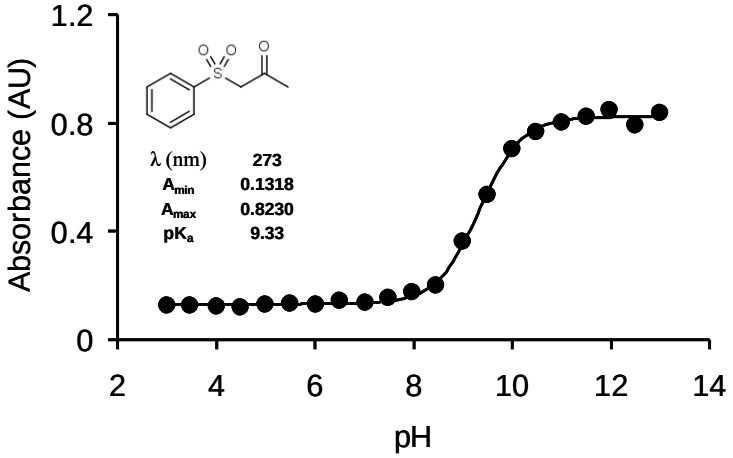

Figure 4.2. Determination of carbon acid **E** aqueous pK_a

Entry	Sulfone	pK_a
D	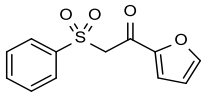	9.2
F	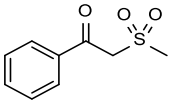	9.3
E	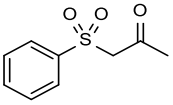	9.3
G	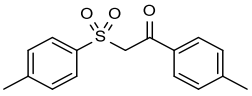	9.7
A	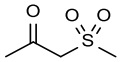	10.0
B	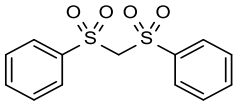	10.9
C	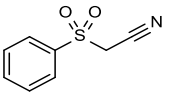	11.0

Table 4.2. Aqueous pK_a values of various sulfones determined at $\mu = 0.2$ M

4.7 Assay development and determination of rate constants for covalent capture of the sulfenyl amide by sulfone-based carbon nucleophiles.

We sought to develop a quantitative relationship between carbon nucleophile structure and ability to capture the sulfenyl amide on the basis of reaction kinetics. To this end, we developed a spectrophotometric assay by which to selectively monitor sulfenyl amide concentration in solution. The assay utilized the colorimetric thiol 5-

sulfanyl-2-nitro benzoic acid (TNB), the reduced form of Ellman's reagent. TNB exists predominantly as a dianion (TNB^{-2}) under our assay conditions and bears a highly reactive aryl thiolate nucleophile.[3536] We determined that this aryl thiolate reacted rapidly with free sulfenyl amide in solution. Reaction of the TNB^{-2} thiolate with the sulfenyl amide was stoichiometric (1:1), affording the corresponding mixed disulfide (Figure 4.3A). This stoichiometry is in accord with precedented thiol-disulfide exchange equilibria involving aryl thiols such as TNB.[37] The TNB^{-2} ion absorbs strongly at 410 nm in aqueous media, but disulfides of TNB do not. Thus, we were able to monitor the concentration of free, unreacted sulfenyl amide during "trapping" reactions by measuring changes in A_{410} over time. In these assays, the model sulfenyl amide was introduced to a large molar excess (10-fold or greater) of carbon nucleophile and allowed to react under similar conditions to those employed in the syntheses described above (1:1 MeOH : pH 7 buffer, r.t.). At various times during the reaction, aliquots were removed from the mixture and assayed for remaining, "untrapped" sulfenyl amide by dilution into assay buffer containing TNB^{-2}. As the trapping reaction proceeded, less free sulfenyl amide was available to react with and consume the TNB^{-2} thiolate, affording rising A_{410} values over time. Plotting A_{410} versus reaction time afforded monophasic curves, consistent with time- and concentration-dependent consumption of the sulfenyl amide by carbon nucleophiles (Figure 4.3B). The kinetic data were analyzed using pseudo first-order kinetic treatment. Plots of the extracted pseudo first-order rate constants versus carbon nucleophile concentration were linear, suggesting processes first-order in nucleophile for each "class" of carbon acid (Figure 4.3C).[38] These results were consistent with an overall second-order process, described by rate law:

$$Rate = -\frac{d[SA]}{dt} = -\frac{d[Nu]}{dt} = \frac{d[P]}{dt} = k_{trap}[SA][Nu]$$

where [SA], [Nu], and [P] are the concentrations of sulfenyl amide, carbon nucleophile, and thioether product, respectively, and k_{trap} is the apparent second-order rate constant for capture of the sulfenyl amide. Reaction order was determined in this way for representative members of each class of carbon nucleophile (compounds **B**, **C**, **D**, and **E**). Apparent second-order rate constants varied from 12 ± 1.5 M^{-1} s^{-1} to 61 ± 8.0 M^{-1} s^{-1} (Table 4.3). Approximate second-order rate constants were determined for three additional β-keto sulfones: **A** (9 M^{-1} s^{-1}), **F** (18 M^{-1} s^{-1}), and **G** (20 M^{-1} s^{-1}, see Table 4.2 for structures). These values were determined by monitoring the kinetics of the trapping reaction at a single concentration of nucleophile and dividing the pseudo first-order rate constant (units of s^{-1}) by the molar concentration of carbon nucleophile, affording apparent second-order rate constants in units of M^{-1} s^{-1}.

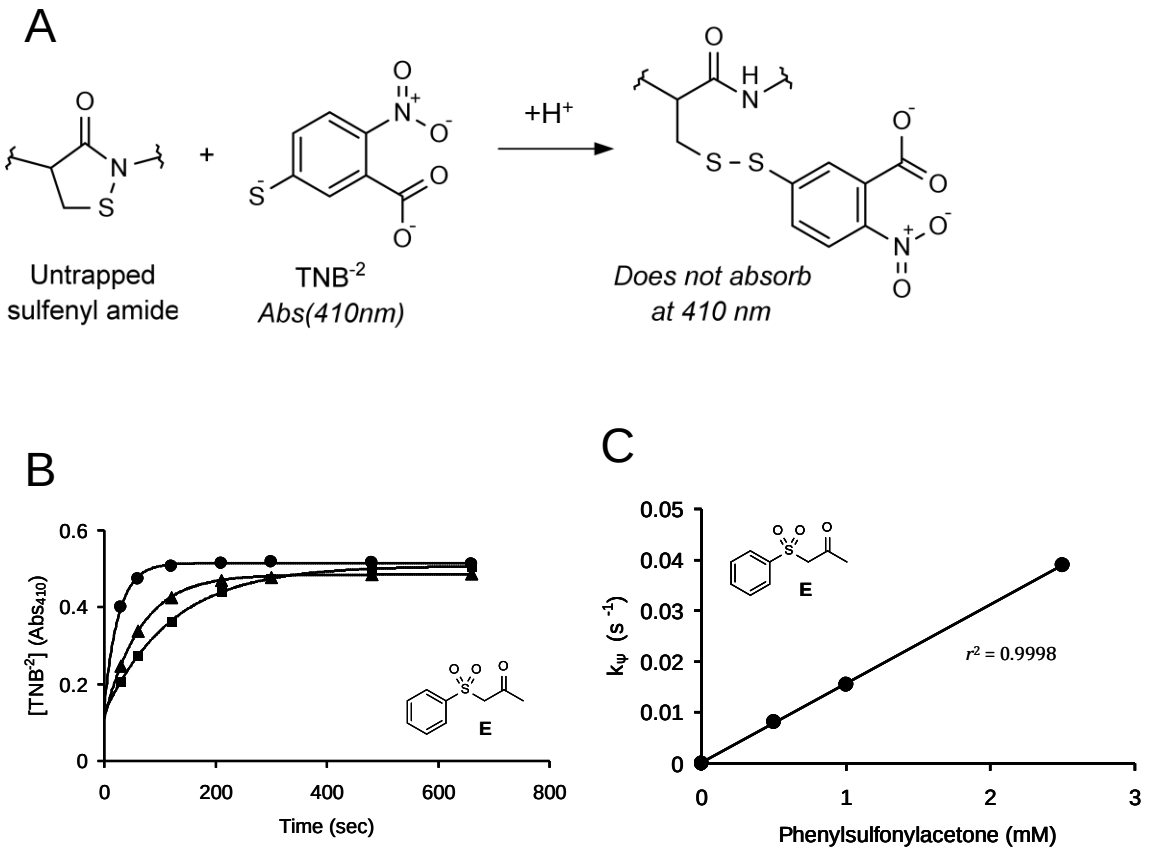

Figure 4.3. Determination of reaction kinetics for trapping the model sulfenyl amide by sulfone-based carbon acids/nucleophiles. (A) The chemical basis for kinetics assays. The free TNB^{-2} ion absorbs strongly at 410 nm; disulfides thereof do not. As sulfenyl amide was consumed by the "trapping reaction" with carbon nucleophiles, less became available to react with the TNB^{-2} ion. Thus, as the trapping reaction proceeded, A_{410} increased, plateauing when all sulfenyl amide had been consumed by carbon nucleophile. (B) Representative traces of kinetic data. Sulfenyl amide (50 μM) was allowed to react with 0.5, 1, or 2.5 mM compound **E** (squares, triangles, and circles, respectively). At predefined time intervals (0.5, 1, 2, 3.5, 5, 8, and 11 min), 10 μL aliquots were removed from the reaction mixture and assayed for remaining sulfenyl amide *via* the TNB^{-2} assay. Kinetics were analyzed in Microsoft Excel *via* non-linear regression analysis, fitting to pseudo first-order kinetic models. From these fits, pseudo first-order rate constants (units of s^{-1}) were extracted. (C) Plotting these rate constants versus the concentration of carbon nucleophile in excess revealed excellent linear dependence of pseudo first-order rate constant on concentration of carbon nucleophile, with the trendline intercepting the origin. These kinetics are consistent with a simple bimolecular reaction. Division of pseudo first-order rate constants by corresponding molar concentrations of carbon nucleophile afforded the apparent second-order rate constant for the reaction (units of M^{-1} s^{-1}). Finally, the apparent second-order rate constants were averaged and the standard deviation computed (15.8 ± 0.5 M^{-1} s^{-1}).

Cmpd	Structure	k_{trap} (M^{-1} s^{-1}) [a]	pK_a [b]
C	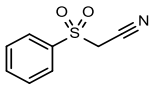	61 ± 8.0	11.0
D	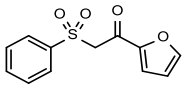	30 ± 2.0	9.2
E	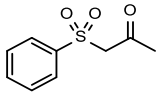	15.8 ± 0.5	9.3
B	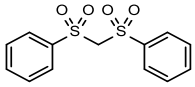	12 ± 1.5	10.9

Table 4.3. Rate constants for trapping the model sulfenyl amide and aqueous acid dissociation constants for sulfone-based nucleophiles. [a]Second-order rate constants for trapping the model sulfenyl amide in 1:1 MeOH : Buffer B (pH 7.0), 23 ± 2 °C. [b]Aqueous pK_a values were determined as reported in the text.

4.8 Conclusion

We demonstrated that structurally-diverse carbon acids containing a sulfone and one additional β-electron-withdrawing group (-COR, -SO_2R, or -CN) were capable of covalently capturing a model dipeptide isothiazolidin-3-one (sulfenyl amide) under mild conditions. Total isolated yields for these reactions ranged from 12 % - 62 %. Presumably, these reactions proceeded in stepwise fashion, where the carbon acid first ionized rapidly in solution, then nucleophilically attacked the sulfenyl amide sulfur. Concomitant cleavage of the S-N bond and ring-opening/proton transfer afforded the thioether products.

Interestingly, we found that some carbon nucleophiles preferentially formed so-called "monoadducts" (**1a – 1c**) or "diadducts" (**2a – 2c**) under our reaction conditions

(1:1 MeOH:buffer pH 7, r.t., 5 min reaction time, Table 1). Monoadducts arose from capture of one equivalent of the sulfenyl amide, whereas diadducts resulted from capture of two equivalents of the sulfenyl amide. Presumably, diadducts (**2b** and **2c**) formed *via* loss of the second acidic proton from monoadduct intermediates **1b** and **1c**, followed by nucleophilic attack on a second equivalent of the sulfenyl amide. Diadduct formation might be expected of these reactions, as monoadduct intermediates **1b** and **1c** were likely more acidic than the parent carbon acids **B** and **C** themselves, due to the presence of an α-sulfenyl group. Interestingly, in the case of β-cyano sulfone **C**, diadduct **2c** was the only product isolated from reaction with the sulfenyl amide (monoadduct **1c** was not isolated or observed by TLC). Conversely, in the case of β-keto sulfone **A**, monoadduct **1a** was the only product isolated from the reaction mixture (no diadduct **2a** was observed). The basis for preferential formation of either mono- or diadducts during reaction with the sulfenyl amide is not yet understood, though it may reflect relative rates or extents of ionization of the parent carbon acids compared to their corresponding monoadduct intermediates.[24]

We then turned our attention to measuring the rates of these reactions. We found that all three "classes" of carbon nucleophile (β-keto sulfones, β-cyano sulfones, and β-disulfones) captured the sulfenyl amide in time- and concentration-dependent fashions. Plots of pseudo first-order rate constants versus carbon nucleophile concentration revealed that these reactions were first order in nucleophile, suggesting bimolecular (second-order) kinetics overall. The apparent second-order rate constants for these reactions fell between approximately 10 – 60 M^{-1} s^{-1}, and were apparently independent of carbon acid pK_a. For example, β-cyano sulfone **C** was the weakest carbon acid studied,

though it trapped the model sulfenyl amide with the largest rate constant (**C**, aqueous pK_a 11.0, k_{trap} 61 ± 8.0 M^{-1} s^{-1}). However, β-disulfone **B** was of comparable acidity (aqueous pK_a 10.9), but trapped the model sulfenyl amide with a much smaller rate constant (k_{trap} = 12 ± 1.5 M^{-1} s^{-1}). Indeed, no apparent correlation appeared to exist between carbon acid pK_a and rate constant for trapping the sulfenyl amide. To further explore this apparent lack of correlation, we measured approximate second-order rate constants and aqueous pK_a values for three additional β-keto sulfones: **A** (pK_a 10.0, k_{trap} 9 M^{-1} s^{-1}), **F** (pK_a 9.3, k_{trap} 18 M^{-1} s^{-1}), and **G** (pK_a 9.7, k_{trap} 20 M^{-1} s^{-1}). Plotting log(k_{trap}) versus carbon acid pK_a again revealed no apparent correlation between the two (Figure 4.4). Consideration of only the β-keto sulfones in this data set afforded a poor linear correlation between log(k_{trap}) and pK_a (r^2 = 0.5855, slope = -0.43). It is unclear why pK_a and rate constant for trapping the sulfenyl amide appear decoupled among sulfone-based carbon nucleophiles, though at least in the context of β-keto sulfones, this may reflect competing factors such as sulfone-promoted enolate formation and hydration of the keto group.[39]

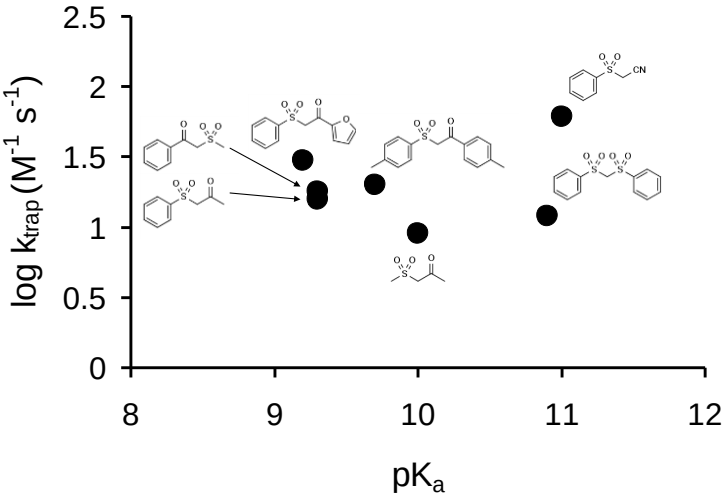

Figure 4.4 A plot of log k_{trap} versus carbon acid pK$_a$ reveals no evident correlation between the two.

4.9 Methods and Materials

Determination of carbon acid ionization constants and kinetics of reaction with the sulfenyl amide were performed exactly as described in Chapter 3.

References

(1) Tonks, N. K. Protein Tyrosine Phosphatases: From Genes, to Function, to Disease. *Nat. Rev. Mol. Cell Biol.* **2006**, *7*, 833–846.

(2) Tanner, J. J.; Parsons, Z. D.; Cummings, A. H.; Zhou, H.; Gates, K. S. Redox Regulation of Protein Tyrosine Phosphatases: Structural and Chemical Aspects. *Antioxid. Redox Signal.* **2011**, *15*, 77–97.

(3) Zhou, H.; Singh, H.; Parsons, Z. D.; Lewis, S. M.; Bhattacharya, S.; Seiner, D. R.; LaButti, J. N.; Reilly, T. J.; Tanner, J. J.; Gates, K. S. The Biological Buffer Bicarbonate/CO2 Potentiates H2O2-Mediated Inactivation of Protein Tyrosine Phosphatases. *J. Am. Chem. Soc.* **2011**, *133*, 15803–15805.

(4) Seiner, D. R.; LaButti, J. N.; Gates, K. S. Kinetics and Mechanism of Protein Tyrosine Phosphatase 1B Inactivation by Acrolein. *Chem. Res. Toxicol.* **2007**, *20*, 1315–1320.

(5) Bhattacharya, S.; LaButti, J. N.; Seiner, D. R.; Gates, K. S. Oxidative Inactivation of Protein Tyrosine Phosphatase 1B by Organic Hydroperoxides. *Bioorg. Med. Chem. Lett.* **2008**, *18*, 5856–5859.

(6) Denu, J. M.; Tanner, K. G. Specific and Reversible Inactivation of Protein Tyrosine Phosphatases by Hydrogen Peroxide: Evidence for a Sulfenic Acid Intermediate and Implications for Redox Regulation†. *Biochemistry (Mosc.)* **1998**, *37*, 5633–5642.

(7) Arabaci, G.; Guo, X.-C.; Beebe, K. D.; Coggeshall, K. M.; Pei, D. A-Haloacetophenone Derivatives As Photoreversible Covalent Inhibitors of Protein Tyrosine Phosphatases. *J. Am. Chem. Soc.* **1999**, *121*, 5085–5086.

(8) Goldstein, B. J.; Mahadev, K.; Kalyankar, M.; Wu, X. Redox Paradox: Insulin Action Is Facilitated by Insulin-Stimulated Reactive Oxygen Species with Multiple Potential Signaling Targets. *Diabetes* **2005**, *54*, 311–321.

(9) Mahadev, K.; Motoshima, H.; Wu, X.; Ruddy, J. M.; Arnold, R. S.; Cheng, G.; Lambeth, J. D.; Goldstein, B. J. The NAD(P)H Oxidase Homolog Nox4 Modulates Insulin-Stimulated Generation of H2O2 and Plays an Integral Role in Insulin Signal Transduction. *Mol. Cell. Biol.* **2004**, *24*, 1844–1854.

(10) Parsons, Z. D.; Gates, K. S. Thiol-Dependent Recovery of Catalytic Activity from Oxidized Protein Tyrosine Phosphatases. *Biochemistry (Mosc.)* **2013**, *52*, 6412–6423.

(11) Dagnell, M.; Frijhoff, J.; Pader, I.; Augsten, M.; Boivin, B.; Xu, J.; Mandal, P. K.; Tonks, N. K.; Hellberg, C.; Conrad, M.; et al. Selective Activation of Oxidized PTP1B by the Thioredoxin System Modulates PDGF-B Receptor Tyrosine Kinase Signaling. *Proc. Natl. Acad. Sci.* **2013**, *110*, 13398–13403.

(12) Combs, A. P. Recent Advances in the Discovery of Competitive Protein Tyrosine Phosphatase 1B Inhibitors for the Treatment of Diabetes, Obesity, and Cancer. *J. Med. Chem.* **2010**, *53*, 2333–2344.

(13) Yue, E. W.; Wayland, B.; Douty, B.; Crawley, M. L.; McLaughlin, E.; Takvorian, A.; Wasserman, Z.; Bower, M. J.; Wei, M.; Li, Y.; et al. Isothiazolidinone Heterocycles as Inhibitors of Protein Tyrosine Phosphatases: Synthesis and Structure-Activity Relationships of a Peptide Scaffold. *Bioorg. Med. Chem.* **2006**, *14*, 5833–5849.

(14) Park, H. Structure-Based Virtual Screening Approach to Identify Novel Classes of PTP1B Inhibitors. *Eur. J. Med. Chem.* **2009**, *44*, 3280–3284.

(15) Shen, K.; Keng, Y.-F.; Wu, L.; Guo, X.-L.; Lawrence, D. S.; Zhang, Z.-Y. Acquisition of a Specific and Potent PTP1B Inhibitor from a Novel Combinatorial Library and Screening Procedure. *J. Biol. Chem.* **2001**, *276:*, 47311–47319.

(16) Johnson, T. O.; Ermolieff, J.; Jirousek, M. R. Protein Tyrosine Phosphatase 1B Inhibitors for Diabetes. *Nat. Rev. Drug Discov.* **2002**, *1*, 696–709.

(17) Combs, A. P.; Zhu, W.; Crawley, M. L.; Glass, B.; Polam, P.; Sparks, R. B.; Modi, D.; Takvorian, A.; McLaughlin, E.; Yue, E. W.; et al. Potent Benzimidazole Sulfonamide Protein Tyrosine Phosphatase 1B Inhibitors Containing the Heterocyclic (S)-Isothiazolidinone Phosphotyrosine Mimetic. *J. Med. Chem.* **2006**, *49*, 3774–3789.

(18) Wiesmann, C.; Barr, K. J.; Kung, J.; Zhu, J.; Erlanson, D. A.; Shen, W.; Fahr, B. J.; Zhong, M.; Taylor, L.; Randal, M.; et al. Allosteric Inhibition of Protein Tyrosine Phosphatase 1B. *Nat. Struct. Mol. Biol.* **2004**, *11*, 730–737.

(19) Salmeen, A.; Andersen, J. N.; Myers, M. P.; Meng, T.-C.; Hinks, J. A.; Tonks, N. K.; Barford, D. Redox Regulation of Protein Tyrosine Phosphatase 1B Involves a Sulphenyl-Amide Intermediate. *Nature* **2003**, *423*, 769–773.

(20) Van Montfort, R. L. M.; Congreve, M.; Tisi, D.; Carr, R.; Jhoti, H. Oxidation State of the Active-Site Cysteine in Protein Tyrosine Phosphatase 1B. *Nature* **2003**, *423*, 773–777.

(21) Haque, A.; Andersen, J. N.; Salmeen, A.; Barford, D.; Tonks, N. K. Conformation-Sensing Antibodies Stabilize the Oxidized Form of PTP1B and Inhibit Its Phosphatase Activity. *Cell* **2011**, *147*, 185–198.

(22) Lushchak, V. I. Glutathione Homeostasis and Functions: Potential Targets for Medical Interventions. *J. Amino Acids* **2012**, *2012*, e736837.

(23) Allison, W. S. Formation and Reactions of Sulfenic Acids in Proteins. *Acc. Chem. Res.* **1976**, *9*, 293–299.

(24) Pearson, R. G.; Dillon, R. L. Rates of Ionization of Pseudo Acids.1 IV. Relation between Rates and Equilibria. *J. Am. Chem. Soc.* **1953**, *75*, 2439–2443.

(25) Mofaddel, N.; Bar, N.; Villemin, D.; Desbène, P. Determination of Acidity Constants of Enolisable Compounds by Capillary Electrophoresis. *Anal. Bioanal. Chem.* **2004**, *380*, 664–668.

(26) Qian, J.; Wani, R.; Klomsiri, C.; Poole, L. B.; Tsang, A. W.; Furdui, C. M. A Simple and Effective Strategy for Labeling Cysteine Sulfenic Acid in Proteins by Utilization of B-Ketoesters as Cleavable Probes. *Chem. Commun.* **2012**, *48*, 4091–4093.

(27) Seo, Y. H.; Carroll, K. S. Quantification of Protein Sulfenic Acid Modifications Using Isotope-Coded Dimedone and Iododimedone. *Angew. Chem. Int. Ed.* **2011**, *50*, 1342–1345.

(28) Trost, B. M.; Curran, D. P. Chemoselective Oxidation of Sulfides to Sulfones with Potassium Hydrogen Persulfate. *Tetrahedron Lett.* **1981**, *22*, 1287–1290.

(29) MAGGIOLO ALLISON; BLAIR E. ALLAN. Ozone Oxidation of Sulfides and Sulfoxides. In *OZONE CHEMISTRY AND TECHNOLOGY*; Advances in Chemistry; AMERICAN CHEMICAL SOCIETY, 1959; Vol. 21, pp. 200–201.

(30) Hirano, M.; Tomaru, J.; Morimoto, T. A Convenient Synthesis of Sulfones by the Oxone Oxidation of Sulfides in an Aprotic Solvent in the Presence of Clay Minerals. *Bull. Chem. Soc. Jpn.* **1991**, *64*, 3752–3754.

(31) Katritzky, A. R.; Abdel-Fattah, A. A. A.; Wang, M. Efficient Conversion of Sulfones into B-Keto Sulfones by N-Acylbenzotriazoles§. *J. Org. Chem.* **2003**, *68*, 1443–1446.

(32) Russell, G. A.; Sabourin, E. T.; Hamprecht, G. .beta.-Keto Sulfoxides. V. Condensation of Dimethyl Sulfoxide and Dimethyl Sulfone with Dibasic Esters. *J. Org. Chem.* **1969**, *34*, 2339–2345.

(33) Morin, R. B.; Gordon, E. M.; Lake, J. R. Chemistry of Dehydropeptides. Formation of Isothiazolones and Isothiazolidones from Cysteinyl Peptides. *Tetrahedron Lett.* **1973**, *14*, 5213–5216.

(34) Pretsch, E.; Bühlmann, P.; Badertscher, M. *Structure Determination of Organic Compounds: Tables of Spectral Data*; 4th ed. 2009 edition.; Springer: Berlin, 2009.

(35) Riddles, P. W.; Blakeley, R. L.; Zerner, B. [8] Reassessment of Ellman's Reagent. In *Methods in Enzymology*; C.H.W. Hirs, S. N. T., Ed.; Academic Press, 1983; Vol. Volume 91, pp. 49–60.

(36) Riddles, P. W.; Blakeley, R. L.; Zerner, B. Ellman's Reagent: 5,5′-dithiobis(2-Nitrobenzoic Acid)—a Reexamination. *Anal. Biochem.* **1979**, *94*, 75–81.

(37) Whitesides, G. M.; Lilburn, J. E.; Szajewski, R. P. Rates of Thiol-Disulfide Interchange Reactions between Mono- and Dithiols and Ellman's Reagent. *J. Org. Chem.* **1977**, *42*, 332–338.

(38) Parsons, Z. D.; Gates, K. S. Redox Regulation of Protein Tyrosine Phosphatases: Methods for Kinetic Analysis of Covalent Enzyme Inactivation. *Methods Enzymol.* **2013**, *528*, 129–154.

(39) Guthrie, J. P. Carbonyl Addition Reactions: Factors Affecting the Hydrate–Hemiacetal and Hemiacetal–Acetal Equilibrium Constants. *Can. J. Chem.* **1975**, *53*, 898–906.

Chapter 5: Covalent Capture of Oxidatively-Inactivated PTP1B by Carbon Nucleophiles

5.1 Introduction

The observation that carbonyl- and sulfone-based carbon acids were capable of covalently capturing a small molecule model sulfenyl amide (Chapters 3 and 4) gave us confidence that such agents might be capable of covalent capturing oxidatively-inactivated PTP1B. Additionally, evidence that these adducts were stable in the presence of thiol suggested that these nucleophilic agents may be capable of preventing thiol-mediated recovery of oxidatively-inactivated PTP1B. As stated earlier, Tonks' group recently reported that antibody-mediated capture of oxidatively-inactivated PTP1B resulted in enhanced phosphorylation of the insulin receptor and prevented phosphine-mediated reactivation of PTP1B.[1] These results suggested that capture of oxidatively-inactivated PTP1B and associated blocking of thiol-mediated recovery of PTP activity in a cell might be a viable approach to attenuating the enzyme's activity *in vivo* for therapeutic purposes. Additionally, it has been established that cyclic and acyclic 1,3-diketone agents may be used for the detection of protein sulfenic acids in cellular environments.[234] Similar to the sulfenyl amide, sulfenic acids feature an electrophilic divalent sulfur atom. Taken together, these results suggest that carbon acids such as those

described in Chapters 3 and 4 may be useful agents for the covalent capture of the electrophilic sulfenyl amide moiety *in vivo.*

Results

5.2 Screening of Nucleophilic Agents for Ability to Prevent Thiol-Mediated Recovery of Oxidatively-Inactivated PTP1B ($PTP1B_{ox}$)

In order to assess whether these agents might be capable of blocking thiol-mediated recovery, we first had to develop an assay by which to monitor this process. In general, these assays involved first generating of a stock of oxidatively-inactivated PTP1B by treatment of the enzyme with H_2O_2 followed by catalase quench and storage on ice. Typically, $PTP1B_{ox}$ stocks were prepared by treating the native enzyme with 1 mM H_2O_2 for 5 minutes at 25°C followed by addition of catalase to ~ 200 un/mL, final concentration. The oxidatively-inactivated PTP was then treated with nucleophilic agent under the desired conditions, aliquots removed from the reaction mixture and diluted into buffer containing an large excess of thiol, and the samples assayed for recovered PTP activity.

We first acquired a modest library of commercially-available compounds bearing "active" methylene or methine groups (-CH_2- or >CH- groups bonded to two or more electron-withdrawing substituents, Table 5.1). Molecules for which aqueous pK_a values were determined (as described in Chapters 3 and 4) are reported in Table 5.1.

Code	Structure	pKa	Code	Structure	pKa
A	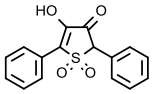	8.6	**S**	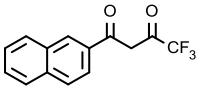	6.0
B	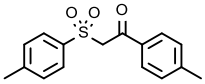	9.7	**T**	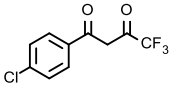	5.6
D	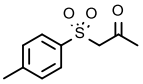	n/a	**U**	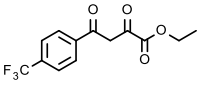	n/a
E		n/a	**W**	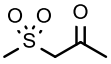	10.0
F	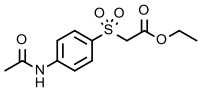	n/a	**X**	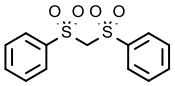	10.9
G	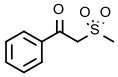	9.3	**Y**	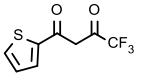	n/a
H	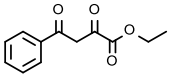	5.6	**Z**	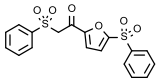	7.0
J	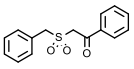	8.6	**AA**	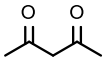	8.8
L	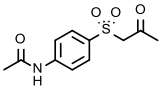	n/a	**BB**	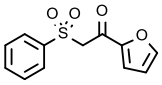	9.2
M	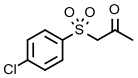	9.1	**CC**	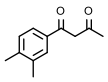	n/a
N	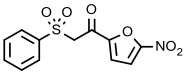	n/a	**DD**		4.9
O	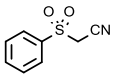	11.0	**FF**	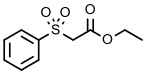	n/a
P	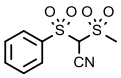	n/a	**GG**	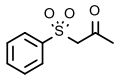	9.3
Q	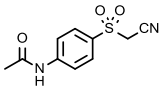	n/a	**HH**	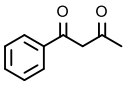	8.3
R	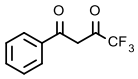	6.0	**JJ**	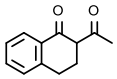	n/a

Table 5.1. Structures and aqueous pK_a values of keto- and sulfone-based carbon acids.

We then assayed these agents in the manner described above for their abilities to prevent thiol-mediated recovery of PTP activity from oxidatively-inactivated PTP1B. We first conducted an assay intended to (a) determine a "rank order" of these agents in their abilities to prevent thiol-mediated recovery of PTP activity, and (b) probe whether these agents might resist displacement by thiol under protracted incubation time. To this end, we treated oxidatively-inactivated PTP1B with a subset of the library presented in Table 5.1. All agents were 1 mM concentration in this assay, and allowed to react with oxidatively-inactivated PTP1B for 105 minutes at 37°C (pH 7.0). Following this time, the samples were diluted with buffer containing glutathione (60 mM, final conc, pH 7.0, 23 ± 2°C) and the samples assayed for recovered PTP activity following 15 minutes' treatment with GSH and again at 105 minutes' treatment with GSH (Figure 5.1). The results of this assay revealed tremendous stratification in these agents' abilities to prevent thiol-mediated recovery of $PTP1B_{ox}$. Most notably, agents **N**, **S**, **Z**, and **T** seemed to be much more efficient at preventing reactivation of oxidatively-inactivated PTP than other agents. These observations suggested that 1,3-diketones (**S** and **T**) and β-keto sulfones (**N** and **Z**) may be equally efficient in capturing $PTP1B_{ox}$. Furthermore, protracted incubation with a large excess of glutathione did not appear to displace these agents, suggesting stable bonds to the oxidatively-inactivated PTP (Figure 5.1B).

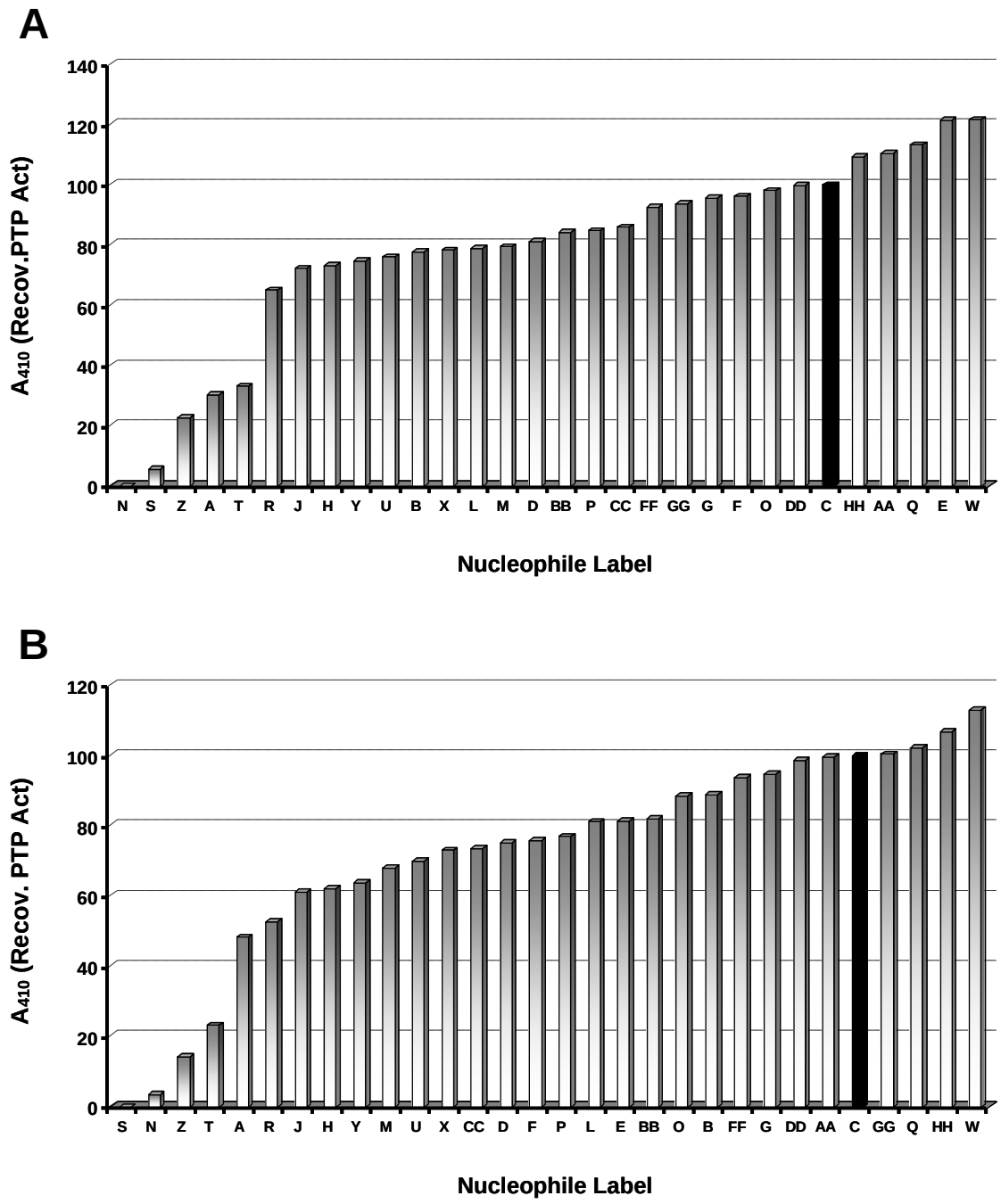

Figure 5.1. Screening of a subset of the carbon acid library for ability to prevent thiol-mediated recovery of PTP1B$_{ox.}$ Carbon nucleophiles (1 mM) were allowed to react with PTP1B$_{ox}$ for 105 min at 37°C (pH 7.0). (**A**) Recovered PTP activity relative to the control (bold bar, "C") after treatment with GSH (60 mM, pH 7.0, 15 min). (**B**) Recovered PTP activity after 105 min treatment with 60 mM GSH.

We then carried out another screening assay with two major modification to that described above: (1) the "trapping phase" of the reaction was conducted at pH 8.0 instead of pH 7.0, and (2) *time-dependent* capture of oxidatively-inactivated $PTP1B_{ox}$ was screened for. Regarding the latter, fixed concentrations of nucleophilic agent were used (1 mM), and the mixtures assayed for thiol-recoverable activity at various times during incubation with agent in pH 8.0 buffer (at 15, 60, and 105 minutes). The reactivation phase was carried out in pH 6.0 buffer containing 60 mM DTT and allowed to proceed for 15 minutes before samples were assayed for recovered PTP activity. The results of this "kinetic screen" are shown in Figure 5.2.

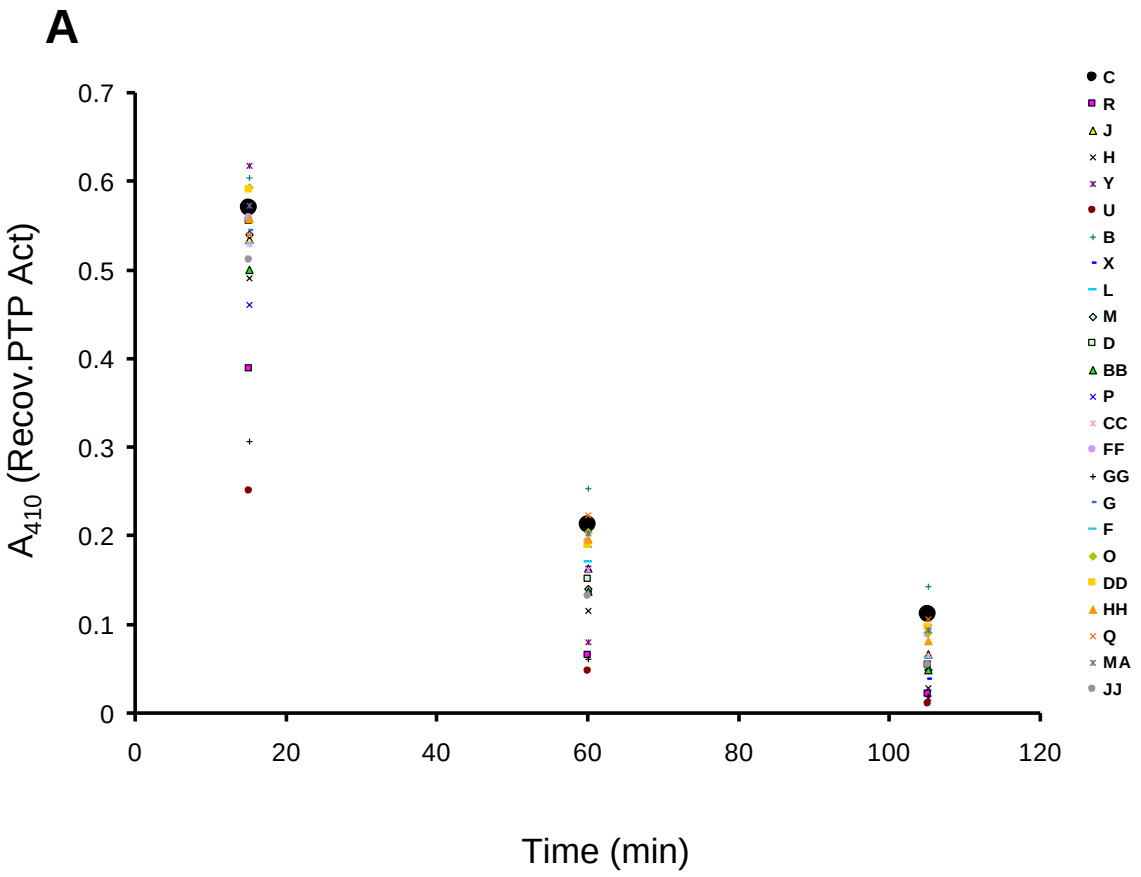

B

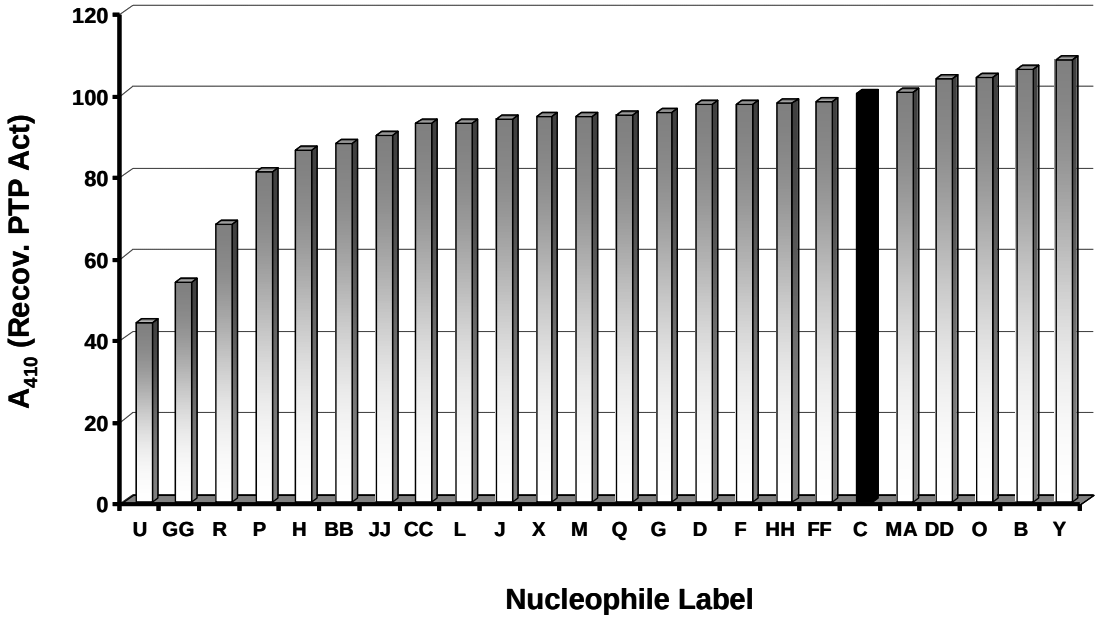
120
100
80
60
40
20
0
A410 (Recov. PTP Act)
U GG R P H BB JJ CC L J X M Q G D F HH FF C MA DD O B Y
Nucleophile Label

C

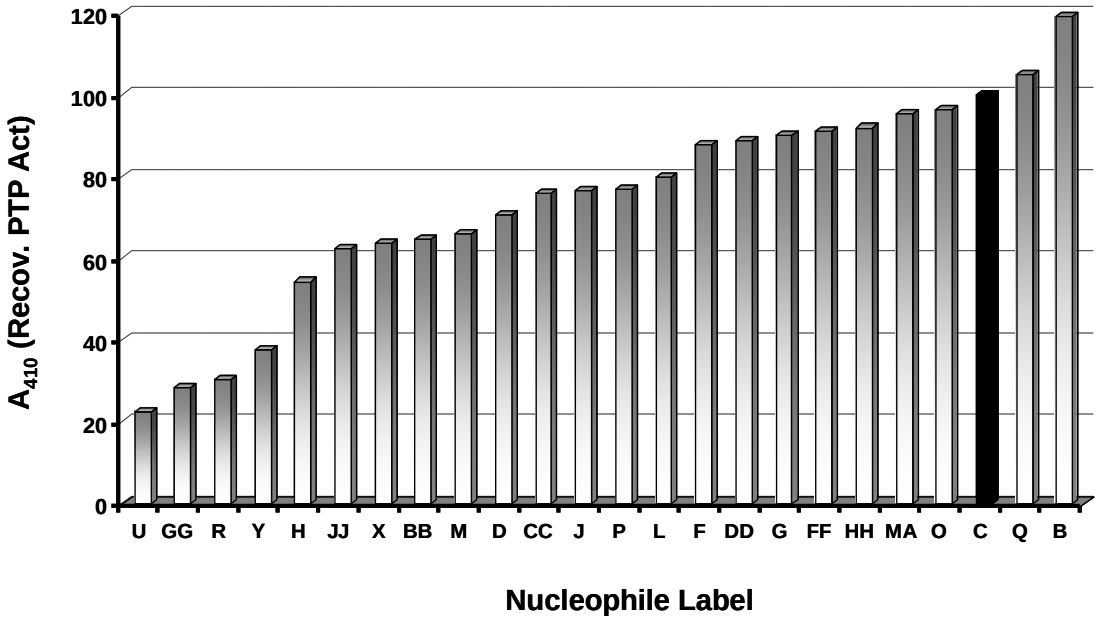
120
100
80
60
40
20
0
A410 (Recov. PTP Act)
U GG R Y H JJ X BB M D CC J P L F DD G FF HH MA O C Q B
Nucleophile Label

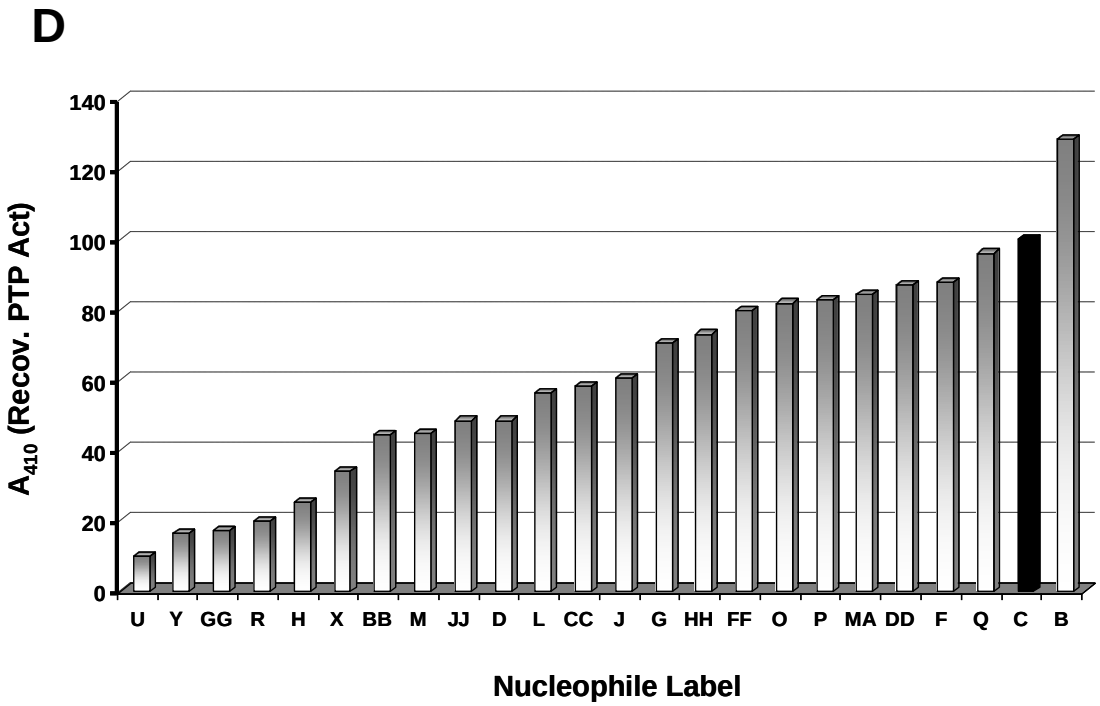

Figure 5.2. "Kinetic screening" of carbon nucleophiles at pH 8.0. Carbon nucleophiles (1 mM) were allowed to react with $PTP1B_{ox}$ at 37°C, pH 8.0. (**A**) Raw data. Recovered PTP activity (A_{410}) versus time of treatment with each nucleophile (15, 60, and 105 min). (**B**) Percent recovered activity (relative to the control) at 15 min. (**C**) Percent recovered activity at 60 min. (**D**) Percent recovered activity at 105 min.

Consistent with expectations, time-dependent loss of thiol-recoverable activity relative to the control was observed in most of the series. Interestingly, we noted time-dependent loss of thiol-recoverable activity in the *absence* of agent, as well (in the control series, C). This observation is explicitly addressed in Chapter 6 of this thesis. Importantly, this assay revealed, for several agents, accelerated loss of thiol-recoverable activity in a time-dependent fashion, relative to the control. Namely, the amount of thiol-recoverable activity decreased with time, consistent with chemical reaction/covalent bond formation. It is worth noting here that agents **N**, **S**, **Z**, and **T** were not screened in this

assay, having proved previously to be among the most potent inhibitors of thiol-mediated recovery of PTP activity in the library. Execution of the assay at pH 8.0 was intended to promote ionization of more weakly-acidic carbon acids and reveal further stratification in the library with regard to these agents' abilities to prevent thiol-mediated recovery of PTP activity. Indeed, differences in the amount of thiol-recovered activity following incubation with agents for 105 minutes (Figure 5.2D) revealed a large spread in abilities to prevent thiol-mediated recovery of PTP activity.

5.3 Nucleophilic Agents do not Inhibit or Inactivate Native PTP1B

We next sought to provide evidence that the loss of thiol-recoverable activity produced by these agents was due to covalent modification of the *oxidized* enzyme, and not to modification of native PTP1B. To this end, we examined prototypical members of the 1,3-diketone and β-keto sulfone classes of carbon acids in assays with native enzyme (Figure 5.3). Along these lines, we conducted assays of two types: a discontinuous or "time-point" assay (Figure 5.3A), and a continuous assay (Figure 5.3B). The time-point assay design allows for straightforward monitoring of time-dependent processes, but sometimes "misses" fast, reversible processes such as enzyme inhibition.[5] The continuous assay, on the other hand, provides less straightforward kinetic data in some cases, but reveals enzyme inhibition processes. In both assays, we found that representative 1,3-diketones and β-keto sulfones did not cause time-dependent loss of PTP activity from native PTP1B (inactivation) or "time-independent" suppression of PTP activity (inhibition).

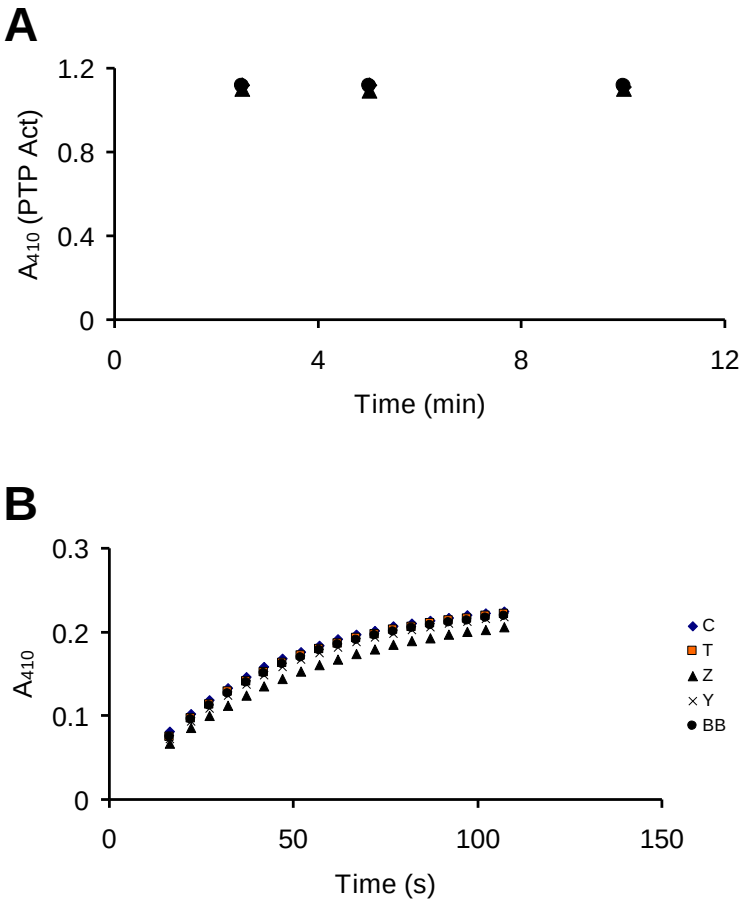

Figure 5.3. Various nucleophilic agents do not inactivate or inhibit native PTP1B. (**A**) Discontinuous assay data. Native PTP1B was treated with 500 μM agent **S** (triangles), **Z** (diamonds), or with no agent (circles) at pH 7.0, 37°C in the presence of 5 mM DTT. No loss of enzyme activity was observed in any series. (**B**) Continuous assay data. Native PTP1B was introduced to a buffered solution (pH 7.0) containing substrate (pNPP, 22 mM) and nucleophilic agent (500 μM). Release of 4-nitrophenol was monitored at A_{410} over time. No apparent inhibition or inactivation by these agents were observed.

5.4 Evidence for Covalent Modification of $PTP1B_{ox}$ by Compound S

Having established that these agents do not inhibit or inactivate native PTP1B under the conditions employed, we turned our attention to providing evidence that these agents function by covalent modification of oxidatively-inactivated PTP1B. Along these

lines, we selected 1,3-diketone **S** as a representative member of the "nucleophilic trappers" and treated oxidatively-inactivated PTP1B with the agent (1 mM, pH 7.0, 37°C, 20 min). Following this time, excess agent was removed by gel filtration and the enzyme stock assayed for thiol-recoverable activity against a control sample treated identically, but without subjection agent **S**. In this case, recovered enzyme activity was monitored during a continuous assay, where the treated and untreated $PTP1B_{ox}$ stocks were added to a cuvette containing both *p*NPP substrate and DTT (17 mM and 40 mM, respectively, pH 7.0, Figure 5.4).

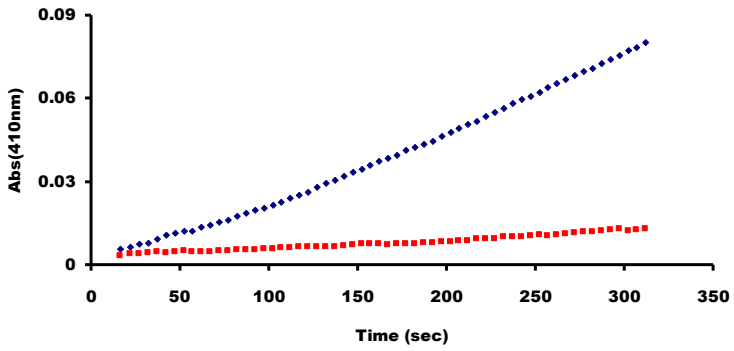

Figure 5.4. Evidence for covalent modification of $PTP1B_{ox}$. Thiol-mediated recovery of PTP activity was inhibited when $PTP1B_{ox}$ had been treated with 1 mM **S** and excess agent removed by gel filtration (red trace), relative to the control (blue trace).

5.5 Nucleophilic Agents can "Outcompete" Thiol for Reaction with $PTP1B_{ox}$

We were interested to determine whether these agents might be capable of trapping $PTP1B_{ox}$ in the *presence* of thiol agent. That is, we wondered if these agents might be capable of "outcompeting" thiol with respect to rate of nucleophilic attack on

the sulfenyl amide. To this end, we introduced oxidatively-inactivated PTP1B to a buffered solution (pH 7.0) containing substrate (20 mM pNPP) and either glutathione alone (10 mM) or in the presence of **S** (1 mM). We found that **S** successfully prevented thiol-mediated recovery of some portion of the oxidatively-inactivated PTP, even in the presence of an order of magnitude greater concentration of thiol (Figure 5.5).

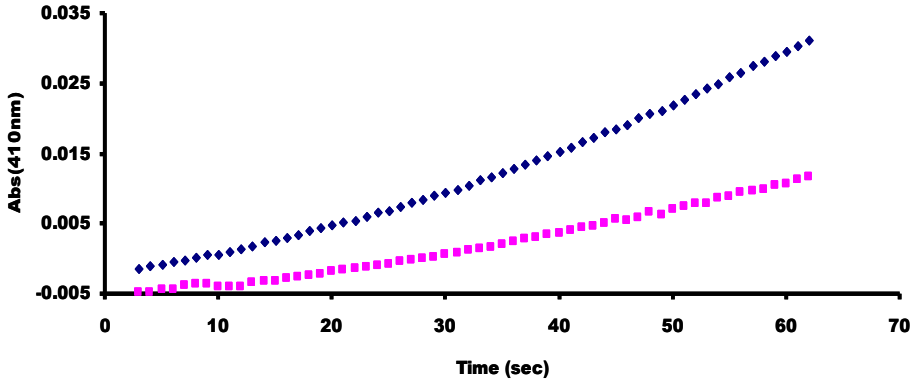

Figure 5.5. Agent **S** (1 mM) successfully captures a portion of the $PTP1B_{ox}$ population, even in the presence of 10-fold excess of glutathione (GSH, 10 mM). Glutathione alone (blue trace), and GSH + 1 mM **S** (pink trace).

5.6 Kinetics of "Trapping" Reactions: Determination of Reaction Order and Rate Constants for Representative Nucleophilic Agents S and Z

To corroborate the proposed mechanism of action of these agents, we set out to determine reaction order and rate constants for the trapping of $PTP1B_{ox}$ by a subset of nucleophilic agents. We selected diketone **S** and β-keto sulfone **Z** as representative members of each class of trapping agent to pursue in these detailed kinetics studies. It is worth noting that, although screening revealed that β-keto sulfone **N** was also efficient at

trapping $PTP1B_{ox}$, it was not pursued in these studies due to overlapping absorbance with the chromaphoric product of enzyme activity assays (4-nitrophenol(ate), A_{410} – compound **N** was ostensibly yellow in solution).

We first treated oxidatively-inactivated PTP1B with large molar excesses of compound **S** at pH 7.0, 37 °C, and assayed the reaction mixture for thiol-recoverable activity at various time points (Figure 5.6A and B). We found that diketone **S** caused time- and concentration-dependent loss of thiol-recoverable activity relative to the control (no agent), in a manner consistent with covalent modification. We then inspected a natural logarithm replot of the data normalized against the control series for linearity (Figure 5.6C). Indeed, linear regressions fit well to the data ($r^2 \geq 0.99$), indicative of (pseudo) first-order processes. A plot of the pseudo first-order rate constants versus molar concentration of **S** afforded a straight line, consistent with a process first-order in diketone and second-order overall (Figure 5.6D). The apparent second-order rate constant for this process was $2.9 \pm 0.3\ M^{-1}\ s^{-1}$. Interestingly, this rate constant is roughly identical to that determined for covalent capture of the *model* dipeptide sulfenyl amide in 1:1 MeOH/pH 7 buffer, as reported in Chapter 3 ($\sim 2\ M^{-1}\ s^{-1}$).

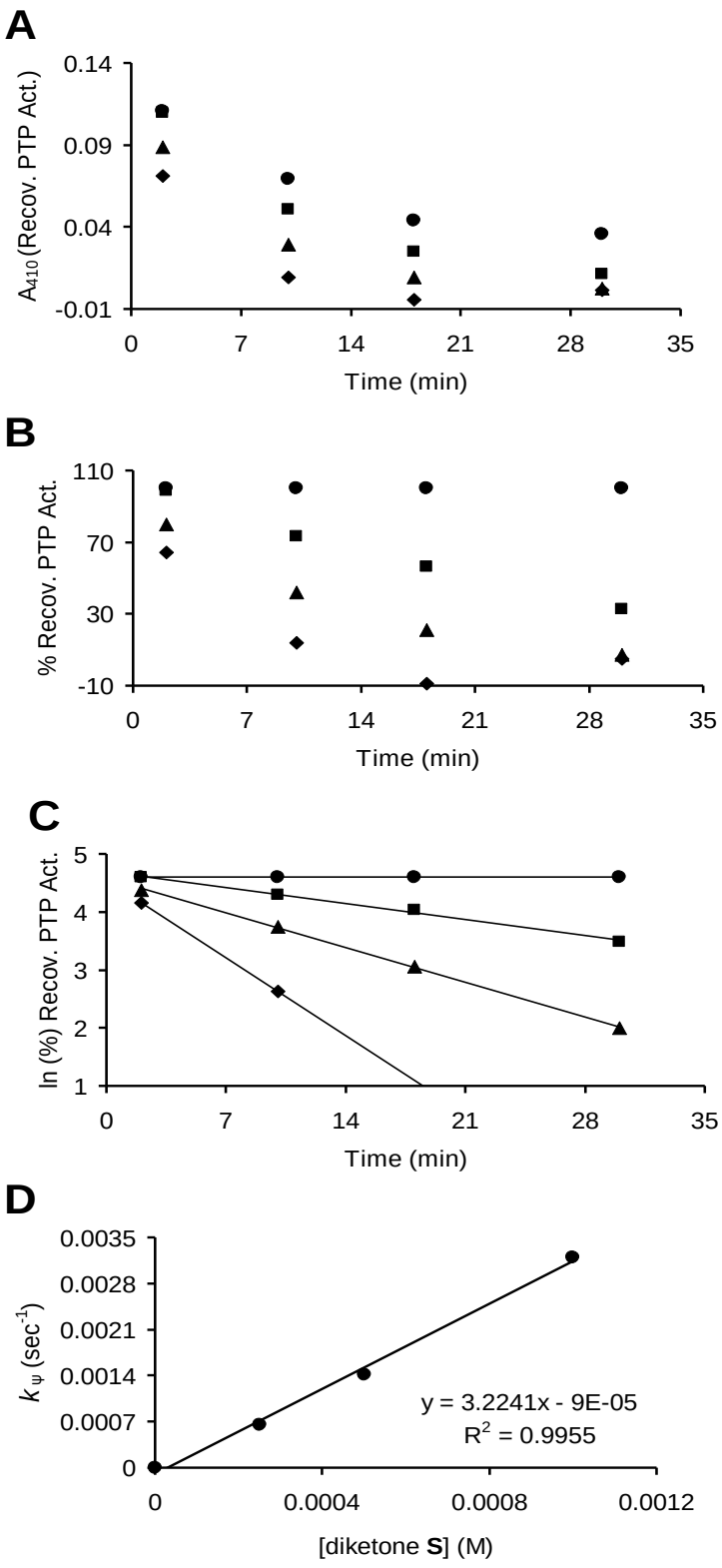

Figure 5.6. Kinetics of trapping $PTP1B_{ox}$ by diketone **S** (pH 7.0, 37 °C). (**A**) Raw data. Recovered PTP activity from $PTP1B_{ox}$ following treatment with 0, 250, 500, or 1000 μM

S (circles, squares, triangles, and diamonds, respectively) for 2, 10, 18, and 30 min (reactivation *via* treatment with 40 mM GSH for 4 min, pH 7.0, r.t.). (**B**) Percent recovered PTP activity, normalized to the control series. (**C**) Natural logarithm replot of the kinetic data. (**D**) Pseudo first-order rate constants (negative slopes of lines from ln plot) versus molar concentration of **S**. Linearity in this plot suggests a process first-order in compound **S** and second-order overall. Averaging the apparent second-order rate constants at each concentration of **S** affords 2.9 ± 0.3 M^{-1} s^{-1}.

We then conducted a similar assay to that directly above to verify these results, examining diketone **S** again and β-keto sulfone **Z** in parallel. Again, we observed time- and concentration-dependent loss of thiol-recoverable activity in the presence of both of these agents (Figure 5.7A). We noted that loss of thiol-recoverable activity was ostensibly faster when $PTP1B_{ox}$ was treated with **Z** relative to **S** at the same concentrations of agent. We analyzed the kinetic data from these trials by non-linear, least-squares regression analysis, fitting pseudo first-order kinetic models to the data. Extraction of pseudo first-order rate constants and plotting them as a function of carbon nucleophile concentration again suggested good linear dependence of k_ψ on nucleophile concentration (Figure 5.7B and C). Importantly, the apparent second-order rate constant determined in this trial for compound **S** matched well that determined above (3.7 ± 0.7 M^{-1} s^{-1}). Consistent with visual inspection of the data, the apparent second-order rate constant for trapping $PTP1B_{ox}$ by β-keto sulfone **Z** was approximately two-fold larger than that observed for **S** (**Z**; k_{trap} = 5.9 ± 0.8 M^{-1} s^{-1}). These results were interesting in light of the work done on trapping of the model sulfenyl amide by diketones and β-keto sulfones described in Chapters 3 and 4 herein. Indeed, in trapping both the model sulfenyl amide and that of $PTP1B_{ox}$, we found that β-keto sulfones were consistently more

efficient (faster) in capturing the sulfenyl amide moiety than 1,3-diketones were, despite the fact that β-keto sulfones were generally less acidic than the corresponding diketones.

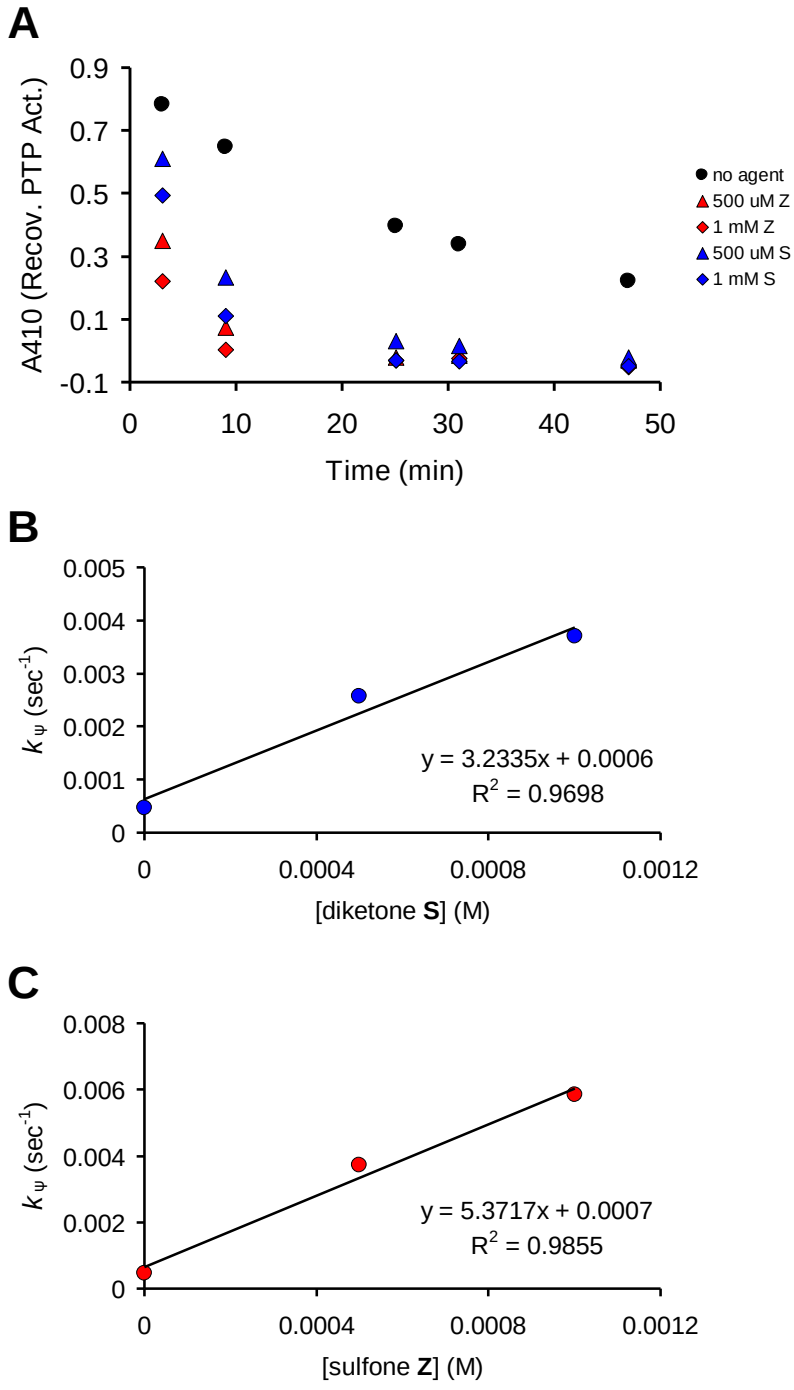

Figure 5.7. Kinetics of trapping $PTP1B_{ox}$ by diketone **S** and β-keto sulfone **Z** (pH 7.0, 37 °C). (**A**) Raw data. Recovered PTP activity following treatment as indicated in the figure

legend. The reactions were assayed at 3, 9, 25, 31, and 47 min and recovery of PTP activity achieved by treatment with 60 mM DTT (pH 8.0, 3 min).

5.7 Diketone S does not Efficiently Capture Oxidatively-Inactivated SHP-2

Finally, we set out to determine whether these nucleophilic agents might display selectivity for capture of oxidatively-inactivated PTP1B (i.e. a sulfenyl amide) over other oxidatively-inactivated PTP family members. SHP-2 is a member of the PTP family involved in immune response and hematopoiesis.[67] Oxidatively-inactivated SHP2 is believed to exist as a surface-exposed disulfide,[8910] in contrast to the sulfenyl amide of $PTP1B_{ox}$. Using well-established protocols,[11] we inactivated SHP-2 with hydrogen peroxide (1 mM) and then treated the resulting $SHP2_{ox}$ with compound **S** under conditions shown previously to prevent thiol-mediated recovery from $PTP1B_{ox}$ (1 mM **S** for 22 min at 37 °C in pH 7.0 buffer, see Figure 5.4 for reference). Following incubation with **S**, we added either treated $SHP2_{ox}$ or untreated $SHP2_{ox}$ to a cuvette containing pNPP substrate (25 mM final conc). We allowed the PTP_{ox} to stand in buffer containing substrate for approximately 1 minute to confirm inactivity before adding DTT to final concentration 40 mM. Indeed, this data revealed that PTP activity was recovered from oxidatively-inactivated SHP2, both when the PTP had been treated or not treated with compound **S** (Figure 5.8). It is not yet clear whether this reflects sluggish reaction kinetics between $SHP2_{ox}$ and the diketone, or if a covalent bond formed between the diketone and the PTP might be thiol-labile. In either case, the data suggests that

nucleophilic capture of oxidatively-inactivated PTPs may offer inherent, reaction-based selectivity.

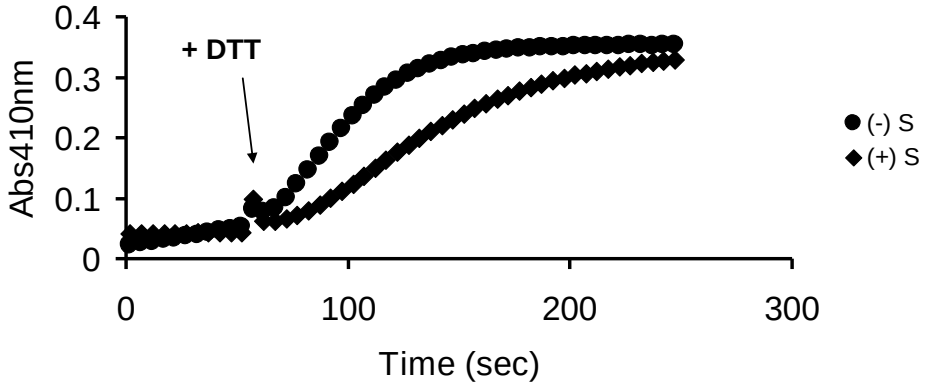

Figure 5.8. Compound **S** does not block thiol-mediated recovery of oxidatively-inactivated SHP2 when employed under the same conditions as those which afford blocking of thiol-mediated recovery of $PTP1B_{ox}$.

5.8. Discussion

Results from the screening assays (Figures 5.1 and 5.2) revealed several interesting structure-activity relationships among the various carbon nucleophiles. Notably, trifluoromethyl 1,3-diketones **S** and **T** were appreciably better at capturing $PTP1B_{ox}$ than the analogous 1,3-diketone **R**, though they all were of similar pK_a values (5.6 – 6.0). Compounds **S** and **T** bore bulkier aryl substituents than the simple phenyl group of **R** (naphthyl and *p*-Cl phenyl, respectively in **S** and **T**). The enhanced abilities of **S** and **T** relative to **R** in preventing thiol-mediated recovery of PTP activity from

$PTP1B_{ox}$ may reflect noncovalent interactions between the oxidized enzyme and hydrophobic naphthyl and *p*-Cl phenyl substituents, driving the trapping reaction. However, pK_a of the parent carbon acid may still play an important role in ability to capture the $PTP1B_{ox}$ sulfenyl amide. For example, compounds **HH** and **R** differ structurally only in substitution of a terminal methyl group for a trifluoromethyl group (-CH_3 in **HH**, -CF_3 in **R**). This substitution has a marked impact on pK_a (pK_a **HH** 8.3, pK_a **R** 6.0) which may be the basis for why compound **R** more effectively prevented thiol-mediated reactivation of $PTP1B_{ox}$ than did **HH** (Figure 5.2). Nevertheless, compound **R** captured the *model* sulfenyl amide more slowly than did compound **HH** (Chapter 3, called **H** and **E** there, respectively). The basis for this apparent "inversion" of sulfenyl amide capturing ability is not yet understood.

Interestingly, known protein sulfenic acid capturing agent dimedone (**DD**)[3] fared quite poorly in capturing the $PTP1B_{ox}$ sulfenyl amide (Figure 5.1 and 5.2). Almost certainly, the fraction of dimedone in nucleophilic, enolate form under our screening assay conditions was near unity (pK_a dimedone ~ 4.9, assay buffers pH 7.0 and 8.0). Results from the "kinetic screening" of nucleophilic agents (Figure 5.2) revealed that dimedone caused slow, time-dependent loss of thiol-recoverable PTP activity. Taken together, these results suggest that the dimedone enolate functions poorly as a nucleophile against the $PTP1B_{ox}$ sulfenyl amide. However, dimedone was "middle of the pack" in rate of trapping the model sulfenyl amide (Chapter 3, k_{trap} ~ 6 M^{-1} s^{-1}). This disparity may reflect an inability of the dimedone enolate α-carbon to access the electrophilic sulfur atom in the $PTP1B_{ox}$ sulfenyl amide (in short: steric occlusion of the carbon nucleophile from the sulfur electrophile, Scheme 5.2). Because rotation about

sigma bonds is restricted in cyclic systems, dimedone and analogues thereof may lack a necessary conformational flexibility for fast reaction with the $PTP1B_{ox}$ sulfenyl amide (a speculated-upon phenomenon we have nicknamed the "bull horn effect"). It is worth pointing out that Meldrum's acid (**MA**), the diester lactone analogue of dimedone, is both equally acidic as dimedone (pK_a **MA** ~ 4.8) and equally as inept at capturing $PTP1B_{ox}$ (Figure 5.2). These speculations may be supported by consideration of reactions wherein roles are reversed: namely, when the PTP functions as the nucleophilic agent and the small molecule the electrophile. For example, Pei's group has shown that α-bromoketones are effective alkylators of native PTP1B.[12] However, work presented in Chapter 8 of this thesis revealed that allyl bromide does *not* alkylate PTP1B. Importantly, an α-bromoketone and an allylic bromide might be considered isosteric to one another (Figure 5.9). Thus, it stands to reason – if modest changes to electrophile structure can abrogate reaction with native PTP1B – that the same structural "intolerance" might be expected upon role reversal (small molecule nucleophiles with electrophilic PTP).

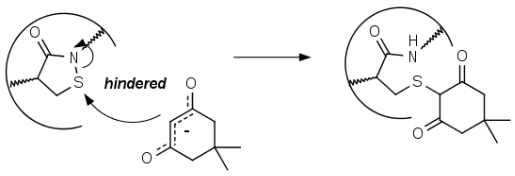

Scheme 5.1. Nucleophilic attack of dimedone enolate α-carbon on the $PTP1B_{ox}$ sulfenyl amide may be sterically-hindered by pairing of conformationally-locked groups in the enolate and occlusion of the sulfenyl amide sulfur.

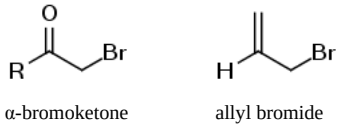

α-bromoketone allyl bromide

Figure 5.8. Allyl bromide and α-bromoketones may be considered isosteric.

5.9. Conclusions

Here we have demonstrated that structurally-diverse carbon acids based predominantly on 1,3-diketo and β-keto sulfone scaffolds are capable of preventing thiol-mediated recovery of PTP activity from oxidatively-inactivated PTP1B ($PTP1B_{ox}$) with greatly varying rates of reaction. We found that these agents prevented thiol-mediated recovery of PTP activity in time- and concentration-dependent fashions, consistent with covalent bond formation. Furthermore, we showed that removal of excess agent by gel filtration following treatment of the oxidized PTP did not reverse the effect of inhibiting thiol-mediated recovery of enzyme activity, suggesting irreversible covalent bond formation. We then determined reaction order and rate constants for trapping oxidized PTP1B by representative agents from each class of carbon acid (compound **S** of the 1,3-diketones and **Z** of the β-keto sulfones). We found that these processes were first-order in carbon nucleophile, consistent with overall bimolecular kinetics. These kinetics were in agreement with a reaction mechanism involving rate-limiting attack of the carbon nucleophile on the PTP sulfenyl amide. Rate constants for these processes were 2.9 ± 0.3 M^{-1} s^{-1} and 5.9 ± 0.8 M^{-1} s^{-1} for compounds **S** and **Z**, respectively (pH 7.0, 37 °C).

Finally, we provided evidence that these agents are selective for covalent capture of oxidatively-inactivated PTP1B over PTP family member SHP2. Crystallographic evidence from multiple groups suggests that oxidative inactivation of PTP1B results in formation of a 5-membered sulfenyl amide, whereas mass spectrometric and kinetic data suggest that oxidatively-inactivated SHP2 forms a surface-exposed disulfide. Taken together, these results may provide evidence that nucleophilic carbon species preferentially react with some sulfur electrophiles found in biomolecules, but not others.

5.10 Methods and Materials

Buffer compositions.

Buffer X (pH 6.0): 100 mM Bis-Tris, 100 mM NaCl, 10 mM DTPA.

Buffer Y (pH 7.0): 50 mM Tris, 50 mM Bis-Tris, 100 mM NaOAc, 10 mM DTPA

Buffer Z (pH 8.0): 100 mM Tris, 100 mM NaOAc, 10 mM DTPA

Buffer A (pH 6.0): 50 mM Bis-Tris, 100 mM NaCl, 10 mM DTPA

Note: an asterisk indicates addition of Tween 80 (0.5 %, v/v) *to the indicated buffer.*

Screening of nucleophilic agents at pH 7.0 for thiol-stability in the presence of glutathione. PTP1B $_{ox}$ (10 μM, in buffer Y*) was prepared by combination of 60 μL 22 μM thiol-free PTP1B with 67 μL 1.9 mM H_2O_2 and incubation at 37 °C for 4 min prior to addition of 2 μL of catalase stock (17,000 un/mL). All agents were prepared in buffer Y*. Stocks of nucleophilic agents (2 mM) were prepared via dilution of concentrated primary

stocks (50 mM in dmso) into buffer Y*. Upon mixing of $PTP1B_{ox}$ and nucleophile (1:1, v/v, 4 μL each), a timer was started. The PTP_{ox} and agents were incubated for 105 minutes at 37 °C before removal of 5 μL aliquots from each mixture and dilution into 45 μL buffer Y* containing GSH (60 mM, final conc). The reactivation phase was allowed to proceed for 15 and 105 min at 23 ± 2 °C before being assayed for recovered PTP activity (10 μL aliquots removed, diluted into 490 μL buffer A containing 20 mM pNPP, 15 min activity assay at 23 ± 2 °C before addition of 500 μL 2 M NaOH to quench).

Screening of nucleophilic agents at pH 8.0. A 1 mL stock of $PTP1B_{ox}$ (2.2 μM in buffer Z*) was prepared by addition of 100 μL of 22 μM thiol-free PTP1B in buffer Z* to 900 μL of 1 mM H_2O_2 in buffer Z*. The mixture was incubated for 5 min at 23 ± 2 °C before quenching of excess hydrogen peroxide by addition of 2 μL of catalase stock (84,400 un/mL, 170 un/mL final). Stocks of nucleophilic agent (2 mM in buffer Z*) were prepared as described above. Upon combination of $PTP1B_{ox}$ and agents at 37 °C, a timer was started and aliquots (10 μL) were removed from the reaction mixtures at 15, 60, and 105 min and diluted into ready-made samples containing DTT in buffer X* (DTT 60 mM, final conc). Samples were incubated with DTT for 15 min at 23 ± 2 °C prior to assay for recovered PTP activity (done as described above).

***Determination of rate constant for trapping the $PTP1B_{ox}$ sulfenyl amide by agents* S.** A stock of $PTP1B_{ox}$ (8 μM in buffer Y*) was prepared in a manner similar to that described earlier. A concentrated stock (200 mM) of compound **S** was prepared in dmso and diluted to 2x concentrations in buffer Y*. Additional dmso was added to each stock as needed to bring the final concentration of dmso in each sample to 1 % (v/v). $PTP1B_{ox}$ and 2x agent were then combined 1:1 (v/v, 5 μL each) and incubated at 37 °C.

At 2, 10, 18, and 30 min intervals, aliquots (2 μL) were removed from the reaction mixtures and diluted into ready-made 18 μL samples of GSH in buffer Y* (GSH 40 mM, final conc). The reactivation phase was allowed to proceed for 4 min at 23 ± 2 °C before samples were assayed for recovered PTP activity as described above.

***Determination of rate constants for trapping oxidized PTP1B: agent Z and reevaluation of agent* S.** Stocks of $PTP1B_{ox}$ (1 μM) and agents **S** and **Z** (2x conc) were prepared in buffer Y* in manners previously described. Upon combination of these stocks at 37 °C, a timer was started and aliquots (10 μL) were removed from the reaction mixtures at 3, 9, 25, 31, and 47 min and diluted into ready-made 40 μL samples containing DTT in buffer Z* (DTT 60 mM, final conc). The reactivation phase was allowed to proceed for 3 min at 23 ± 2 °C before the samples were assayed for recovered PTP activity via direct addition of 450 μL of 22.2 mM pNPP in buffer X to the samples. The activity assay was allowed to proceed at 23 ± 2 °C for 10 min before quenching with 500 μL of 2 M NaOH.

***Evidence of covalent modification of $PTP1B_{ox}$ by agent* S.** $PTP1B_{ox}$ (3 μM in buffer Y*) was prepared in a manner similar to that described above. The stock was split into two 85 μL portions. To one portion were added 1.7 μL of 50 mM agent **S** in dmso; to the other portion, 1.7 μL of dmso alone were added. Both treated and untreated stocks were incubated at 37 °C for 20 min prior to being subjected to gel filtration, as previously described.[11138] Then, 30 μL of either treated or untreated PTP were added to cuvettes containing 470 μL DTT and pNPP (final concentrations: DTT 40 mM, pNPP 17 mM, and PTP 180 nM). A similar protocol was followed in the case of work done with SHP2.

References

(1) Haque, A.; Andersen, J. N.; Salmeen, A.; Barford, D.; Tonks, N. K. Conformation-Sensing Antibodies Stabilize the Oxidized Form of PTP1B and Inhibit Its Phosphatase Activity. *Cell* **2011**, *147*, 185–198.

(2) Qian, J.; Wani, R.; Klomsiri, C.; Poole, L. B.; Tsang, A. W.; Furdui, C. M. A simple and effective strategy for labeling cysteine sulfenic acid in proteins by utilization of [small beta]-ketoesters as cleavable probes. *Chem. Commun.* **2012**, *48*, 4091–4093.

(3) Seo, Y. H.; Carroll, K. S. Quantification of Protein Sulfenic Acid Modifications Using Isotope-Coded Dimedone and Iododimedone. *Angew. Chem. Int. Ed.* **2011**, *50*, 1342–1345.

(4) Pan, J.; Carroll, K. S. Chemical biology approaches to study protein cysteine sulfenylation. *Biopolymers* **2013**.

(5) Parsons, Z. D.; Gates, K. S. Redox regulation of protein tyrosine phosphatases: methods for kinetic analysis of covalent enzyme inactivation. *Methods Enzymol.* **2013**, *528*, 129–154.

(6) Nabinger, S. C.; Chan, R. J. Shp2 function in hematopoietic stem cell biology and leukemogenesis. *Curr. Opin. Hematol.* **2012**, *19*, 273–279.

(7) Salmond, R. J.; Alexander, D. R. SHP2 forecast for the immune system: fog gradually clearing. *Trends Immunol.* **2006**, *27*, 154–160.

(8) Parsons, Z. D.; Gates, K. S. Thiol-Dependent Recovery of Catalytic Activity from Oxidized Protein Tyrosine Phosphatases. *Biochemistry (Mosc.)* **2013**, *52*, 6412–6423.

(9) Tanner, J. J.; Parsons, Z. D.; Cummings, A. H.; Zhou, H.; Gates, K. S. Redox regulation of protein tyrosine phosphatases: structural and chemical aspects. *Antioxid. Redox Signal.* **2011**, *15*, 77–97.

(10) Chen, C.-Y.; Willard, D.; Rudolph, J. Redox regulation of SH2-domain-containing protein tyrosine phosphatases by two backdoor cysteines. *Biochemistry (Mosc.)* **2009**, *48*, 1399–1409.

(11) Zhou, H.; Singh, H.; Parsons, Z. D.; Lewis, S. M.; Bhattacharya, S.; Seiner, D. R.; LaButti, J. N.; Reilly, T. J.; Tanner, J. J.; Gates, K. S. The Biological Buffer Bicarbonate/CO2 Potentiates H2O2-Mediated Inactivation of Protein Tyrosine Phosphatases. *J. Am. Chem. Soc.* **2011**, *133*, 15803–15805.

(12) Arabaci, G.; Guo, X.-C.; Beebe, K. D.; Coggeshall, K. M.; Pei, D. α-Haloacetophenone Derivatives As Photoreversible Covalent Inhibitors of Protein Tyrosine Phosphatases. *J. Am. Chem. Soc.* **1999**, *121*, 5085–5086.

(13) Seiner, D. R.; LaButti, J. N.; Gates, K. S. Kinetics and Mechanism of Protein Tyrosine Phosphatase 1B Inactivation by Acrolein. *Chem. Res. Toxicol.* **2007**, *20*, 1315–1320.

Chapter 6: Oxidative Inactivation of PTP1B – Evidence for Formation of Multiple Oxoforms of PTP1B in Solution, Including a Hydrolytically-Labile, Thiol-Recoverable Form

6.1 Introduction

Results from our work on the kinetics and mechanisms associated with thiol-mediated recovery of oxidatively-inactivated PTP1B[1] (Chapter 3) suggested that multiple oxoforms of PTP1B may exist in solution following H_2O_2-mediated inactivation of the enzyme. Most strikingly, we observed that the enzymatic reducing system Trx/TrxR recovered markedly *less* PTP activity than small molecule thiols did, although the enzymatic reducing system was much *faster* in recovering PTP activity. This result may suggest (1) that multiple oxoforms of PTP1B might be generated during hydrogen peroxide-mediated inactivation, and (2) that enzymatic systems might discriminate between the various oxoforms of PTP1B. Conversely, small molecule thiols such as DTT appeared to indiscriminately reduce all thiol-recoverable PTP1B oxoforms. Additionally, during our work on the covalent capture of oxidatively-inactivated PTP1B by carbon nucleophiles (Chapter 5), we noted time-dependent loss of thiol-recoverable PTP activity in the absence of nucleophilic agent (i.e. loss of thiol-recoverable PTP activity in buffer alone). This data may suggest that an oxoform of PTP1B present in solution is hydrolytically-unstable, but thiol-recoverable. Thus, we set out to explicitly examine the

possibility that treatment of PTP1B with hydrogen peroxide generates multiple, "chemically-distinct" oxoforms in solution, and whether one of the putative oxoforms is hydrolytically-labile, but may be returned to catalytically-active PTP by thiol agents.

Work conducted previously by our group[2,3] showed that a small, aryl chemical model sulfenyl amide could be converted to the corresponding sulfoxide and sulfone by oxidation with dimethyldioxirane (Scheme 6.1). The sulfoxide derivative of a sulfenyl amide is colloquially referred to as a 'sulfinyl amide', and the sulfone analogue a 'sulfonyl amide'. Treatment of both the sulfenyl and sulfinyl amides with an excess of thiol (2-mercaptoethanol) resulted in conversion to the free aryl thiol (Scheme 6.2). Additionally, the model sulfinyl amide was found to be hydrolytically unstable. Upon standing in 1:1 (v/v) acetonitrile/pH 7 buffer, the sulfinyl amide was converted to the corresponding sulfinic acid with a rate constant of $4.5 \pm 0.2 \times 10^{-4}$ s^{-1} ($t_{1/2}$ = 26 min, Scheme 6.3). The sulfonyl amide, however, did not react with 2-mercaptoethanol and was stable in buffer (pH 7). These results suggest that the *sulfinyl amide* may be a hydrolytically-labile, thiol-recoverable functionality, but that the sulfonyl amide is irrecoverable by thiol agents. This led us to suspect that time-dependent loss of thiol-recoverable activity from oxidatively-inactivated PTP1B in buffer alone might be due to formation and hydrolysis of a sulfinyl amide (Scheme 6.4).

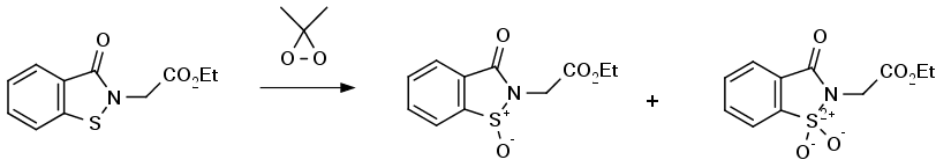

sulfenyl amide *sulfinyl amide* *sulfonyl amide*

Scheme 6.1. Oxidation of a chemical model sulfenyl amide affords the corresponding sulfoxide and sulfone ("sulfinyl amide" and "sulfonyl amide", respectively).

Scheme 6.2. The model sulfinyl amide may be fully reduced by thiol agent to afford free aryl thiol.

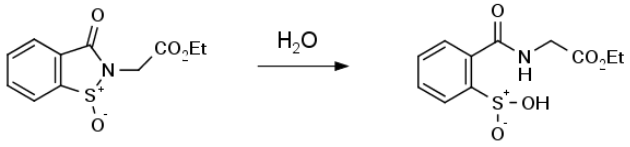

Scheme 6.3. The model sulfinyl amide is hydrolytically-labile.

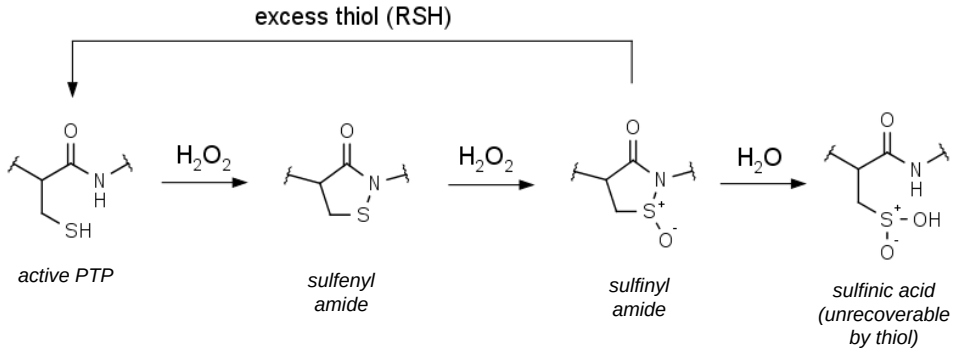

Scheme 6.4. Oxidation of PTP1B by excess hydrogen peroxide is suspected to result in formation of a hydrolytically-labile, thiol-recoverable sulfinyl amide.

Results

6.2 Evidence for a Hydrolytically-Labile, Thiol-Recoverable Oxoform of PTP1B Following Hydrogen Peroxide-Mediated Inactivation.

We envisioned treating PTP1B with a large excess of hydrogen peroxide might "force" over-oxidation of the enzyme, yielding sulfinyl and sulfonyl amide oxoforms. Along these lines, we treated native PTP1B with large molar excesses of H_2O_2 for a fixed amount of time (2 min), quenched the excess peroxide with catalase (500 un/mL), and allowed the PTP to stand in pH 7.4 buffer. At various time points, aliquots were removed from the mixture containing PTP in buffer, treated with dithiothreitol (DTT, 60 mM, 4 min, pH 7.4), and the amount of recovered PTP activity determined (Figure 6.1).

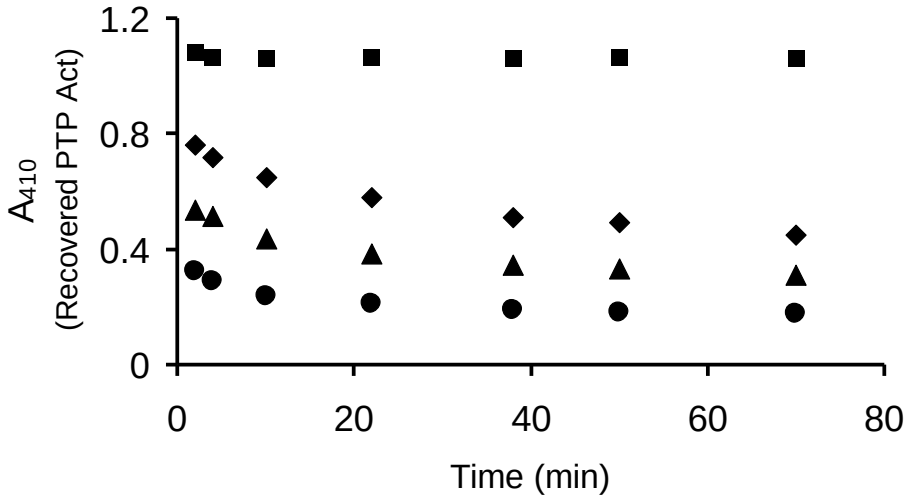

Figure 6.1. Time-dependent loss of thiol-recoverable PTP activity from oxidatively-inactivated PTP in buffer alone (pH 7.4). Native PTP1B was treated with 0 mM (squares), 2.5 mM (diamonds), 5 mM (triangles), or 10 mM (circles) H_2O_2 in pH 7.4 buffer for 2 min. Catalase was added to the mixtures to quench excess hydrogen peroxide (catalase 500 un/mL, final conc). A timer was started and aliquots were removed from the mixture and diluted into buffer containing 60 mM DTT at 2, 4, 10, 22, 38, 50, and 70 minute intervals. DTT-mediated reactivation was allowed to proceed for 4 min before the samples were assayed for recovered PTP activity.

Time-dependent loss of thiol-recoverable activity from the oxidatively-inactivated PTP in buffer alone was observed, consistent with a hydrolytically-unstable species. Importantly, the amount of thiol-recoverable PTP activity in each series "tracked" with the concentration of hydrogen peroxide used in the inactivation phase. Namely, increasing H_2O_2 concentration in the inactivation phase afforded decreasing amounts of thiol-recoverable activity following incubation in buffer. This result was consistent with H_2O_2-mediated formation of a hydrolytically-labile sulfinyl amide, where higher concentrations of hydrogen peroxide afforded larger amounts of sulfinyl amide and correspondingly less remaining sulfenyl amide.

We utilized nonlinear, least-squares regression analysis to estimate endpoints (A_f) of the putative hydrolysis reactions and extract associated pseudo first-order rate constants (k_ψ, Figure 6.2 A inset). First-order kinetic models fit very well to the data ($r^2 >$ 0.98). Surprisingly, the pseudo first-order rate constants for hydrolytic decay of PTP activity depended linearly on concentration of hydrogen peroxide used in the *inactivation* phase (Figure 6.2 B, $k_{apparent}$ = 0.12 M^{-1} s^{-1}). The cause for this apparent dependence of rate of *hydrolysis* on oxidant concentration is not yet understood. In any case, apparent pseudo first-order rate constants for hydrolytic loss of PTP activity varied from 0.04 – 0.10 min^{-1}, corresponding to half-lives of 7 – 17 min for loss of thiol-recoverable PTP activity (25°C, pH 7.4). These rates are comparable to that determined for hydrolysis of the chemical model sulfinyl amide under alternate conditions ($t_{1/2}$ = 26 min, *vide supra*).

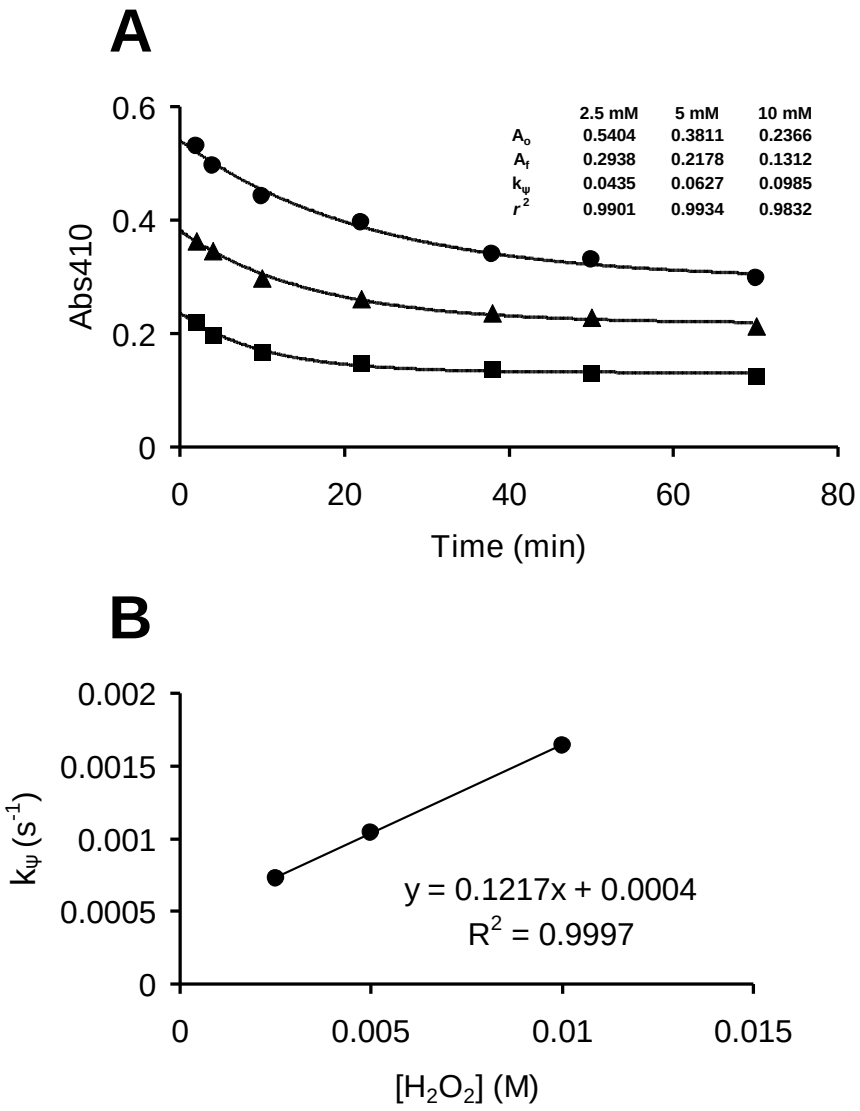

Figure 6.2. Kinetics of loss of thiol-recoverable activity from oxidatively-inactivated PTP1B. (**A**) Curve-fitting analysis of decay of recoverable PTP activity. First-order kinetic models fit excellently to the data and optimized parameters for each series (A_o, A_f, and k_ψ) are reported in the inset. Pseudo first-order rate constants reported in the inset have units of min^{-1}. (**B**) Pseudo first-order rate constants for spontaneous decay of thiol-recoverable PTP activity in buffer depended linearly on the concentration of hydrogen peroxide utilized in the inactivation phase of the assay. The slope of the linear regression trendline is the apparent second-order rate constant for the operative process, 0.12 M^{-1} s^{-1}. Importantly, the non-zero intercept (0.0004 s^{-1}) suggests a possible equilibrating reaction.

6.3 On the pH-Dependence of Hydrolytic Decomposition Rates and Evidence for Multiple Hydrolytically or Conformationally-Unstable PTP1B Oxoforms

We next set out to explore whether a pH-rate dependence for the putative hydrolysis reaction might exist. To this end, we executed an assay similar to that described above, but employing uniform oxidative inactivation conditions (2.5 mM H_2O_2 for 2 min), followed by a catalase quench of excess H_2O_2 and dilution into pH 6, 7, or 8 buffer. Following dilution into pH 6 – 8 buffer, a timer was started, and aliquots were removed at various time points for determination of thiol-recoverable activity (Figure 6.3). From this data, two important features were noted: (1) rates of hydrolysis increased with increasing pH, and (2) the reactions appeared to exhibit biphasic kinetics. For example, loss of thiol-recoverable PTP activity at pH 8 occurred rapidly early in the reaction, but slowed down at around 40 minutes (Figure 6.3, diamonds). Conversely, the loss of thiol-recoverable activity at pH 6 and 7 occurred more slowly in the early stages of the reaction, but "caught up" to the reaction occurring at pH 8 at around t = 70 min. These results are consistent with simultaneous processes contributing to the loss of thiol-recoverable PTP activity, one of which may be hydroxide-ion dependent.

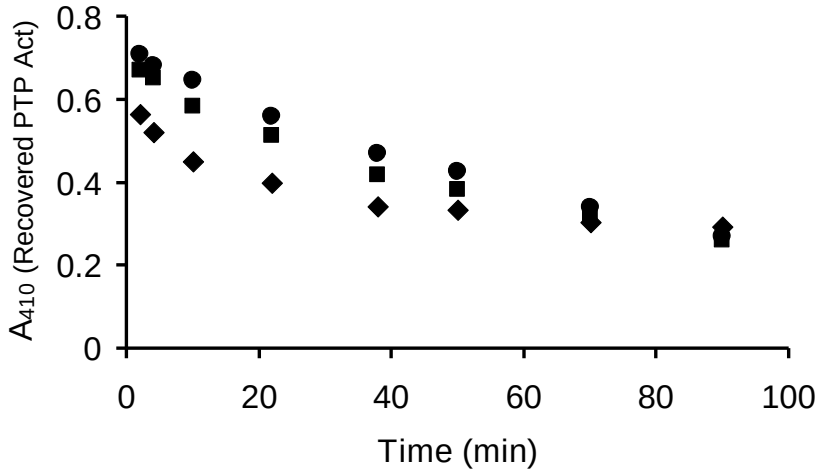

Figure 6.3. The rate of loss of thiol-recoverable activity from oxidatively-inactivated PTP1B is both pH-dependent and biphasic. Following treatment of native PTP1B with 2.5 mM H_2O_2 for 2 min in pH 6 buffer, aliquots were diluted into pH 6 (circles), pH 7 (squares), or pH 8 (diamonds) buffer containing catalase (500 un/mL). A timer was then started and aliquots were removed at 2, 4, 10, 22, 38, 50, 70, and 90 minute intervals for determination of thiol-recoverable PTP activity (60 mM DTT, pH 8, 4 min).

To verify the observed biphasic kinetics and further explore whether the process was indeed sensitive to attenuated hydroxide ion concentration, we conducted a similar assay to that above, extending both the incubation time in buffer and the pH range studied to pH 5 – 8 (Figure 6.4). We again noted clear evidence for biphasic kinetic behavior at pH 8; loss of thiol-recoverable PTP activity occurred rapidly from $t = 0$ to approximately $t = 40$ min, then slowed down. Loss of thiol-recoverable activity occurred more slowly in the early stages of the reaction at pH 7 relative to pH 8, but then "caught up" and "overtook" the rate of decay of PTP activity at pH 8 at $t = 70$ min. Importantly, if a *single* chemical process were operative (affording monophasic kinetics), a slower reaction should never "catch up" to a faster one (until $t = \infty$). Interestingly, loss of thiol-recoverable PTP activity occurred most rapidly at pH 5, and appeared to occur in

monophasic fashion. It is not yet clear whether this kinetic profile is due to a single hydrolytic process, closely-overlapping biphasic processes, or to an alternative mechanism of loss of PTP activity such as enzyme denaturation. It is worth noting that enzyme denaturation might also afford time-dependent loss of thiol-recoverable PTP activity, and that at least some denaturation processes are known to follow first-order kinetics.[4]

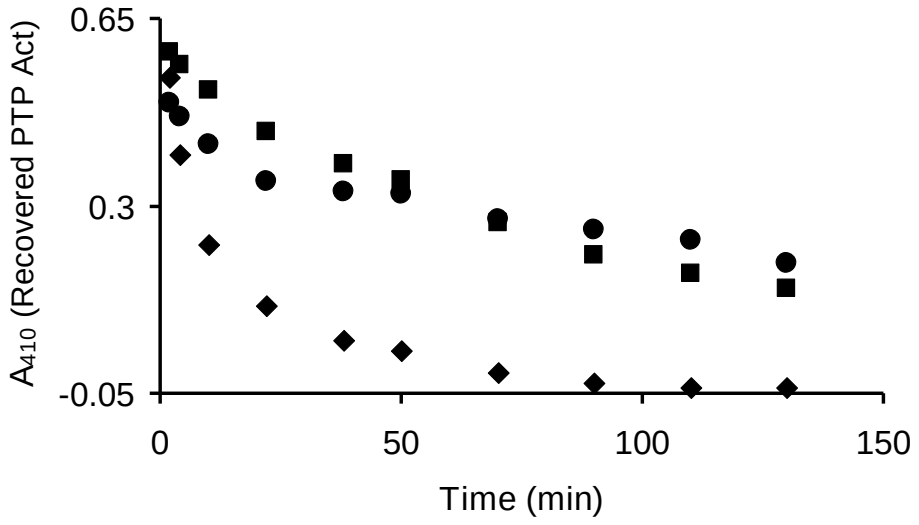

Figure 6.4. Loss of thiol-recoverable PTP activity at pH 5 (diamonds), pH 7 (squares), and pH 8 (circles). Assay methodology was similar to that described above, where native PTP was treated with hydrogen peroxide under uniform conditions, diluted into buffer (pH 5 – 8) containing catalase, a timer started, and the amount of DTT-recoverable PTP activity determined at 2, 4, 10, 22, 38, 50, 70, 90, 110, and 130 minute intervals.

6.4 Efforts to Determine the Rate of "Over-Oxidation" of PTP1B

We were interested in determining the rate of formation of the hydrolytically-labile, thiol-recoverable oxoform of PTP1B – the putative sulfinyl amide. Results from the previous experiments led us to suspect that the rapidly-hydrolyzing species at pH 8

might be the sulfinyl amide, and the oxoform which decayed more slowly the sulfenyl amide. As both were suspected to be thiol-recoverable oxoforms, we had to devise a way to "decouple" them, such that we might selectively monitor either loss of sulfenyl amide (starting material) or formation of sulfinyl amide (product). We envisioned that capitalizing on the rapid hydrolysis of the putative sulfinyl amide at pH 8 might allow us to "scrub out" any contribution to thiol-recoverable activity from that species, allowing us to selectively monitor sulfenyl amide oxidation. Thus, the experimental design rationale for monitoring the rate of "over-oxidation" (conversion of the sulfenyl amide to the sulfinyl amide) was as follows: (1) treat native PTP1B with a large excess of hydrogen peroxide while monitoring reaction time, (2) at various times, remove aliquots from the reaction mixture and dilute them into pH 8 buffer containing catalase, (3) allow the $PTP1B_{ox}$ to stand in pH 8 buffer for 50 min to completely "scrub out" the rapidly-hydrolyzing species, (4) treat the PTP with thiol for sufficient time to recover all recoverable PTP activity, (5) assay for recovered PTP activity.

The reaction scheme that was expected to be operative in these experiments is given in Scheme 6.5. The rate of oxidative-inactivation of PTP1B by H_2O_2 (k_{inact}) is well-documented, coming from work conducted both in our laboratory and by other groups.[56] Additionally, work conducted by Salmeen *et al.* suggests that the dehydrative cyclization involved in converting the cysteine sulfenic acid to the sulfenyl amide is rapid (faster than the initial oxidation event).[7] Data on the rates of hydrolytic loss of thiol-recoverable PTP activity reported above reveal that incubation of $PTP1B_{ox}$ for 50 minutes in pH 8.0 buffer should be sufficient for complete conversion of the putative sulfenyl amide to the thiol-*irrecoverable* sulfinic acid. Finally, treatment of the oxidatively-inactivated PTP

with 40 mM DTT for 10 minutes should ensure complete recovery of any thiol-recoverable PTP activity. All points taken together, we anticipated kinetic data such as that 'simulated' in Figure 6.5 A, revealing time- and H_2O_2 concentration-dependent loss of thiol-recoverable PTP activity, as the sulfenyl amide would be oxidized to the sulfinyl amide and hydrolytically cleaved. We expected the rate constant for "over-oxidation" (k_{overox} in Scheme 6.5 and Figure 6.5 B) to be less than the rate of oxidation of the native PTP1B cysteine thiolate (k_{inact}, approximately 15 M^{-1} s^{-1}). The expectation that k_{overox} would be much smaller than k_{inact} is in agreement with reported rates of oxidation or covalent modification of small molecule thiolates compared to their corresponding neutral thiols or disulfides.[8,9]

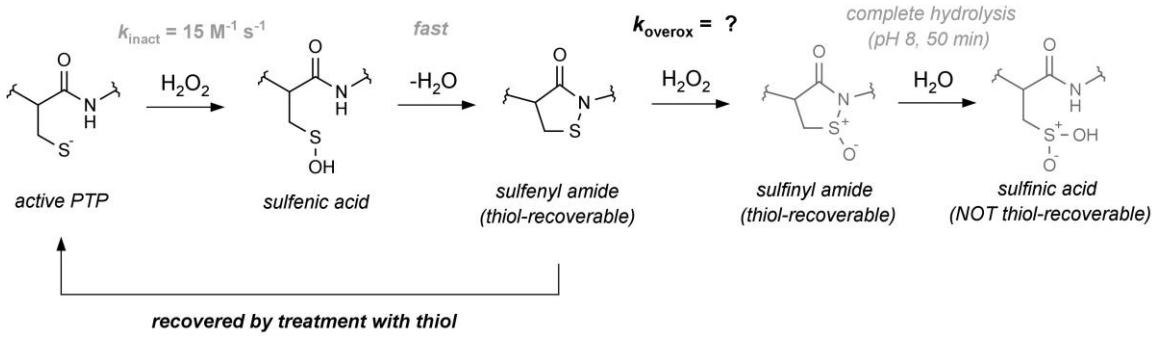

Scheme 6.5. Anticipated reaction scheme and associated kinetic steps for "over-oxidation" of PTP1B. It was expected that treating native PTP1B with a large excess of hydrogen peroxide followed by catalase quench and incubation in pH 8 buffer would afford kinetic data reflective of rate-determining oxidation of the sulfenyl amide (k_{overox}).

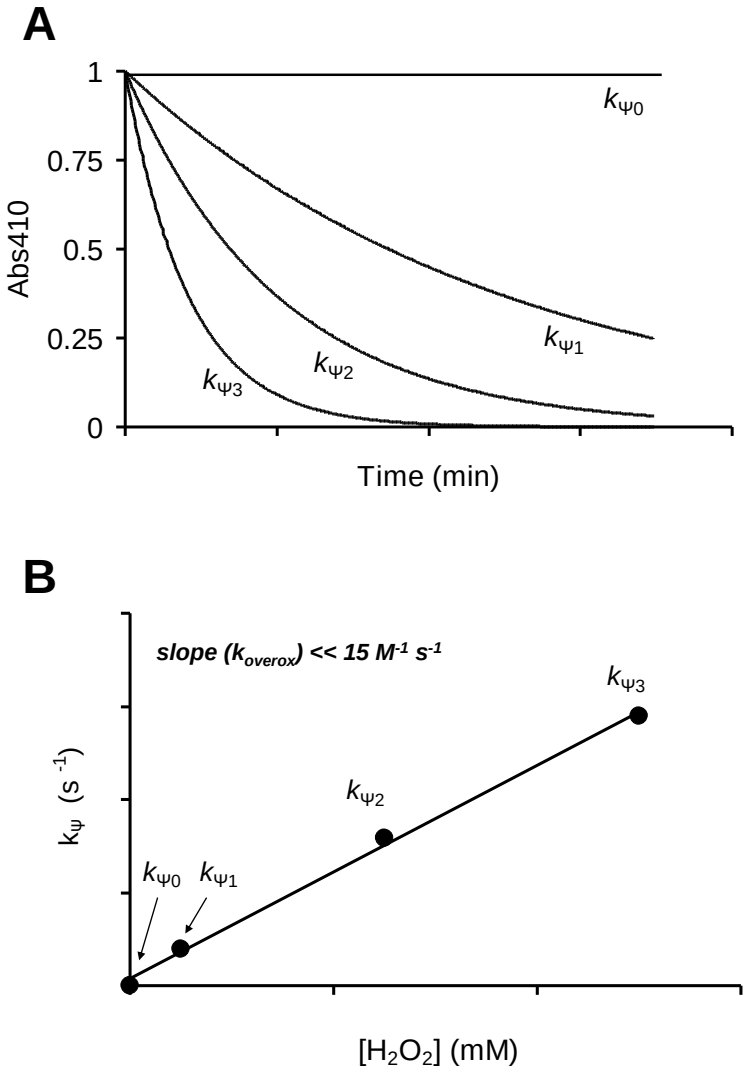

Figure 6.5. Mock data: expected kinetics of "over-oxidation" of PTP1B. (**A**) As hydrogen peroxide concentration increased, correspondingly faster loss of thiol-recoverable PTP activity and larger pseudo first-order rate constants (k_{ψ}) were anticipated. Additionally, it was expected that the amount of thiol-recoverable activity would go to zero, as complete oxidation of the sulfenyl amide would afford only thiol-*irrecoverable* sulfinic acid following hydrolysis of the intermediate sulfinyl amide. (**B**) It was expected that "over-oxidation" would follow second-order kinetics, where the pseudo first-order rate constants for oxidation would depend linearly on H_2O_2 concentration. Also, an apparent second-order rate constant less than 15 M^{-1} s^{-1} was expected, as the nucleophile in the putative reaction mechanism is a sulfenyl sulfur, rather than a thiolate.

Figure 6.6 presents the results of three independent trials conducted as described in the experimental design above. Native PTP1B was treated with concentrations of hydrogen peroxide indicated in the Figure legends (pH 7.4, 25°C), aliquots were drawn from the reaction mixture at various times and diluted into ready-made solutions of catalase (500 – 750 un/mL, pH 8) and allowed to stand at room temperature (23 ± 2°C) for 40 – 55 minutes before being treated with DTT (40 mM, 16 – 20 min, pH 8, r.t.). Thereafter, the samples were assayed for recovered PTP activity. In our nomenclature, we consider the activity recovered here "non-hydrolytically-labile, thiol-recoverable" PTP activity, and have traditionally presumed this species to be the sulfenyl amide.

As expected, time- and H_2O_2 concentration-dependent loss of thiol-recoverable activity was observed in each trial. The "flatness" of the control series containing no hydrogen peroxide confirm that the assay provided uniform concentrations of PTP in the activity assay, and that the PTP activity assay was consistent throughout the course of the experiment. Thus, we may confidently assert that subtle trends in the kinetic data reflect actual chemical events.

Most notably "outside of expectations" was that loss of non-hydrolytically-labile, thiol-recoverable activity did not go to completion. In other words, the decay of thiol-recoverable PTP activity did not go to zero. Consistently and independent of H_2O_2 concentration used, the amount of non-hydrolytically-labile, thiol-recoverable PTP activity decayed to approximately 30%. Additionally, there consistently appeared to be a subtle *increase* in the amount of non-hydrolytically-labile, thiol-recoverable activity at around 6 – 12 minutes during the oxidative inactivation/over-oxidation phase. The bases for these observations is not yet understood, but speculated upon below.

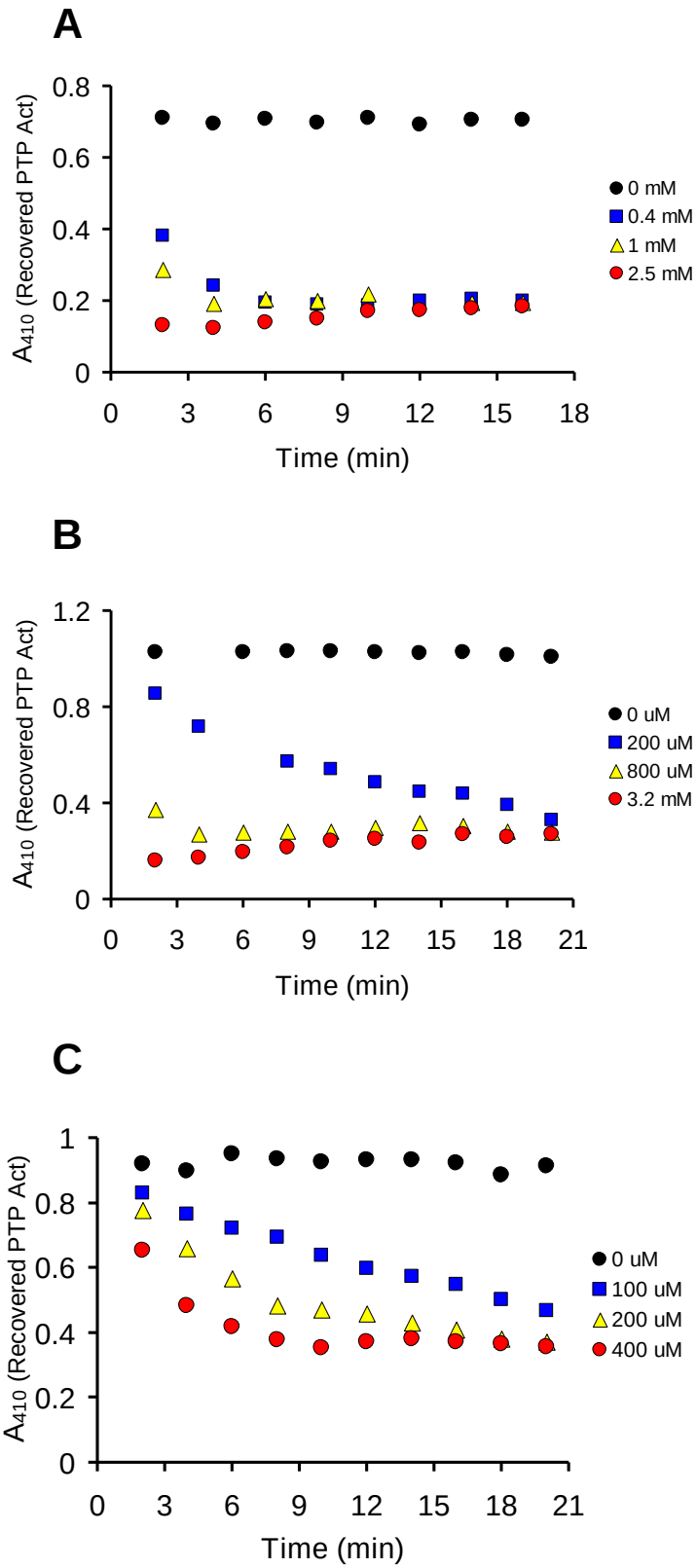

Figure 6.6. Kinetic data for the "over-oxidation" of PTP1B. Native PTP1B was treated

with the indicated concentrations of hydrogen peroxide at 25°C in pH 7.4 buffer. During this treatment, aliquots were withdrawn at various time points and diluted into pH 8 buffer containing catalase (500 – 750 un/mL). The samples were incubated at 23 ± 2°C for 40 – 55 minutes before being assayed for thiol-recoverable activity (40 mM DTT, pH 8, 16 – 20 min).

Treating the kinetic data above as a set of pseudo first-order processes and plotting the extracted rate constants as a function of hydrogen peroxide concentration revealed a relatively crude linear relationship of k_{obs} (s^{-1}) on [H_2O_2] (r^2 = 0.89, Figure 6.7). The apparent second-order rate constant for this process was 15 ± 5.0 M^{-1} s^{-1}. Surprisingly, this rate constant is *equal* to that determined for oxidative inactivation of the native PTP1B cysteine thiolate. It is not yet clear whether this is a meaningful observation, or merely a coincidence.

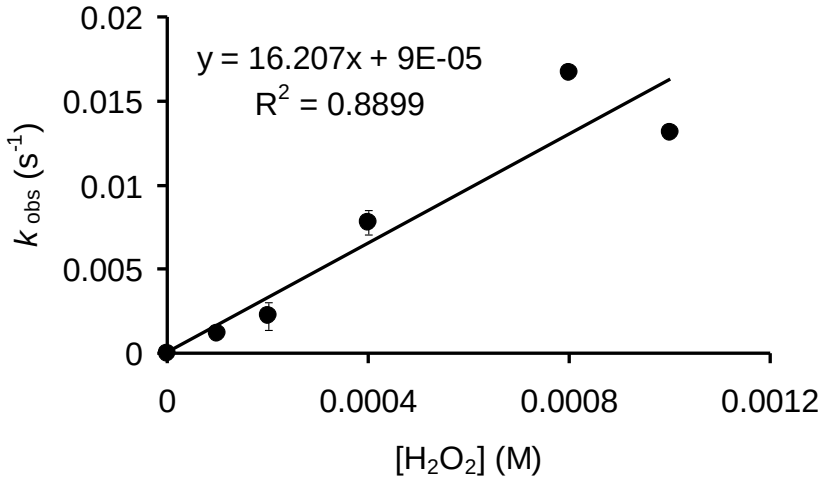

Figure 6.7. Apparent pseudo first-order rate constants for "over-oxidation" of PTP1B versus associated concentration of hydrogen peroxide.

6.5. Discussion

The rate of hydrolysis of the putative sulfinyl amide at pH 7.4, generated by treatment of PTP1B with varying concentrations of H_2O_2, provided evidence that increasing concentrations of hydrogen peroxide afford correspondingly less thiol-recoverable PTP activity, but also that the rate of hydrolytic loss of PTP activity was relatively insensitive to hydrogen peroxide concentration. These results were in agreement with the expectations that larger concentrations of H_2O_2 would generate more hydrolytically-labile sulfinyl amide, but that the rate of hydrolysis of this intermediate should be roughly constant under a given set of conditions. Additionally, the rates observed for hydrolysis of the putative PTP1B sulfinyl amide (0.04 – 0.1 min^{-1}) were comparable to the rate reported for hydrolysis of a small chemical model sulfinyl amide in 1:1 acetonitrile:pH 7 buffer (approx. 0.03 min^{-1}).[2]

Results from the set of experiments intended to investigate the rate of hydrolytic decomposition of $PTP1B_{ox}$ at varying pH were somewhat more surprising. Indeed, the apparent rates of hydrolysis of oxidized PTP1B depended on buffer pH. However, evidence that *both* the sulfinyl and sulfenyl amides might be hydrolytically-labile was observed. The reaction exhibited biphasic kinetic behavior most obvious at pH 8, where rapid loss of thiol-recoverable PTP activity was followed by a slower decay. At pH 5, complete and rapid (within 90 min) loss of all thiol-recoverable activity was observed. At intermediate pH values (6 and 7), biphasic kinetic behavior was less pronounced and loss of thiol-recoverable activity much slower than at pH 5 (~ 50 % PTP activity still recovered at 90 min at both pH values). Assuming only hydrolytic processes were at play,

it is possible that the decay kinetics at various pH values reflect a combination of water-mediated, hydroxide ion-mediated, and acid-catalyzed loss of thiol recoverable PTP activity. For example, if the rapidly-hydrolyzing species at pH 8 were the *sulfinyl* amide and the slower-decaying species at pH 8 were the sulfenyl amide, that may implicate hydroxide as the effective nucleophile during hydrolysis of the sulfinyl amide at pH 8 (Scheme 6.6). Thus, hydrolysis of the sulfinyl amide might be expected to be much slower at pH 7 or 6, where hydroxide ion concentration would be 10 and 100-fold lower, respectively. Additionally, water-mediated hydrolysis of the sulfinyl amide may also occur, but perhaps at a slower rate.

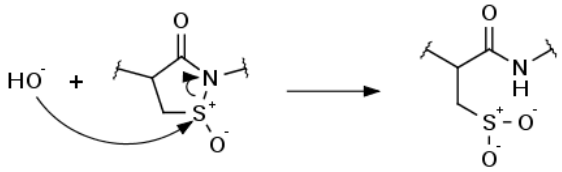

Scheme 6.6. Hydroxide-ion mediated hydrolysis of the sulfinyl amide.

If the sulfinyl and sulfenyl amides were the only thiol-recoverable oxoforms of PTP1B present in solution, then complete loss of thiol-recoverable activity must have resulted from decomposition of *both* oxoforms. At pH 5, rapid and complete loss of all thiol-recoverable PTP activity was observed. Under these conditions, hydrolysis of the sulfinyl amide may still occur by reaction with water, rather than with hydroxide ion. However, swift loss of all thiol-recoverable PTP activity suggests rapid decomposition of

the sulfenyl amide as well. This may implicate an acid-catalyzed process during decomposition of the sulfenyl amide. For example, protonation of the sulfenyl amide may afford a reactive intermediate potentially susceptible to cleavage by multiple chemical mechanisms (Scheme 6.7). Two possible mechanisms by which the protonated sulfenyl amide may be cleaved are shown in Scheme 6.7 B and C. As illustrated in Scheme 6.7 B, an E2-type elimination resulting in cleavage of the sulfenyl amide S-N bond may occur, giving rise to a thioaldehyde intermediate. The thioaldehyde may then undergo further hydrolysis to yield the corresponding aldehyde and hydrogen sulfide (H_2S).[10] Alternatively, water-mediated deprotonation of the α-carbon may promote C-S bond cleavage to afford the α,β,-unsaturated, thio-substituted amide in Scheme 6.7 C. This intermediate Michael acceptor may then undergo a variety of reactions involving water, thiol, or buffer components to give a diverse array of products.

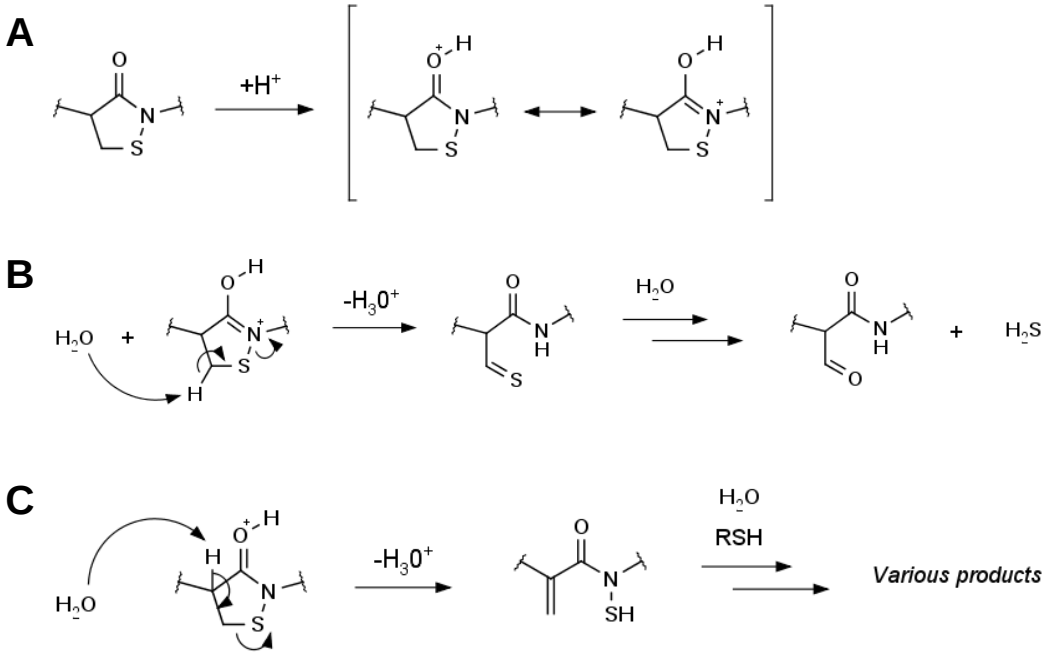

Scheme 6.7. Protonation of the sulfenyl amide may promote multiple pathways for water-mediated degradation.

Finally, results from assays intended to determine rate and extent of "over-oxidation" of PTP1B may suggest that the sulfinyl amide forms as a mixture of diastereomers. Independent of the concentration of hydrogen peroxide used in oxidation of PTP1B, roughly 30 % of PTP activity remained thiol-recoverable and hydrolytically-*stable* at pH 8. Presumably, forcing conditions such as 3.2 mM H_2O_2 for 20 minutes would have afforded complete conversion of the sulfenyl amide to the sulfinyl amide. Thus, retention of thiol-recoverable activity following such treatment *and* incubation in pH 8 buffer for 50 minutes may be due to formation of a thiol-recoverable, hydrolytically-*stable* sulfinyl amide isomer. Oxidation of the sulfenyl amide may potentially lead to two chiral sulfoxides (sulfinyl amide isomers, Figure 6.8). Importantly, acyclic chiral sulfoxides are known to retain configuration under biological conditions.[11,12] Thus, it is likely that isomers of the cyclic sulfinyl amide would not undergo pyramidal inversion either.

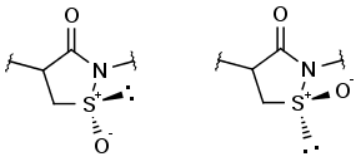

Figure 6.8. Oxidation of the sulfenyl amide may afford diastereomeric sulfinyl amides.

If both sulfinyl amide isomers were thiol-recoverable but one were hydrolytically-labile, then data such as that in Figure 6.6 might be expected. Namely, complete conversion of the sulfenyl amide to sulfinyl amides may occur, but the population of sulfinyl amide

resistant to hydrolysis would persist as thiol-recoverable activity, even after incubation in pH 8 buffer for 40 – 55 minutes. Furthermore, under a given set of conditions during the oxidation phase, it might be expected that the ratio of the two sulfinyl amide isomers formed would be roughly constant, independent of hydrogen peroxide concentration. That indeed seemed to be the case, as the amount of thiol-recoverable activity in each series decayed to roughly 30%, independent of concentration of H_2O_2 employed. Finally, it is not yet understood why the apparent second-order rate constant for "over-oxidation" of PTP1B was equal to that for oxidation of the native PTP1B cysteine thiolate (~15 M^{-1} s^{-1}). Undoubtedly, this will be the subject of further investigation.

6.6 Methods and Materials

***Determination of the Rate of Hydrolysis of the Putative Sulfinyl Amide*.** Stocks of H_2O_2 at 2x concentrations were prepared in buffer A (100 mM Tris, 100 mM NaCl, 10 mM DTPA, 0.5 % Tween 80, pH 7.4). Thiol-free PTP1B (4 μM) was prepared in the same buffer. PTP1B and H_2O_2 stocks were mixed 1:1 (v/v, 20 μL each) and allowed to react for 2 minutes, affording 2 μM PTP and the reported concentrations of H_2O_2. Following incubation at 25°C for 2 min, 20 μL aliquots were removed from the PTP-H_2O_2 reaction mixtures and diluted into ready-made 180 μL solutions of catalase in buffer A (600 un/mL). These samples were incubated at 25°C and at various time points 20 μL aliquots were removed and diluted into ready-made 80 μL portions of DTT (75 mM) in buffer A. DTT-mediated reactivation was allowed to proceed at 23 ± 2°C for 4 min before 400 μL of 25 mM pNPP in pH 6 buffer B was added (100 mM Bis-Tris, 100

mM NaCl, 10 mM DTPA). The activity assay was allowed to proceed for 10 min before quenching by addition of 500 μL of 2M NaOH.

Determination of Rate and Extent of Over-Oxidation of PTP1B. General assay methodology for experiments of this type are as follows: a 20 μL aliquot of thiol-free PTP1B (1.5 μM) in buffer containing 50 mM Tris, 50 mM Bis-Tris, 100 mM NaCl, 10 mM DTPA, and 0.5% Tween 80, pH 7.0 was added to ready-made, 100 μL solutions of 1.2x H_2O_2 in buffer A (15 mM Tris, 100 mM NaCl, 10 mM DTPA, 0.5% Tween 80, pH 7.4, held at 25°C). Immediately upon addition of PTP, a timer was started and aliquots (10 μL) were removed from the reaction mixtures every 2 min up to 20 minutes. Aliquots from the reaction mixture were diluted into ready-made 80 μL portions of catalase in pH 8 buffer (100 mM Tris, 100 mM NaCl, 10 mM DTPA, 0.5% Tween 80, 500 – 750 units/mL catalase, final). The samples were then allowed to stand at 23 ± 2°C for 40 – 55 minutes before addition of 400 μL of 25 mM pNPP in pH 6 buffer (100 mM Bis-Tris, 100 mM NaCl, 10 mM DTPA, 0.5% Tween 80). The activity assay was allowed to proceed for 20 min at 23 ± 2°C before being quenched with 500 μL of 2M NaOH.

References

(1) Parsons, Z. D.; Gates, K. S. Thiol-Dependent Recovery of Catalytic Activity from Oxidized Protein Tyrosine Phosphatases. *Biochemistry* **2013**, *52*, 6412–6423.

(2) Sivaramakrishnan, S.; Keerthi, K.; Gates, K. S. A Chemical Model for Redox Regulation of Protein Tyrosine Phosphatase 1B (PTP1B) Activity. *J. Am. Chem. Soc.* **2005**, *127*, 10830–10831.

(3) Sivaramakrishnan, S.; Cummings, A. H.; Gates, K. S. Protection of a Single-Cysteine Redox Switch from Oxidative Destruction: On the Functional Role of Sulfenyl Amide Formation in the Redox-Regulated Enzyme PTP1B. *Bioorg. Med. Chem. Lett.* **2010**, *20*, 444–447.

(4) London, M.; McHugh, R.; Hudson, P. B. Unified Theory of Enzyme Catalysis and Denaturation. *J. Gen. Physiol.* **1962**, *46*, 57–73.

(5) Tanner, J. J.; Parsons, Z. D.; Cummings, A. H.; Zhou, H.; Gates, K. S. Redox Regulation of Protein Tyrosine Phosphatases: Structural and Chemical Aspects. *Antioxid. Redox Signal.* **2011**, *15*, 77–97.

(6) Zhou, H.; Singh, H.; Parsons, Z. D.; Lewis, S. M.; Bhattacharya, S.; Seiner, D. R.; LaButti, J. N.; Reilly, T. J.; Tanner, J. J.; Gates, K. S. The Biological Buffer, Bicarbonate/CO2, Potentiates H2O2-Mediated Inactivation of Protein Tyrosine Phosphatases. *J. Am. Chem. Soc.* **2011**, *133*, 15803–15805.

(7) Salmeen, A.; Andersen, J. N.; Myers, M. P.; Meng, T.-C.; Hinks, J. A.; Tonks, N. K.; Barford, D. Redox Regulation of Protein Tyrosine Phosphatase 1B Involves a Sulphenyl-Amide Intermediate. *Nature* **2003**, *423*, 769–773.

(8) Bednar, R. A. Reactivity and pH Dependence of Thiol Conjugation to N-Ethylmaleimide: Detection of a Conformational Change in Chalcone Isomerase. *Biochemistry (Mosc.)* **1990**, *29*, 3684–3690.

(9) Betterton, E. A.; Hoffmann, M. R. Kinetics and Mechanism of the Oxidation of Aqueous Hydrogen Sulfide by Peroxymonosulfate. *Environ. Sci. Technol.* **1990**, *24*, 1819–1824.

(10) *Comprehensive Organic Functional Group Transformations II: A Comprehensive Review of the Synthetic Literature 1995 - 2003*; Elsevier, 2004.

(11) Marom, H.; Biedermann, P. U.; Agranat, I. Pyramidal Inversion Mechanism of Simple Chiral and Achiral Sulfoxides: A Theoretical Study. *Chirality* **2007**, *19*, 559–569.

(12) Morrow, R. J.; Millership, J. S.; Collier, P. S. Diastereotopic Analysis of Mesoridazine Besylate (serentil). *Chirality* **2004**, *16*, 534–540.

Chapter 7: Computational Prediction of 1,2,4-benzotriazine-based Nitrogen Mustard Reactivities

7.1 Introduction

Nitrogen mustards are aryl or aliphatic amines which bear at least one N-alkyl chain containing a leaving group attached to a β-carbon (beta position with respect to the nitrogen atom). Several nitrogen mustards are currently employed as chemotherapeutic agents for the treatment of various types of cancer, with mechlorethamine (**1**) being the first nitrogen mustard reported in such an application.[12]

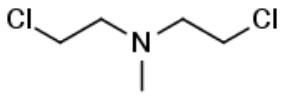

1

The biological activity of nitrogen mustards arises from their propensity to form highly electrophilic aziridinium ions.[3] Aziridinium ion formation occurs when the nitrogen atom engages in nucleophilic attack on a proximal β-carbon, displacing the leaving group and resulting in formation of a cationic, 3-membered heterocycle (an aziridinium ion, Scheme 7.1). Following its formation, the aziridinium ion may then undergo reaction with adventitious nucleophiles such as water or those present in biomolecules like DNA or proteins (Scheme 7.1).[456]

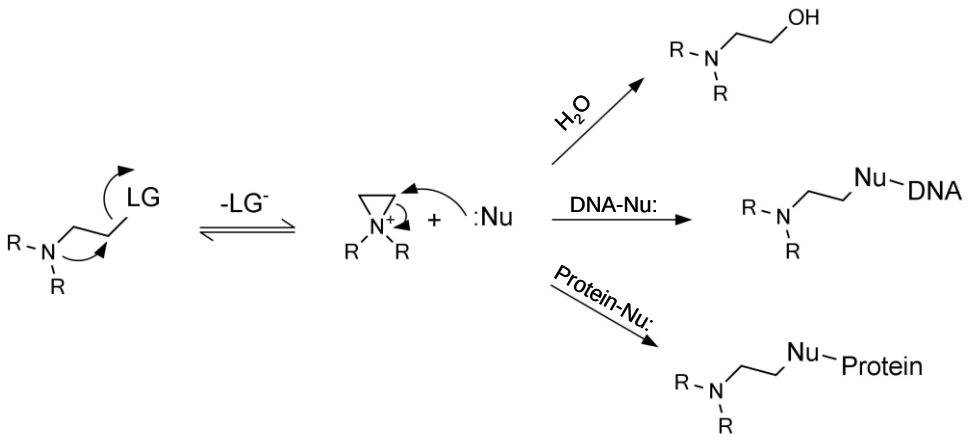

Scheme 7.1. Generalized mechanism for formation and reactions of aziridinium ions. Examples of common sources of nucleophiles *in vivo* are given above forward reaction arrows.

Clearly, modification of biomolecules such as DNA and/or protein can have profound biological consequences. Indeed, the pharmacological effects of clinically-used nitrogen mustards stem from modification of biological targets, particularly DNA.[3] These chemotherapeutics alkylate various nucleophilic sites on DNA, often at endocyclic nitrogens of the purine and pyrimidine bases.[7] Because these molecules typically have little or no inherent selectivity for modifying biomolecules in cancerous cells over normal somatic cells, modification of off-target DNA and protein occurs, resulting in severe adverse side-effects.[2] In fact, nitrogen mustards like mechlorethamine were originally utilized as *chemical warfare agents*, not therapeutics.[8] For this reason, development of chemotherapeutic molecules capable of selective modification of malignant tissue or cells is of tremendous importance. Clearly, identification of chemical, structural, or compositional differences between normal and cancer cells is of critical importance for the rational design of agents capable of selective modification of cancer cells/tissue.

Consistently, human solid tumor masses contain much lower concentrations of molecular oxygen than normal tissues (~10-fold or less).[91011] Often, this tumor hypoxia results from the tumor mass being spatially separated from vasculature, beyond the distance which O_2 diffuses. Unsurprisingly, there have been substantial efforts dedicated to the exploitation of this compositional difference with the intent of achieving selectivity in damaging tumor tissue over normal tissue.[109121314] Perhaps the best-studied molecule amongst the hypoxia-selective antitumor agents is tirapazamine (TPZ).[1012] Tirapazamine (3-amino-1,2,4-benzotriazine 1,4-dioxide, **2**) is a substituted 1,2,4-benzotriazine (**3**) which undergoes enzyme-mediated one-electron reduction *in vivo*, followed by homolytic deoxygenation and release of hydroxyl radical (•OH, Scheme 7.2).[151617] Neither TPZ itself nor the deoxygenated metabolite **3** are appreciably cytotoxic, but the hydroxyl radical released is potently so.

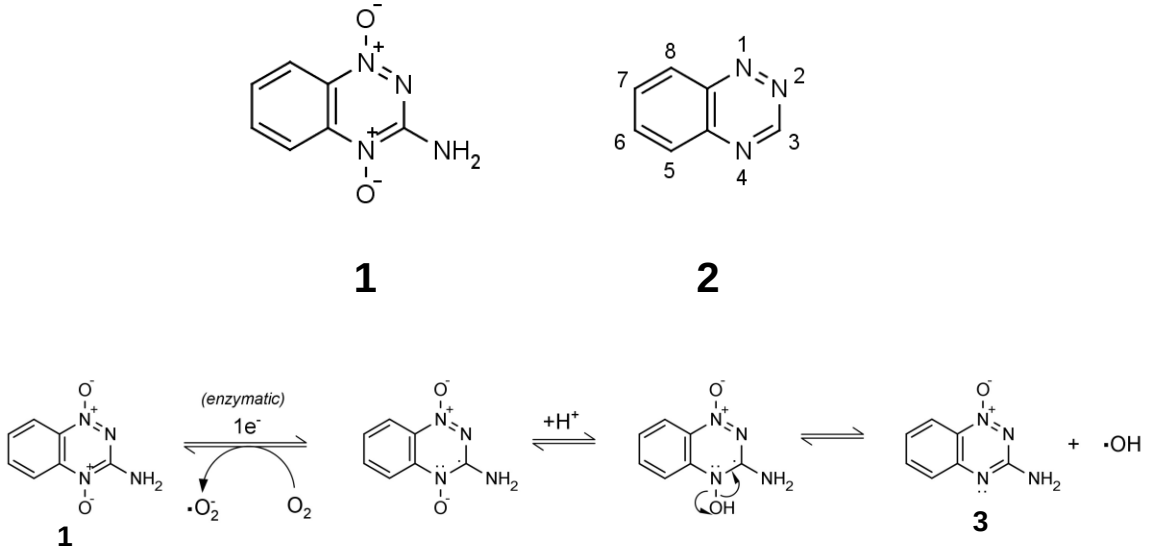

Scheme 7.2. Reduction of TPZ results in deoxygenation and release of hydroxyl radical.

Importantly, the radical anion formed by reduction of TPZ may be re-oxidized by O_2 before release of hydroxyl radical, recovering TPZ and preventing cytotoxicity (first reverse reaction, Scheme 7.2). Thus, adequate concentrations of oxygen such as those present in normal tissue may prevent deoxygenation of TPZ. However, under hypoxic conditions, insufficient O_2 exists to prevent forward reaction, and deoxygenated compound **3** is produced.

We envisioned that the hypoxia-selective cytotoxicity of a TPZ analogue might be enhanced relative to TPZ if, in addition to releasing hydroxyl radical, the analogue of deoxygenated metabolite **3** were cytotoxic. However, in order to maintain *hypoxia-selective* cytotoxicity, the parent 1,4-dioxide of the analogue should remain inert. Thus, this approach hinged on exploitable chemical/electronic changes associated with reduction of the parent 1,4-dioxo compound to the corresponding 1-oxide. Along these lines, we anticipated that a nitrogen mustard functionality attached to the benzotriazine core might meet these requirements. Indeed, it has been demonstrated that N-aryl nitrogen mustard activity (aziridinium ion formation) is suppressed when electron-withdrawing substituents such as a *p*-nitro group are attached to the N-aryl ring.[186] Reduction of the nitro group to the hydroxylamine or amine, however, affords electron-donating groups which promote aziridinium ion formation, ultimately resulting in cytotoxicity (Figure 7.3).[18] Thus, we were interested in predicting whether reduction of benzotriazine 1,4-dioxides to the corresponding 1-oxides might constitute a similar "electronic switch" and at which position along the benzotriazine core this effect might be greatest. We were most interested in predicting these effects at carbons 6 and 7 due to parallel synthetic efforts.[19]

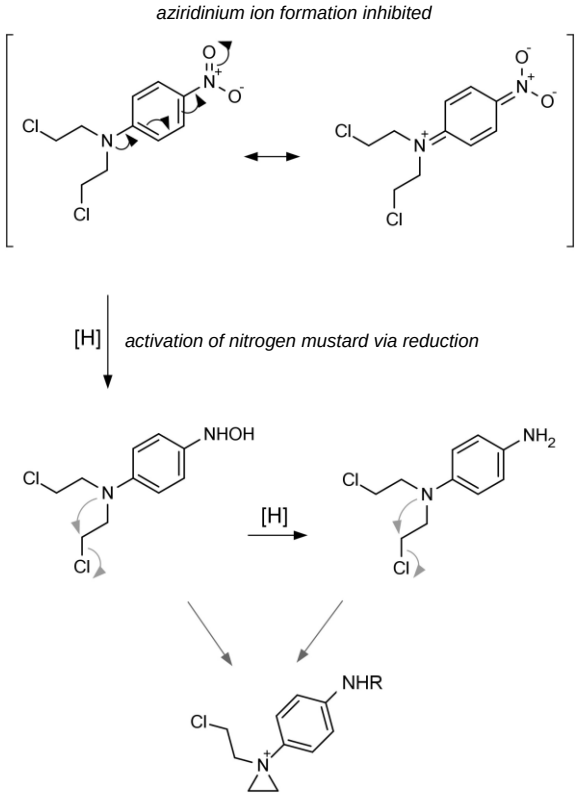

Scheme 7.3. Reduction of an electron-withdrawing nitro group to corresponding hydroxylamino or amino groups constitutes an "electronic switch" that "turns on" aziridinium ion formation.

7.2 Method development and selection of a training set for computational prediction of substituent effects.

Arguably the best-established means by which to quantify the electron-withdrawing or donating power of a group is the Hammett substituent constant (σ).[2021222324] By convention, electron-withdrawing groups are assigned positive σ values, electron-donating groups negative σ values, and σ is defined as zero when hydrogen is

the substituent ($\sigma = 0$ when –H). Originally based on the ionization constants of a series of meta- and para-substituted benzoic acids,[24] the Hammett σ parameter has since been applied to numerous, diverse reactions with success in establishing quantitative relationships between Hammett substituent constants and reaction rates and equilibria.[252627] Importantly, it has been established that the rate at which N-aryl nitrogen mustards form aziridinium ions correlates well with Hammett substituent constants.[6] Thus, we were interested in developing a rapid, reliable, but "user-friendly" method by which we might predict Hammett substituent constants for several benzotriazine derivatives. Electronic structure calculations appealed to us, as modern computational techniques have been repeatedly shown to produce excellent agreement with experiment,[28] and contemporary computing power allows rapid processing of computational jobs in many cases. Thus, we pursued a method by which to predict Hammett substituent constants for substituted benzotriazines based on the results of *ab initio* calculations.[29]

In the interest of simplicity, we wished to use a metric by which to predict σ values based on relatively "routine" electronic structure calculations. This prompted us to consider molecular properties which might be readily extracted from optimized structures of substituted benzotriazines. Examination of the canonical resonance structures associated with aryl-mediated electron withdrawal from nitrogen (Figure 7.3) led us to consider C-N bond length, C-N stretching frequency, and extent of pyramidalization at nitrogen as possible observables which might correlate with Hammett substituent constants. A survey of the literature revealed that work conducted by Seybold's group[30] on a series of substituted anilines showed that C-N bond length correlates but modestly

with Hammett σ values when structures were optimized at the HF/6-311G(d,p) level of theory (r^2 = 0.797). Consequently, we opted to not pursue this metric for prediction of σ values. Furthermore, we quickly realized that coupling of vibrational modes prevents C-N stretching frequencies from being usable metrics for prediction of Hammett σ values.[31] Thus, we pursued pyramidalization angle about nitrogen as the measure of substituent electronic effects. We anticipated that electron-withdrawing substituents would decrease pyramidalization around nitrogen, whereas electron-donating substituents would increase it.

Surprisingly, we found that several methods have been proposed for calculation of "degree of pyramidalization" or the "pyramidalization angle" at a given center.[3233] Among these methods, Haddon's π-orbital axis vector (POAV)[3435] seemed the most robust and quantitative measure of this apparently-elusive quantity. This method, in accord with traditional teachings of molecular geometry, defines trigonal planar centers containing σ-σ bond angles ($\theta_{\sigma\text{-}\sigma}$) of 120° and π-σ interorbital angles ($\theta_{\pi\text{-}\sigma}$) of 90° as having *no* pyramidal character (strictly sp^2 hybridized). Alternatively, sp^3 hybridized centers exhibit uniform σ-σ bond angles of 109.5^0 (in an ideal, carbon-centered tetrahedron). Thus, the angle defined by the POAV and any of the σ bonds ranges from 90^0 at sp^2-hybridized centers (no pyramidalization) to 109.5^0 in sp^3-hybridized carbon centers (complete pyramidalization). Consequently, pyramidalization angles (defined as $\theta_{\pi\text{-}\sigma}$ – 90°) typically range from 0 – 19.5° (Figure 7.3). An excellent graphical depiction of the interplay amongst these parameters is presented in Figure 6 of Haddon's paper.[34] Though this method was originally developed to describe the extent of pyramidalization

at carbon centers, it has been successfully extended to other elements, including nitrogen.[3637] Here, we refer to this measure of pyramidalization as θ_H for Haddon's theta.

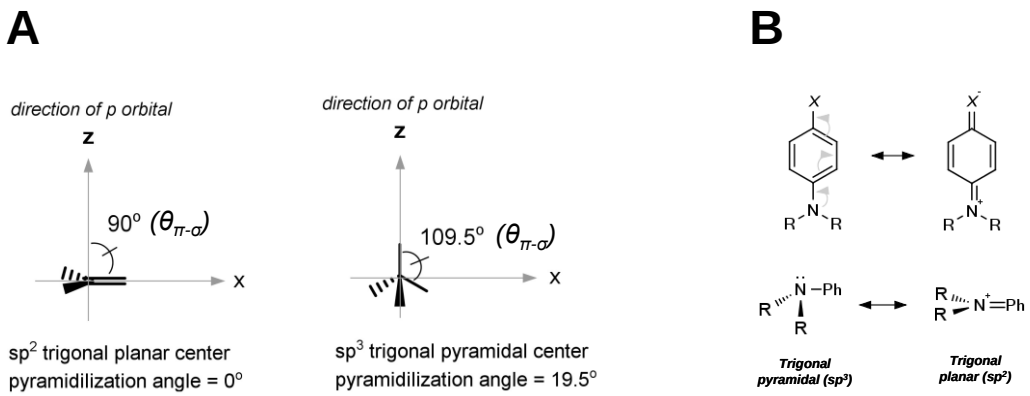

Figure 7.3. Graphical representations of the basis for determination of Haddon's measure of pyramidalization (POAV). (**A**) Degree of pyramidalization is computed as a function of the angle between the π-orbital axis vector and any of the σ bond angles. (**B**) Electron-withdrawing substituents attached to an aryl amine should decrease the degree of pyramidalization about nitrogen.

Though the θ_H parameter has seen widespread application in a variety of systems, to our knowledge no attempt has been made to correlate this value with Hammett substituent constants. Thus, we first examined a set of structurally-diverse meta- and para-substituted anilines to test for correlation between θ_H and Hammett substituent constants. We found when substituted anilines were optimized to minima using DFT B3LYP/6-311+G** and θ_H computed from bond angles taken from the optimized geometries, excellent linear correlation (r^2 = 0.96) was observed between θ_H and Hammett σ values (Figure 7.4). Using the equation derived from linear regression through this data, we then "back-calculated" predicted σ values for the aniline training set

as a means of forecasting the error associated with these predictions. We found that the average difference between predicted and experimental σ values was ± 0.07, corresponding to an average error in estimation of σ of 17% (Table 7.1). It is worth noting that visual inspection of pyramidalization is not an advisable method by which to assess strength of electron-donating or withdrawing substituent, as subtle changes in θ_H correspond to large changes in σ. Consider *p*-methoxyaniline and *p*-nitroaniline (Figure 7.5). Although a visible change in pyramidalization has occurred, it may appear to the "casual viewer" a subtle one, although the difference in σ values of the substituents is large (approximately 1.5).

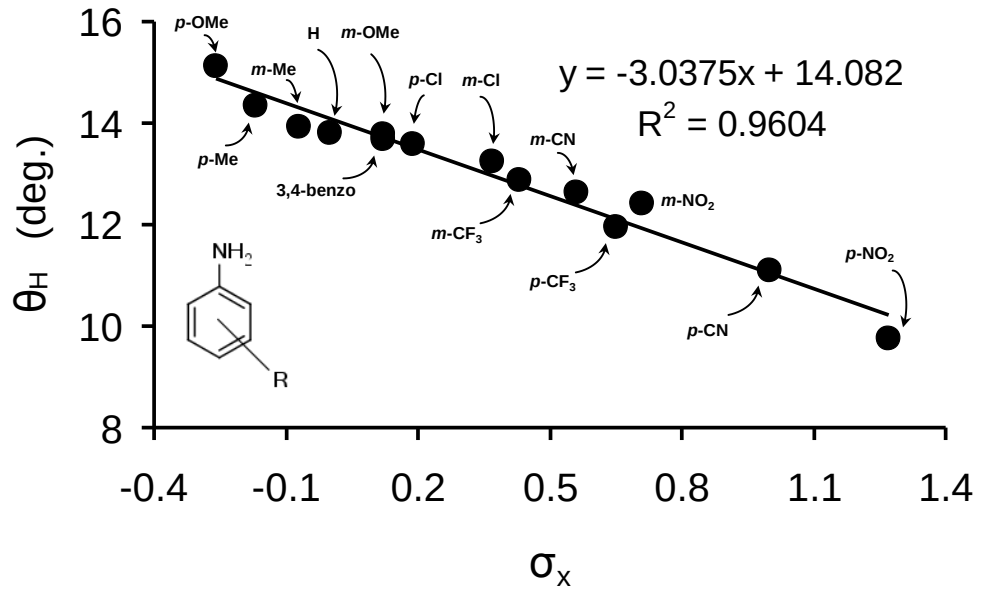

Figure 7.4. A plot of computationally-predicted pyramidalization angles (θ_H) versus experimentally-determined Hammett substituent constants taken from the literature.[2120]

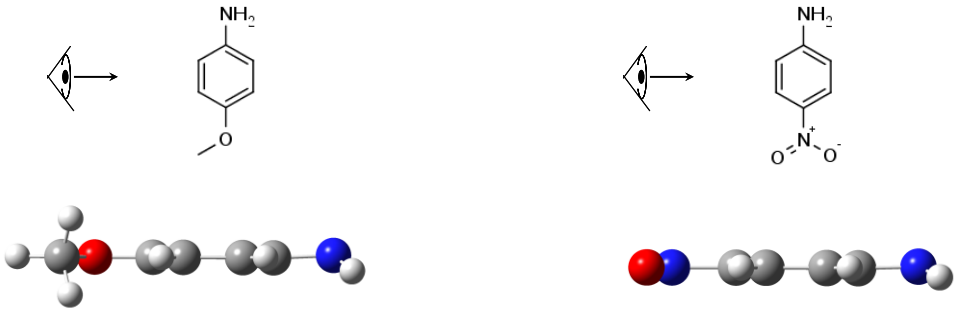

Figure 7.5. Optimized structures of *p*-methoxyaniline and *p*-nitroaniline.

Substituent	Θ_H	σ_{exp}	σ_{pred}	$\sigma_{pred} - \sigma_{exp}$
p-OMe	15.13	-0.26	-0.34	-0.08
p-Me	14.34	-0.17	-0.08	0.09
m-Me	13.93	-0.07	0.05	0.12
-H	13.81	0	0.09	0.09
m-OMe	13.79	0.12	0.10	-0.02
3,4-benzo	13.69	0.12	0.13	0.01
p-Cl	13.58	0.19	0.17	-0.02
m-Cl	13.23	0.37	0.28	-0.09
m-CF_3	12.88	0.43	0.40	-0.03
m-CN	12.62	0.56	0.48	-0.08
p-CF_3	11.95	0.65	0.70	0.05
m-NO_2	12.41	0.71	0.55	-0.16
p-CN	11.11	1	0.98	-0.02
p-NO_2	9.75	1.27	1.43	0.16

$\Sigma \mid \sigma_{exp} \mid = 5.92$ $\Sigma \mid \sigma_{pred} - \sigma_{exp} \mid = 1.03$

n = 14 *Avg. dev. = ± 0.07 (17%)*

Table 7.1. Predicted pyramidalization angles (θ_H), experimental Hammett substituent constants (σ_{exp}), predicted Hammett substituent constants (σ_{pred}), and arithmetic differences between predicted and experimentally-determined substituent constants ($\sigma_{pred} - \sigma_{exp}$) for various meta- and para-substituted anilines. The sum of the absolute differences between experimental and predicted substituent constants (1.03) divided by the sum of the absolute values of σ (5.92) reveals an average 17 % error in estimations.

7.3 Prediction of Hammett substituent constants for a series of substituted benzotriazines.

Having established that computationally-predicted pyramidalization angles might be used to predict Hammett substituent constants, we turned our attention to modeling a series of substituted 6- and 7-amino benzotriazines. Structure optimizations were again carried out at the B3LYP/6-311+G(d,p) level of theory and bond angles around nitrogen used in calculation of θ_H were read out from confirmed minima. Using the linear relationship derived from the aniline training set series, Hammett substituent constants were computed for the benzotriazines (Table 7.2). We find that all benzotriazines are electron-withdrawing with predicted σ^- values ranging from 0.26 to 1.86. For comparison, a *p*-Br substituent has a σ^- value of 0.25 and a perfluoro-*tert*-butylsulfonyl group ($-SO_2C(CF_3)_3$) a σ^- value of 1.81.[21] Thus, benzotriazines may be considered modestly electron-withdrawing to powerfully-electron withdrawing substituents.

We found that the calculations suggested that benzotriazines are much more electron-withdrawing to substituents located at the 6-position relative to the 7-position for a given benzotriazine core. For example, the *minimum* difference between predicted σ^- values for 6- versus 7-positioned amines attached to a given benzotriazine was 0.39 (**1b** versus **2b**). Conversely, the maximum predicted difference in σ^- was 1.03, observed in compounds **3c** and **4c.** These differences and their "directionalities" were in agreement with what might be expected by examining canonical resonance structures (Figure 7.6) and corroborate the experimental observation that nitrogen mustards grafted to the 6-

position hydrolyzed more slowly than those at the 7-position, for a given benzotriazine core and leaving group.[19]

No.	Structure	Θ_H (6-NH_2)	σ^- (pred.)
3b	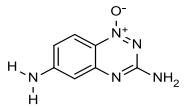	**10.5**	**1.19**
3a	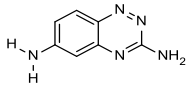	**10.3**	**1.24**
1b	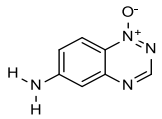	**9.7**	**1.43**
1a	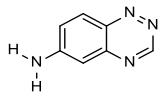	**9.7**	**1.44**
3c	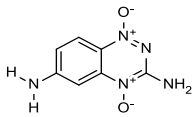	**8.8**	**1.75**
1c	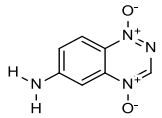	**8.4**	**1.86**

No.	Structure	Θ_H (7-NH_2)	σ^- (pred.)
4a	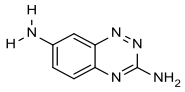	**13.3**	**0.26**
4b	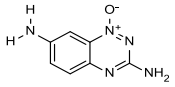	**12.8**	**0.41**
4c	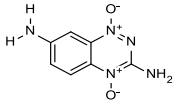	**11.9**	**0.72**
2a	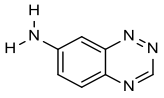	**11.4**	**0.88**
2b	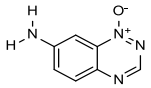	**10.9**	**1.04**
2c	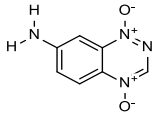	**9.9**	**1.38**

Table 7.2. Pyramidalization angles (θ_H) of 6- or 7-positioned amino groups attached to various benzotriazines and predicted Hammett σ^- values.

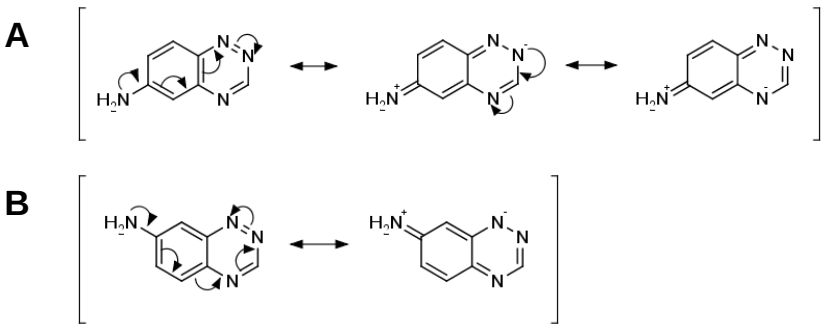

Figure 7.6. Canonical resonance structures of 6- and 7-amino benzotriazines. (**A**) Extensive resonance delocalization suggests that the 6-position may be more strongly electron-withdrawing than the 7-position (pictured in **B**).

Of greatest interest to us was determining which of these benzotriazines might exhibit the largest decrease in σ^- upon reduction from the 1,4-dioxide to the 1-oxide species (a transformation analogous to that which TPZ undergoes under hypoxic conditions). Four systems were examined for this transition: benzotriazines either bearing or lacking a 3-amino group, with nitrogen mustards grafted to either the 6- or 7-position of the benzotriazine core. The "desamino" benzotriazines (lacking a 3-amino group) exhibited decreases in σ^- of 0.43 and 0.34 for 6- and 7-positioned anilinic substituents, respectively (compare compounds **1c** to **1b,** and **2c** to **2b**). The TPZ-like compounds bearing a 3-amino group exhibited decreases in σ^- of 0.56 and 0.31 for 6- and 7-positioned amino groups, respectively (compounds **3c** to **3b**, and **4c** to **4b**). Thus, the pair of compounds exhibiting the largest "electronic switching effect" were tirapazamine-like compounds **3c** and **3b**, where the amino group of interest was attached at the 6-position. This scaffold was pursued in work conducted in our laboratory by Kevin M. Johnson, wherein the nitrogen mustard moiety $-N(CH_2CH_2OMs)_2$ was attached at the 6-position of either 3-amino-1,2,4-benzotriazine 1,4-dioxide or 1-monoxide cores (Figure 7.6). These agents were then assayed for their ability to damage (alkylate) duplex DNA, as in Scheme 7.1. In this work, he found that when the nitrogen mustard unit was attached to the 3-amino-1,2,4-benzotriazine 1,4-dioxide core, little DNA damage was observed. However, when the nitrogen mustard unit was attached to the corresponding benzotriazine 1-oxide (monoxide) core, DNA alkylation was enhanced roughly 30-fold.[19] Presumably, this "switching-on" of DNA-damaging ability is due to the decrease in electron-withdrawing power of the 1-oxide relative to the 1,4-dioxide benzotriazine core, and concomitant "activation" of aziridinium ion formation (Scheme 7.4). These results

corroborate the original hypothesis that the "electronic switching" associated with metabolism of tirapazamine under hypoxic conditions might be exploited to generate a (second) cytotoxic species and that computational methods may be used to predict which compounds may undergo such "electronic switching".

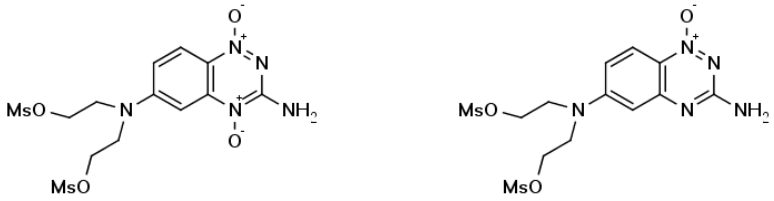

Figure 7.6. Nitrogen mustards prepared and assayed for DNA-damaging ability by Kevin Johnson. The 1,4-dioxide mustard (left) poorly damaged DNA, while 1-oxide (right) was 30-fold more potent in alkylating duplex DNA.

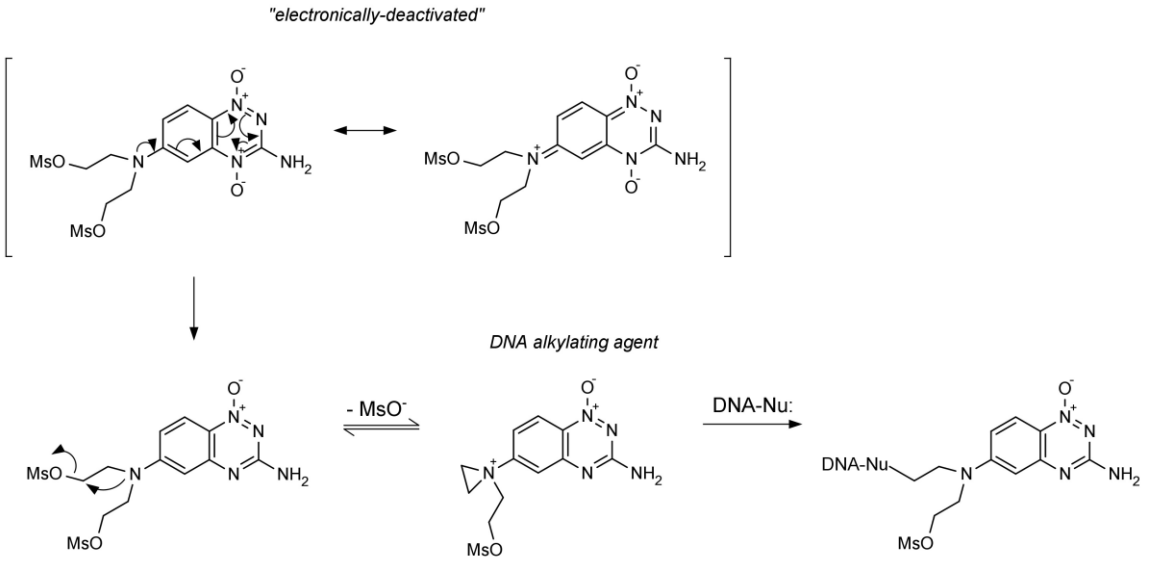

Scheme 7.4. Proposed mechanism for induction of DNA damage by nitrogen mustard-containing 3-amino-1,2,4-benzotriazine 1-oxide.

Work conducted in our laboratory by Kevin Johnson revealed that the 6-hydroxy analogues of **3b** and **3c** have pK_a values of 6.3 and 5.3, respectively (Figure 7.6). Using the ρ value 2.23 suggested by Biggs and Robinson for the ionization of phenols,[20] we calculate that the Hammett σ^- constants for these benzotriazine substituents are 1.64 and 2.10, respectively (difference = 0.46). This data reveals an apparent systematic underestimation in predicted σ^- values of **3c** and **3b** of 0.4 on average, but good agreement between predicted and experimental *differences* in σ^- ($\Delta\sigma^-_{pred} = 0.56$, $\Delta\sigma^-_{exp} = 0.46$). It would be interesting to pursue the basis for this apparent systematic error, in an effort to develop a more accurate prediction method of absolute values of Hammett substituent constants for structurally-diverse systems.

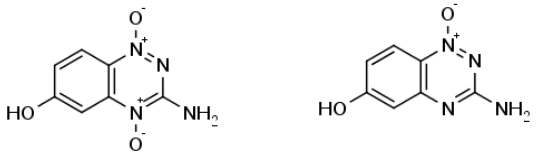

$pK_a = 5.3$ $\sigma^- = 2.10$ $pK_a = 6.3$ $\sigma^- = 1.64$

Figure 7.6. Phenolic analogues of **3b** and **3c** used in experimental pK_a and σ determinations.

7.4 Conclusions

Here, we have described a novel method by which to computationally predict Hammett substituent constants with reasonable accuracy. Importantly, the calculations involved are straightforward and do not require computing power beyond that of a typical

desktop computer. Within the anilinic training set of molecules used in development of this method, we found that predicted σ values varied from those determined experimentally by an average of 17 %. Application of this method to predicting σ constants for a series of benzotriazines suggested a systematic underestimation in σ of ~0.4, though differences in σ for a given pair of benzotriazine oxides agreed reasonably well with experiment (22 % error). Thus, this method may be viewed as a convenient and rapid means by which to predict "electronic switching effects" associated with changes in structure of various aryl amines. Finally, utilization of known ρ values should allow for extension of this predictive method to phenolic and other systems.

7.5 Computational Methods

Electronic structure calculations were performed using the Gaussian 03[38] software package run on an SGI Altix BX2 NUMA architecture machine with 64 1.5 GHz Intel Itanium2 processors. All optimizations were performed using the hybrid density functional B3LYP[3940] with the 6-311+G** basis set. For molecules with asymmetric rotational conformers, both rotamers were optimized to minima and the conformer of lower energy (evaluated on the basis of zero point-corrected energies) was used in the study. Typically, these rotational conformers differed by less than 0.1 kcal/mol (zero point-corrected energies). All stationary points were confirmed minima by vibrational frequency analysis (zero imaginary frequencies). To verify that structures exhibiting N-aryl conjugation were not simply local minima, we performed structure optimizations at the same level of theory on the training set "endpoints" p-methoxyaniline and p-

nitroaniline, where input structures had amino and aryl groups orthogonal to one another. These structures optimized to the same geometries as those found when starting the two groups roughly coplanar.

Bond angles about anilinic nitrogens in the training set or at 6- or 7-positions of 1,2,4-benzotriazines were read from the atomic coordinates of optimized structures using GaussView. From these bond angles the degree of pyramidalization at nitrogen was computed according to the method of Haddon, using an Excel spreadsheet kindly made freely-available by him.[35] To evaluate the correlation between extent of pyramidalization at nitrogen and σ values, σ^- values were taken from the literature[21] and pyramidalization angles plotted as a function of these values. From this plot was extracted the equation for the linear regression trendline (θ_H = -3.0375(σ) + 14.082, r^2 = 0.96, n = 14). The equation was rearranged (solved for σ) and used in prediction of Hammett substituent constants for 1,2,4-benzotriazine cores on the basis of pyramidalization angles extracted from their optimized structures.

References

(1) Goodman LS; Wintrobe MM; Dameshek W; Goodman MJ; Gilman A; McLennan MT. Nitrogen Mustard Therapy: Use of Methyl-Bis(beta-Chloroethyl)amine Hydrochloride and Tris(beta-Chloroethyl)amine Hydrochloride for Hodgkin's Disease, Lymphosarcoma, Leukemia and Certain Allied and Miscellaneous Disorders. *JAMA* **1984**, *251*, 2255–2261.

(2) Staff, P. D. R. *Physicians' Desk Reference, 66th Edition*; 2012 Edition edition.; PDR Network: Montvale, N.J., 2011.

(3) Beown, S. S. Nitrogen Mustards and Related Alkylating Agents. In *Advances in Pharmacology*; Silvio Garattini and Parkhurst A. Shore, Ed.; Advances in Pharmacology; Academic Press, 1963; Vol. Volume 2, pp. 243–295.

(4) Fung, L. W.; Ho, C.; Roth, E. F.; Nagel, R. L. The Alkylation of Hemoglobin S by Nitrogen Mustard. High Resolution Proton Nuclear Magnetic Resonance Studies. *J. Biol. Chem.* **1975**, *250*, 4786–4789.

(5) Mattes, W. B.; Hartley, J. A.; Kohn, K. W. DNA Sequence Selectivity of guanine–N7 Alkylation by Nitrogen Mustards. *Nucleic Acids Res.* **1986**, *14*, 2971–2987.

(6) O'Connor, C. J.; Denny, W. A.; Fan, J.-Y.; Gravatt, G. L.; Grigor, B. A.; McLennan, D. J. Hydrolysis and Alkylating Reactivity of Aromatic Nitrogen Mustards. *J. Chem. Soc. Perkin Trans. 2* **1991**, 1933–1939.

(7) Gates, K. S. An Overview of Chemical Processes That Damage Cellular DNA: Spontaneous Hydrolysis, Alkylation, and Reactions with Radicals. *Chem. Res. Toxicol.* **2009**, *22*, 1747–1760.

(8) Patrick, G. L. *An Introduction to Medicinal Chemistry*; 5 edition.; Oxford University Press: Oxford, 2013.

(9) Brown, J. M. Tumor Hypoxia in Cancer Therapy. *Methods Enzymol.* **2007**, *435*, 297–321.

(10) Brown, J. M.; Wilson, W. R. Exploiting Tumour Hypoxia in Cancer Treatment. *Nat. Rev. Cancer* **2004**, *4*, 437–447.

(11) Shannon, A. M.; Bouchier-Hayes, D. J.; Condron, C. M.; Toomey, D. Tumour Hypoxia, Chemotherapeutic Resistance and Hypoxia-Related Therapies. *Cancer Treat. Rev.* **2003**, *29*, 297–307.

(12) Brown, J. M. The Hypoxic Cell A Target for Selective Cancer Therapy—Eighteenth Bruce F. Cain Memorial Award Lecture. *Cancer Res.* **1999**, *59*, 5863–5870.

(13) Anderson, R. F.; Shinde, S. S.; Hay, M. P.; Gamage, S. A.; Denny, W. A. Radical Properties Governing the Hypoxia-Selective Cytotoxicity of Antitumor 3-Amino-1,2,4-Benzotriazine 1,4-Dioxides. *Org. Biomol. Chem.* **2005**, *3*, 2167–2174.

(14) Hay, M. P.; Gamage, S. A.; Kovacs, M. S.; Pruijn, F. B.; Anderson, R. F.; Patterson, A. V.; Wilson, W. R.; Brown, J. M.; Denny, W. A. Structure−Activity Relationships of 1,2,4-Benzotriazine 1,4-Dioxides as Hypoxia-Selective Analogues of Tirapazamine. *J. Med. Chem.* **2003**, *46*, 169–182.

(15) Junnotula, V.; Sarkar, U.; Sinha, S.; Gates, K. S. Initiation of DNA Strand Cleavage by 1,2,4-Benzotriazine 1,4-Dioxide Antitumor Agents: Mechanistic Insight from Studies of 3-Methyl-1,2,4-Benzotriazine 1,4-Dioxide. *J. Am. Chem. Soc.* **2009**, *131*, 1015.

(16) Yin, J.; Glaser, R.; Gates, K. S. On the Reaction Mechanism of Tirapazamine Reduction Chemistry: Unimolecular N-OH Homolysis, Stepwise Dehydration, or Triazene Ring-Opening. *Chem. Res. Toxicol.* **2012**, *25*, 634–645.

(17) Daniels, J. S.; Gates, K. S. DNA Cleavage by the Antitumor Agent 3-Amino-1,2,4-Benzotriazine 1,4-Dioxide (SR4233): Evidence for Involvement of Hydroxyl Radical. *J. Am. Chem. Soc.* **1996**, *118*, 3380–3385.

(18) Gu, Y.; Guise, C. P.; Patel, K.; Abbattista, M. R.; Li, J.; Lie, J.; Sun, X.; Atwell, G. J.; Boyd, M.; Patterson, A. V.; et al. Reductive Metabolism of the Dinitrobenzamide Mustard Anticancer Prodrug PR-104 in Mice. *Cancer Chemother. Pharmacol.* **2011**, *67*, 543–555.

(19) Johnson, K. M.; Parsons, Z. D.; Barnes, C. L.; Gates, K. S. Toward Hypoxia-Selective DNA-Alkylating Agents Built by Grafting Nitrogen Mustards onto the Bioreductively Activated, Hypoxia-Selective DNA-Oxidizing Agent 3-Amino-1,2,4-Benzotriazine 1,4-Dioxide (Tirapazamine). *J. Org. Chem.* **2014**.

(20) Biggs, A. I.; Robinson, R. A. 69. The Ionisation Constants of Some Substituted Anilines and Phenols: A Test of the Hammett Relation. *J. Chem. Soc. Resumed* **1961**, 388–393.

(21) Hansch, C.; Leo, A.; Taft, R. W. A Survey of Hammett Substituent Constants and Resonance and Field Parameters. *Chem. Rev.* **1991**, *91*, 165–195.

(22) Tsuruta, T.; Fueno, T.; Furukawa, J. A Molecular Orbital Discussion of the Hammett Equation : Semi-Empirical Interpretation on the Abnormality of the

Benzyl Anion Type Substituent. *Bull. Inst. Chem. Res. Kyoto Univ.* **1956**, *34*, 214–223.

(23) Jaffé, H. H. A Reëxamination of the Hammett Equation. *Chem. Rev.* **1953**, *53*, 191–261.

(24) Hammett, L. P. The Effect of Structure upon the Reactions of Organic Compounds. Benzene Derivatives. *J. Am. Chem. Soc.* **1937**, *59*, 96–103.

(25) Brinchi, L.; Di Profio, P.; Germani, R.; Savelli, G.; Spreti, N.; Bunton, C. A. The Hammett Equation and Micellar Effects on SN2 Reactions of Methyl Benzenesulfonates ?ms The Role of Micellar Polarity. *Eur. J. Org. Chem.* **2000**, *2000*, 3849–3854.

(26) Cayzergues, P.; Georgoulis, C.; Mathieu, G. On the Acree Relation. VII. Hammett Correlations with the Rate Constants of "Ions" and "Ion Pairs", Ki and Kp Respectively, in a Nucleophilic Substitution Reaction on Benzylic Substrates. *J Chim Phys Phys-Chim Biol* **1987**, *84*, 63–70.

(27) Ritchie, C. D.; Sager, W. F. An Examination of Structure-Reactivity Relationships. In *Progress in Physical Organic Chemistry*; Cohen, S. G.; Jr, A. S.; Taft, R. W., Eds.; John Wiley & Sons, Inc., 1964; pp. 323–400.

(28) Foresman, J. B.; Frisch, Ae. *Exploring Chemistry With Electronic Structure Methods: A Guide to Using Gaussian*; 2 edition.; Gaussian: Pittsburgh, PA, 1996.

(29) Whether DFT Methods Are Formally Ab Initio Calculations or Not Will Not Be Addressed Here.

(30) Gross, K. C.; Seybold, P. G. Substituent Effects on the Physical Properties and pKa of Aniline. *Int. J. Quantum Chem.* **2000**, *80*, 1107–1115.

(31) Cremer, D.; Wu, A.; Larsson, A.; Kraka, E. Some Thoughts about Bond Energies, Bond Lengths, and Force Constants. *Mol. Model. Annu.* **2000**, *6*, 396–412.

(32) Radhakrishnan, T. P.; Agranat, I. Measures of Pyramidalization. *Struct. Chem.* **1991**, *2*, 107–115.

(33) Vázquez, S.; Camps, P. Chemistry of Pyramidalized Alkenes. *Tetrahedron* **2005**, *61*, 5147–5208.

(34) Haddon, R. C. Pi-Electrons in Three Dimensions. *Acc. Chem. Res.* **1988**, *21*, 243–249.

(35) Haddon, R. C. Comment on the Relationship of the Pyramidalization Angle at a Conjugated Carbon Atom to the Σ Bond Angles. *J. Phys. Chem. A* **2001**, *105*, 4164–4165.

(36) WALSH, J. D.; A.-F, M. Flavin reduction potential tuning by substitution and bending. *Comput. Theor. Chem.* **623**, 2003.

(37) Rojisha, V. C.; De, S.; Parameswaran, P. Electronic Structure of Six-Membered N-Heterocyclic Carbenes and Its Heavier Analogues: Reactivity of the Lone Pair versus the Exocyclic Double Bond. *Inorg. Chem.* **2012**, *51*, 8265–8274.

(38) Frisch, M.; Trucks, G.; Schlegel, H.; Scuseria, G.; Robb, M.; Cheeseman, J.; Montgomery, J.; Vreven, T.; Kudin, K.; Burant, J.; et al. Gaussian 03, Revision E. 01. *Gaussian 03 Revis. E 01* **2003**.

(39) Becke, A. D. Density‐functional Thermochemistry. III. The Role of Exact Exchange. *J. Chem. Phys.* **1993**, *98*, 5648–5652.

(40) Stephens, P. J.; Devlin, F. J.; Chabalowski, C. F.; Frisch, M. J. Ab Initio Calculation of Vibrational Absorption and Circular Dichroism Spectra Using Density Functional Force Fields. *J. Phys. Chem.* **1994**, *98*, 11623–11627.

Chapter 8: Alkylation of Biologically-Relevant Nucleophiles by Garlic-Derived Phytochemicals – Allyl Transfer from Organic Polysulfides

8.1 Introduction

The medicinal benefits of garlic consumption have been recognized since antiquity.[1] However, it has only been recently (since the late 20th century) that a systematic examination of the bioactive constituents of garlic and their cellular/physiological effects has been undertaken.[2] Garlic and other members of the genus *Allium* are rich in organic polysulfide compounds, which have the potential to undergo a variety of redox and other reactions with small molecule and protein nucleophiles – particularly thiols – *in vivo*. Clearly, modification of biomolecules such as proteins can have profound biological and physiological consequences. These organic polysulfides have thus been the focus of studies aimed at linking consumption of garlic to various physiological effects.[3,4] For example, one study found that the *allium* constituent ajoene inhibited cyclooxygenase 2 (COX 2) activity in cells, in similar fashion to the therapeutic mechanism of action of non-steroidal, anti-inflammatory drugs (NSAIDs) such as aspirin.[5] However, the chemical mechanism by which ajoene inhibited COX 2 was not determined. Indeed, there is a dearth of information regarding the chemical mechanisms by which garlic-derived phytochemicals (GDPs) achieve physiological effects. Thus, we set out to characterize some of the fundamental chemical processes in

which GDPs might be involved by employing discrete organic polysulfides commonly found in garlic under well-defined reaction conditions.

Results

8.2. Preparation of 1-*tert*-butyl-4-(prop-2-en-1-ylsulfanyl)benzene (2) *via* Reaction of 4-*tert*-butylbenzenethiol (1) with Allyl Bromide: an Authentic Standard for Transallylation Reactions

Among the reactions envisioned to be possible between biological nucleophiles and organic polysulfides, alkylation (allyl transfer) was of greatest interest to us.[67] Thus, we began this work by synthesizing an authentic standard of the product arising from allyl transfer from an organic polysulfide to 4-*t*-butylbenzenethiol (**1**). The authentic standard 1-*tert*-butyl-4-(prop-2-en-1-ylsulfanyl)benzene (**2**) was prepared by treating **1** with allyl bromide (1.05 equiv) in THF in the presence of TEA (1.1 equiv, Scheme 8.1). The reaction was deemed quantitative by thin layer chromatography (TLC) and the isolated product afforded spectral data consistent with allylation of the aryl thiol (Figure 8.1). We chose **1** as a model thiol for these studies due to its desirable chemical and physical properties. Namely, it was expected that reactions **1** undergo might be similar to those expected for "active" biological thiol(ate)s, as aryl thiols are generally more acidic than alkyl thiols, and would thus afford greater fractions of reactive thiolate under mild conditions.[89] Additionally, the aryl ring in **1** is chromophoric with respect to UV light, rendering the molecule readily visible by thin layer chromatography (TLC), and the

4-*tert*-butyl group affords both a characteristic ^{1}H NMR signal useful in structural characterization and greatly decreases the vapor pressure (and thus the stench) of the molecule relative to benzenethiol (b.p. 4-*t*-butylbenzenthiol 238°C, benzenethiol 169°C).[10]

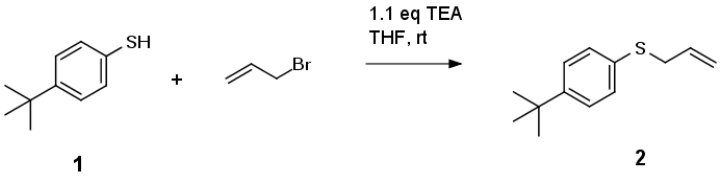

Scheme 8.1 Preparation of an authentic standard of **2** by allylation of **1** with allyl bromide.

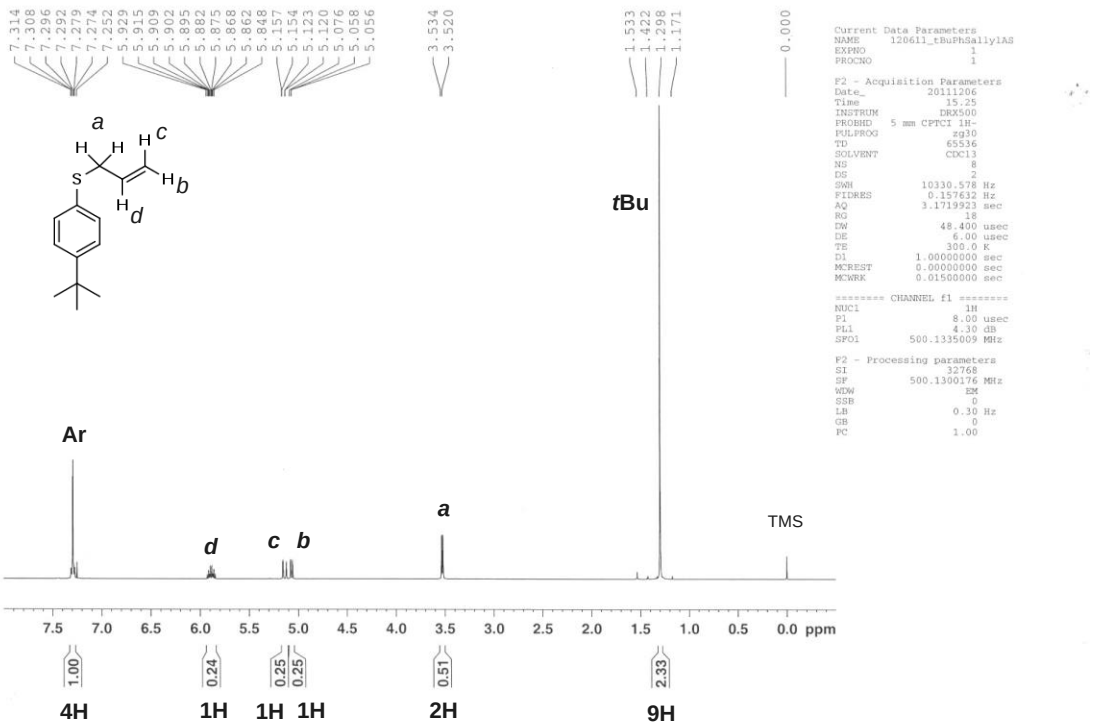

Figure 8.1. Alkylation of **1** by allyl bromide readily afforded **2**.

8.3. Reaction of Diallyl Disulfide (DADS) with 4-*tert*-butylbenzenethiol

Diallyl disulfide (DADS, Figure 8.2) is a major organic polysulfide constituent of garlic.[11] We were interested in characterizing its reactions with the model thiol **1** at various stoichiometric ratios, as we expected that thiol-disulfide exchange would likely precede alkylation and influence product distribution (Scheme 8.2A). Thus, we anticipated that equimolar concentrations of **1** and DADS might afford predominantly products associated with thiol-disulfide exchange processes. Indeed, we found that, when **1** and DADS were combined in equimolar proportion, the major product of the reaction seemed to be aryl allyl disulfide **3**. Aryl disulfide **4** also seemed to form in moderate yield (Scheme 8.2A and B). Putative products **3** and **4** were of identical R_f value on TLC (a single spot), and so were inseparable by column chromatography over silica gel. Proton NMR spectral peaks of the spot did not match either the allylated product **2** nor the thiol starting material. However, the spectrum contained multiple aryl proton clusters, two *t*Bu singlets, and a proton pattern indicative of an allyl group. Thus, we attribute these spectral peaks to products **3** and **4**, arising from thiol-disulfide exchange reactions. Product distributions were estimated from relative integrals in the ^{1}H NMR spectrum of the mixture. The estimated ratio of **3**:**4** was roughly 3:1.

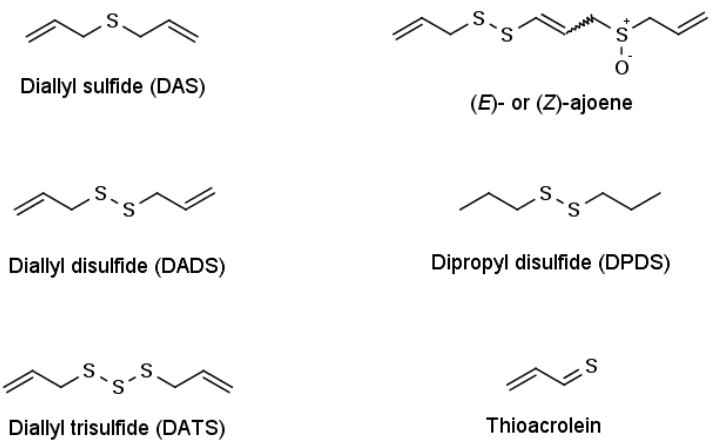

Figure 8.2. Organosulfur compounds found in garlic.

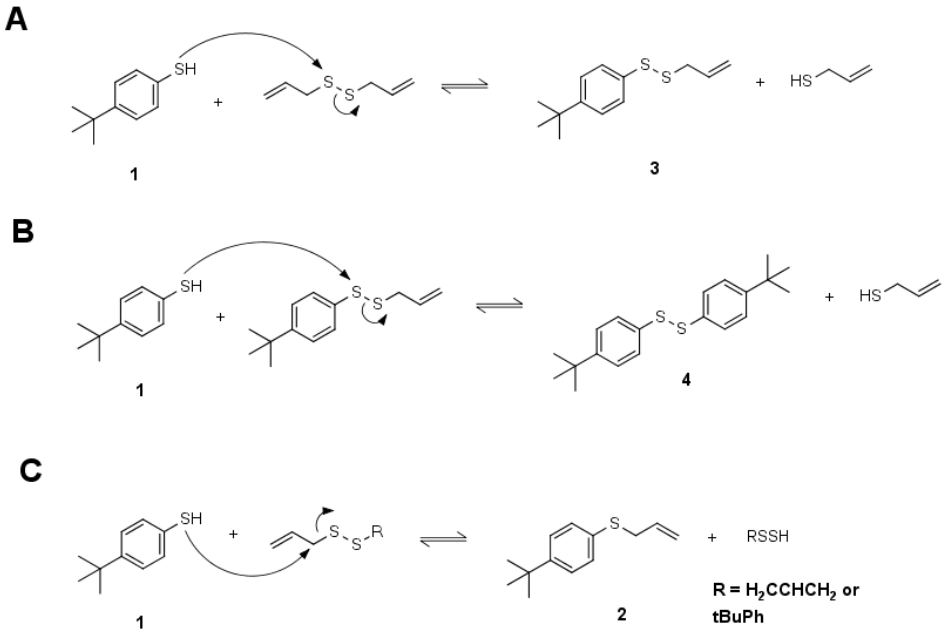

Figure 8.2. Reactions pathways available between thiol **1** and DADS. Pathways **A** and **B** are thiol-disulfide exchange reactions; pathway **C** involves alkylation of thiol **1** either by DADS directly or by the intermediate allyl aryl disulfide **3**.

We then conducted a reaction under the same conditions, but employing excesses thiol **1** (3 equiv, relative to DADS). We anticipated that the presence of excess **1** might promote allyl transfer from thiol-disulfide exchange product **3** to the aryl thiol. Indeed, we isolated product **2** from this reaction in 9 % yield. The isolated yield was probably underrepresentative of the reaction total yield, as a substantial amount of material was lost during the purification process. Importantly, this reaction represents the first, direct spectroscopic evidence of alkylation (allyl transfer) from organic polysulfides found in garlic to biologically-relevant nucleophiles.

We then examined whether allyl transfer from DADS to an oxygen nucleophile might be possible. We employed phenol (5 equiv) as a model oxygen nucleophile in the presence of DADS (1 equiv) under the same reaction conditions as described above (MeOH, 40°C, 1.1 equiv TEA). After 24h reaction time had elapsed, we observed no formation of allyl phenyl ether by TLC, compared against commercially-available authentic standard.

8.4 Reactions of Various Organic Polysulfides with Model Thiol 1

We next examined reaction of model thiol **1** with various organic polysulfides found in garlic under uniform reaction conditions. We explored reaction of **1** with diallyl sulfide (DAS), diallyl disulfide (DADS), diallyl trisulfide (DATS), and dipropyl disulfide (DPDS, Figure 8.2). Consistently, **1** was present in 5-fold molar excess to the organic

polysulfide, and reactions were conducted in methanol held at 40°C for 24h. Yields of allylated product **2** from these reactions are given in Table 8.1.

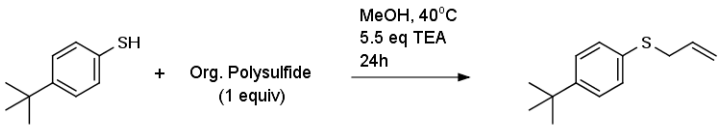

1 (5 equiv) **2**

Entry	Name	Structure	(%) Yield (2)
1	DAS	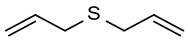	0
2	DADS	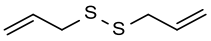	52
3	DATS	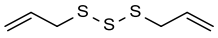	0 (*20)
4	DPDS	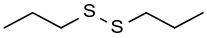	0 (*PhSPr*)

Table 8.1. Percent yields of allyl transfer product **2** from reaction of **1** with various organic polysulfides in MeOH, 40°C for 24h. (*) After 24h, 2 equiv more **1** was added and the reaction allowed to stir for an additional 24h.

Interestingly, we observed no formation of **2** when DAS was the potential allyl donor. This may suggest that the leaving group ability of the allyl mercaptan thiolate is insufficient to allow the substitution reaction to occur. In accord with our earlier observations, treatment of DADS with excess **1** afforded alkylated product **2** in 53 % yield. Treatment of the trisulfide DATS with 5 equiv of **1** afforded no allylated product **2** after 24 h reaction time. However, upon addition of another 2 equiv of **1** and an additional 24 h reaction time, **2** was isolated from the reaction mixture in 17 % yield. These results may suggest consumption of the majority of the 5 equiv of **1** by redox processes, but that a larger excess of the free thiol promotes alkylation. Finally, we investigated whether the saturated analogue of DADS – dipropyl disulfide (DPDS) –

might also be capable of alkylating model thiol **1** *via* propyl transfer. We found no evidence of propyl transfer to **1** from DPDS under these reaction conditions. These observations are consistent with previous reports indicating that allylic substrates are superior to propyl substrates in S_N2-type reactions.[12]

8.5 Organic Polysulfides do not Inactivate PTP1B

Finally, we were interested in determining whether the organic polysulfides found in garlic might be capable of inactivating PTP1B. Ethanolic garlic extracts have been shown to have anti-diabetic properties in chemically-induced diabetic rat models, of greater potency than the anti-diabetic drug glibenclamide.[13] The mechanisms of action by which garlic extracts achieve these anti-diabetic effects are unknown, though diallyl disulfide has been implicated as a major player.[14] It is plausible that organic polysulfides might achieve anti-diabetic effects *via* inactivation of PTP1B by oxidation or alkylation of Cys215. Thus, we examined whether DADS or DATS might be capable of inactivating PTP1B. We found that when PTP1B was treated with DADS or DATS in pH 7 buffer (25°C), no loss of enzyme activity occurred (Figure 8.3), suggesting no modification of the enzyme by these agents. As a "positive control" for alkylation of PTP1B by allylic electrophiles, we treated native PTP1B with allyl bromide. Again, no loss of enzyme activity was observed. These results are intriguing in light of previous work conducted by our group, where the α,β-unsaturated aldehyde acrolein was found to be a potent inactivator of the enzyme.[15] Taken together, these results suggest that PTP1B is not susceptible to alkylation by allylic electrophiles in the context of the S_N2 or S_N2'

mechanisms, but is so in the context of 1,4-additions. This suggests that organic polysulfides likely do not modify PTP1B *in vivo*, although oxidized metabolites such as diallyl sulfone or the corresponding epoxide may.

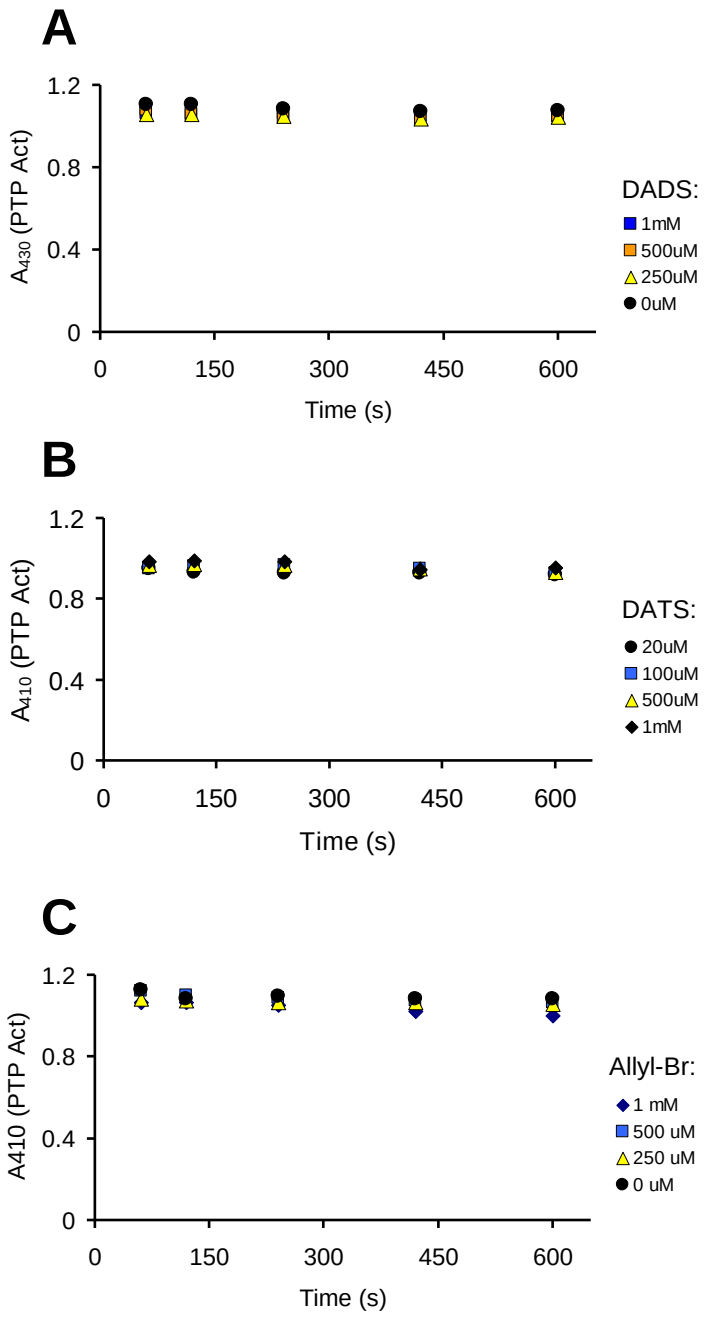

Figure 8.3. Allylic substrates DADS (**A**), DATS (**B**), and allyl bromide (**C**) do not inactivate PTP1B (pH 7.0, 25°C).

8.6 Methods and Materials

General synthetic methods. All reagents except DATS were from Sigma-Aldrich or Fischer Scientific. Diallyl trisulfide was from Cayman Chemical, and was sold as a 0.5 M solution in acetone. Anhydrous organic solvents were prepared by treating the solvents with no less than 20 % (v/v) activated 4Å molecular sieves. Purifications were performed by flash chromatography over silica gel as stationary phase. Hexane (100 %) or dichloromethane:hexane (6:94) were used as eluent. NMR spectra (^{1}H and ^{13}C) were collected on a Bruker Avance III 500 MHz spectrometer using TMS as an internal reference. Anhydrous solvents were deoxygenated either by bubbling N_2 through the solvent prior to introduction of reagents or by iterative (3x) evacuations of atmosphere from the sealed reaction apparatus followed by back-filling with dry N_2 (1 atm). To stirred solutions of **1** (1 equiv) and TEA (1.1 equiv) were added allylic electrophiles (0.2 – 1.0 equiv). Reactions were sealed and stirred at 40°C under positive N_2 pressure (1 atm) for 13 – 24 hr. Thereafter, reactions were removed from heat, solvent removed under reduced pressure, and crude reaction mixtures purified by column chromatography.

***Preparation of authentic standard 1-tert-butyl-4-(prop-2-en-1-ylsulfanyl)benzene* (2).** To a stirred solution of **1** (1 mmol) and TEA (1.1 mmol) in 10 mL THF were added 1.05 mmol allyl bromide. Within minutes of stirring at 40°C, a white precipitate formed (presumably triethylammonium bromide salt). The reaction was left stirring for 30 min, the solid filtered off, and the solvent removed *in vacuo.* Purification over silica gel afforded spectroscopically pure **2** as a clear oil (R_f = 0.17 vs

hexane, R_f = 0.28 vs dichloromethane:hexane, 6:94, ^{1}H NMR ($CDCl_3$, 500 MHz): δ 7.29 (m, 4H), δ 5.87 (m, 1H), δ 5.13 (dd, J = 17 Hz, J = 1 Hz, 1H), δ 5.06 (d, J = 10 Hz, 1H), δ 3.52 (d, J = 7 Hz, 1H). ^{13}C NMR ($CDCl_3$, 125 MHz): δ 149.4, δ 133.8, δ 132.3, δ 129.8, δ 125.7, δ 117.4, δ 37.4, δ 34.4, δ 31.2.

Preparation of* 2 *via reaction of* 1 *with diallyl disulfide (5 equiv). To a stirred solution of **1** (1 mmol) in methanol (3 mL) containing TEA (1.1 mmol) were added 32 μL diallyl disulfide (0.2 mmol). The reaction was sealed and left stirring at 40 °C overnight. Thereafter, solvent was removed *in vacuo* and the crude mixture purified by flash chromatography. Compound **2** was isolated as a clear oil and spectral data matched that of the authentic standard **2** (21.8 mg, 0.106 mmol, 53 % yield).

Preparation of* 2 *via reaction of* 1 *with diallyl disulfide (3 equiv). To a stirred solution of **1** (1 mmol) in methanol (5 mL) containing TEA (1.1 mmol) were added 50 μL (0.3 mmol) diallyl disulfide. The mixture was sealed and stirred overnight at 40 °C. Solvent was removed by rotary evaporation and the crude purified by flash chromatography to afford spectroscopically pure **2** as a clear oil (5.5 mg, 0.027 mmol, 9 % yield). *Note: this yield is an underestimate of reaction yield. Material was lost in transfer.*

Preparation of* 2 *by reaction of* 1 *with diallyl trisulfide. To a stirred solution of **1** (1 mmol) in methanol (4 mL) containing TEA (1.1 mmol) were added 357 μL (0.2 mmol) diallyl trisulfide (sold and used as a solution in acetone: 100 mg/mL, or 560 mM). The reaction exhibited a burst of yellow color upon addition of DATS. The mixture was sealed and left stirring at 40 °C for 24 hrs. TLC revealed no formation of product **2** following this time. An additional 69 μL (0.039 mmol) diallyl trisulfide were added and

the reaction left stirring for another 24 hrs. After 48 hrs time total, solvent was removed under reduced pressure and the crude material purified by column chromatography. The isolated yield of spectroscopically-pure **2** was 8.2 mg (0.04 mmol, 17 %).

***Dipropyl disulfide does not alkylate* 1**. The reaction was set up identically to those described above, but with 0.2 equiv dipropyl disulfide (31.3 μL, 0.2 mmol) as electrophile. In parallel, a reaction mixture containing **1** (0.12 mmol), TEA (0.22 mmol), and propyl bromide (0.11 mmol) was set up in methanol (1 mL) for preparation of an authentic standard of the anticipated S-propyl adduct. After 20 min, a new spot (R_f = 0.28 vs hexane) appeared in the reaction mixture containing propyl bromide, consistent with alkylation of **1** by propyl bromide. Following 24 hr reaction time, no new spot was observed in the reaction mixture containing dipropyl disulfide.

PTP inactivation assay methodology. PTP inactivation assays were carried out using previously described methodology.[1617] Briefly, PTP stocks were made thiol-free by gel filtration and diluted to 2x concentration (0.7 μM) in pH 7.0 buffer A (50 mM Tris, 50 mM Bis-Tris, 100 mM NaOAc, 10 mM DTPA, 0.5 % v/v Tween 80). Stocks of allylic electrophiles (DADS, DATS, and allyl bromide) were prepared in dmso and diluted to 2x concentration in buffer A containing 10 % dmso (v/v), final. Upon introduction of the PTP to the electrophile, a timer was started and the reaction monitored at 1, 2, 4, 7, and 10 min intervals by dilution of a 10 μL aliquot of the mixture into 490 μL of pH 6.0 buffer containing 20 mM 4-nitrophenyl phosphate (50 mM Bis-Tris, 100 mM NaCl, 10 mM DTPA, pH 6.0). The activity assay was allowed to proceed for exactly 10 min at 30 °C before being quenched *via* addition of 500 μL of 2 M NaOH in ddH_2O. Absorbances at 410 nm were then measured and plotted as a function of time.

References

(1) Rivlin, R. S. Is Garlic Alternative Medicine? *J. Nutr.* **2006**, *136*, 713S–715S.

(2) Block, E. The Organosulfur Chemistry of the Genus Allium – Implications for the Organic Chemistry of Sulfur. *Angew. Chem. Int. Ed. Engl.* **1992**, *31*, 1135–1178.

(3) Benavides, G. A.; Squadrito, G. L.; Mills, R. W.; Patel, H. D.; Isbell, T. S.; Patel, R. P.; Darley-Usmar, V. M.; Doeller, J. E.; Kraus, D. W. From the Cover: Hydrogen sulfide mediates the vasoactivity of garlic. *Proc. Natl. Acad. Sci.* **2007**, *104*, 17977–17982.

(4) Truong, D.; Hindmarsh, W.; O'Brien, P. J. The molecular mechanisms of diallyl disulfide and diallyl sulfide induced hepatocyte cytotoxicity. *Chem. Biol. Interact.* **2009**, *180*, 79–88.

(5) Dirsch, V. M.; Vollmar, A. M. Ajoene, a natural product with non-steroidal anti-inflammatory drug (NSAID)-like properties? *Biochem. Pharmacol.* **2001**, *61*, 587–593.

(6) Benavides, G. A.; Squadrito, G. L.; Mills, R. W.; Patel, H. D.; Isbell, T. S.; Patel, R. P.; Darley-Usmar, V. M.; Doeller, J. E.; Kraus, D. W. Hydrogen sulfide mediates the vasoactivity of garlic. *Proc. Natl. Acad. Sci. U. S. A.* **2007**, *104*, 17977–17982.

(7) Bonaventura, J.; Rodriguez, E. N.; Beyley, V.; Vega, I. E. Allylation of intraerythrocytic hemoglobin by raw garlic extracts. *J. Med. Food* **2010**, *13*, 943–949.

(8) Parsons, Z. D.; Gates, K. S. Thiol-Dependent Recovery of Catalytic Activity from Oxidized Protein Tyrosine Phosphatases. *Biochemistry (Mosc.)* **2013**, *52*, 6412–6423.

(9) Sivaramakrishnan, S.; Keerthi, K.; Gates, K. S. A Chemical Model for Redox Regulation of Protein Tyrosine Phosphatase 1B (PTP1B) Activity. *J. Am. Chem. Soc.* **2005**, *127*, 10830–10831.

(10) http://www.sigmaaldrich.com.

(11) Liu, C.-T.; Hse, H.; Lii, C.-K.; Chen, P.-S.; Sheen, L.-Y. Effects of garlic oil and diallyl trisulfide on glycemic control in diabetic rats. *Eur. J. Pharmacol.* **2005**, *516*, 165–173.

(12) Carrion, F.; Dewar, M. J. S. Ground states of molecules. 59. MNDO study of SN2 reactions and related processes. *J. Am. Chem. Soc.* **1984**, *106*, 3531–3539.

(13) Eidi, A.; Eidi, M.; Esmaeili, E. Antidiabetic effect of garlic (Allium sativum L.) in normal and streptozotocin-induced diabetic rats. *Phytomedicine* **2006**, *13*, 624–629.

(14) Chang, M. L.; Johnson, M. A. Effect of garlic on carbohydrate metabolism and lipid synthesis in rats. *J. Nutr.* **1980**, *110*, 931–936.

(15) Seiner, D. R.; LaButti, J. N.; Gates, K. S. Kinetics and Mechanism of Protein Tyrosine Phosphatase 1B Inactivation by Acrolein. *Chem. Res. Toxicol.* **2007**, *20*, 1315–1320.

(16) Parsons, Z. D.; Gates, K. S. Redox regulation of protein tyrosine phosphatases: methods for kinetic analysis of covalent enzyme inactivation. *Methods Enzymol.* **2013**, *528*, 129–154.

(17) Zhou, H.; Singh, H.; Parsons, Z. D.; Lewis, S. M.; Bhattacharya, S.; Seiner, D. R.; LaButti, J. N.; Reilly, T. J.; Tanner, J. J.; Gates, K. S. The Biological Buffer, Bicarbonate/CO2, Potentiates H2O2-Mediated Inactivation of Protein Tyrosine Phosphatases. *J. Am. Chem. Soc.* **2011**, *133*, 15803–15805.

Vita

Zachary Daniel Parsons was born January 8, 1984 in Cape Girardeau, Missouri, to Phyllis and Steven Parsons. Zack was raised by his mother and step-father, Phyllis and Charles Esserine. He graduated from Goddard High School (Goddard, KS) in 2002 and went on to pursue a bachelor's degree – in what, he knew not – at Wichita State University (Wichita, KS). While studying biology at Wichita State, he was invited to join Mike Van Stipdonk's group in the Department of Chemistry, where he grew to appreciate the art of mass spectrometry and developed a (never before-felt) love of chemistry. After receiving his bachelor's degree in chemistry from WSU, he then returned to Missouri, where he worked in Kent Gates' lab and ultimately received his Ph.D. from the University of Missouri in 2014.